DISSERTATION

MULTIFACETED PROTECTION FROM OBESOGENIC DIET-INDUCED DYSFUNCTION BY WHOLE-FOOD COOKED BEAN

Submitted by

Tymofiy Lutsiv

Graduate Degree Program in Cell and Molecular Biology

In partial fulfillment of the requirements

For the Degree of Doctor of Philosophy

Colorado State University

Fort Collins, Colorado

Fall 2025

Doctoral Committee:

Advisor: Henry Thompson

Jessica Davis
Michelle Foster
Tiffany Weir

ABSTRACT

MULTIFACETED PROTECTION FROM
OBESOGENIC DIET-INDUCED DYSFUNCTION
BY WHOLE-FOOD COOKED BEAN

Background. Underconsumption of dietary fiber and the milieu of chemicals with which it is associated is a health concern linked to the increasing global burden of chronic diseases such as clinical obesity and metabolic dysfunction-associated steatotic liver disease (MASLD) caused by disrupted metabolic homeostasis due to dietary challenges. Weight control by improving diet quality is a component of the standard of care in the prevention and control of these metabolic diseases. The benefits of fiber are partially attributed to modulation of the gut microbiota, whose composition and function depend on the amount and quality of microbiota-accessible substrates in the diet. Inclusion of pulses, such as common bean (*Phaseolus vulgaris* L.), is an affordable yet neglected approach to improving diet quality and metabolic outcomes. Whole-food cooked bean is a food type rich in fiber as well as other prebiotics, posing a great potential to positively impact diet-microbiota-host interactions. Regular consumption of common bean, thus, reduces the risk of metabolic impairment. However, its effective dose, the impact of biological sex, and the underlying mechanisms of action are unknown.

Methodology. We fed female and male C57BL6/J mice with obesogenic yet isocaloric diets containing 0%, 17.5%, 35%, and 70% of total dietary protein derived from cooked whole-food bean. The microbial communities in the ceca of female and male mice were

evaluated via 16S rRNA gene sequencing. Liver tissue was collected for histopathology, lipid quantification, and RNA-seq analyses. Based on the obtained results and using biospecimens from several similarly designed studies, cecal content, feces, liver tissue, and plasma samples were subjected to total bile acid analysis and untargeted metabolomics to further complement the findings.

Results. As the bean dose increased, the Bacillota:Bacteroidota ratio (formerly referred to as the Firmicutes:Bacteroidetes ratio) was reduced and α-diversity decreased, whereas the community composition was distinctly different between the diet groups according to β-diversity. These effects were more pronounced in female mice compared to male mice. Compositional analyses identified a dose-responsive bean-induced shift in microbial composition. With an increasing bean dose, Rikenellaceae, *Bacteroides*, and RF39, which are associated with health benefits, were enhanced. More taxa, however, were suppressed, among which were *Allobaculum*, *Oscillospira*, *Dorea*, and *Ruminococcus*, which are predominantly associated with chronic disease risk. Moreover, Beans qualitatively and quantitatively diminished hepatic fat deposition at the 35% dose in female mice and 70% dose in male mice. Bean-induced differentially expressed genes (DEGs) most significantly mapped to hepatic steatosis and revealed dose-responsive inhibition of *de novo* lipogenesis markers (*Acly*, *Acaca*, *Fasn*, *Elovl6*, *Scd1*) and triacylglycerol biosynthesis, activation of triacylglycerol degradation, and downregulation of sterol regulatory element-binding transcription factor 1 (SREBF1) signaling. Upregulated fatty acid β-oxidation was more prominent in females, while suppression of *Cd36*-mediated fatty acid uptake—in males. Sex-dependent bean effects also involved DEGs patterns downstream of peroxisome proliferator-activated receptor α (PPARα) and MLX-interacting protein-like (MLXIPL). Finally, bean-fed mice had increased

cecal bile acid content and excreted more bile acids per gram of feces. Consistent with these effects, increased synthesis of bile acids in the liver was observed. Microbial composition and capacity to metabolize bile acids were markedly altered by bean, with greater prominence of secondary bile acid metabolites in bean-fed mice, i.e., microbial metabolites of chenodeoxycholate/lithocholate increased while metabolites of hyocholate were reduced.

Conclusions. Investigation of the origins of the dose-dependent and biological sex differences in response to common bean consumption may provide insights into bean-gut microbiota-host interactions important to developing food-based precision approaches to chronic disease prevention and control. In rendering mice resistant to obesogenic diet-induced MASLD and obesity, lipid metabolism emerges as one of the main targets of bean effects, especially in the liver. Inhibited uptake of free fatty acids and *de novo* biosynthesis thereof appear to be central molecular responses to bean consumption in the liver, rendering suppressed accumulation of lipid therein. Furthermore, bean consumption sequesters bile acids, increasing their hepatic synthesis and enhancing their diversity through microbial metabolism. Bean-induced changes in bile acid metabolism have the potential to improve dyslipidemia.

ACKNOWLEDGEMENTS

This dissertation is dedicated to the valiant Armed Forces of Ukraine, heroic defenders of my homeland, resilient and indomitable people of Ukraine. In countless ways, I could not have brought this work to fruition without their steadfast courage, their unyielding fight for freedom, and their relentless pursuit of truth amid this war designed to erase our identity, culture, and history. I thank them for their protection, sacrifice, and unconquerable spirit!

Слава Україні! Героям Слава!

TABLE OF CONTENTS

CHAPTER I. Introduction

The problem we address

The term 'pandemic' has recently become popular enough to become the word of the year 2020. Unquestionably, it is associated with the COVID-19 outbreak and therefore carries inherently a certain degree of novelty in its sense. However, unlike this rapid coronavirus-driven one, there is a whole collection of diseases that have been gradually and efficiently growing public health concerns worldwide over the past ~40 years [1], reaching pandemic levels yet not getting a respective spotlight—*obesity*.

In 2022, 1 in 8 people worldwide were living with obesity. Since the 1990s, this number doubled for adults (43% overweight and 16% obese) and quadrupled for children and adolescents (390 million children and adolescents overweight, including 160 million obese) [1]. Obesity is a risk factor for developing cardiovascular disease, type 2 diabetes mellitus, chronic respiratory disease, and different types of cancer. These chronic diseases, also known as noncommunicable diseases (NCDs), constitute seven of the top ten leading causes of mortality worldwide in 2019, accounting for 74% of all deaths and more than three-quarters of years lived with disability, according to estimates from the World Health Organization [2, 3]. The rate of deaths associated with chronic diseases has increased by 75% since 2000 and is projected to account for 86% of all deaths worldwide by 2048 [3]. The development of NCDs is based on genetic, physiological, environmental, and behavioral factors and their intricate combinations.

Recently, clinical obesity has been deemed to join the list of NCDs as 'a chronic, systemic illness characterized by alterations in the function of tissues, organs, the entire individual, or a combination thereof, due to excess adiposity' [4]. Clinical obesity can lead to

severe organ damage and thus life-altering and potentially life-threatening complications (e.g., heart attack, stroke, and kidney failure). In contrast, preclinical obesity is 'a state of excess adiposity with preserved function of other tissues and organs and a varying, but generally increased, risk of developing clinical obesity and several other non-communicable diseases (e.g., type 2 diabetes, cardiovascular disease, certain types of cancer, and mental disorders)'. Even though such a differentiation was performed for clinical and policy-related purposes, the authors admit that the risk of mortality and obesity-associated diseases can rise as a continuum across increasing levels of fat mass.

Such rethinking also affected the metabolic dysfunction-associated steatotic liver disease (MASLD), whose close associations with insulin resistance, cardiometabolic comorbidities, gut microbial dysbiosis, and especially obesity, as well as shared risk factors (e.g., behavioral, lifestyle, and metabolic risk factors), altogether also strongly suggest that MASLD is, in fact, an NCD [5]. Around a third of the world's population is affected by MASLD [6, 7]. To reduce the limitations associated with the previous terminology, non-alcoholic fatty liver disease (NAFLD) was first renamed to metabolic dysfunction-associated fatty liver disease (MAFLD) and later to MASLD. To date, the latter two terms are commonly used with the differences in the policy-level and diagnostic criteria, which rather have a clinical impact [8]. As such, while both MAFLD and MASLD criteria require the presence of metabolic dysfunction, MASLD generally encompasses a larger population, capturing also lean patients with lower risk of disease progression to metabolic dysfunction-associated steatohepatitis (MASH), fibrosis, cirrhosis, hepatocellular carcinoma (HCC) [9, 10].

Biologically speaking, the various degrees of metabolic balance dysregulation in the body underpin their etiology [11, 12], and current global trends in dietary patterns such as the Western type, unsurprisingly, appear to be a root cause of numerous NCDs [11, 13, 14]. Consequently, improving dietary habits remains to this day the most effective way to prevent metabolic disorders.

The solution we suggest

"*Tell me what you eat, and I will tell you what you are*," said Anthelme Brillat-Savarin, a French politician-turned-gastronome in 1826. "*Man is what he eats*," echoed German philosopher Ludwig Feuerbach. Even though originally these words were intended to relate food choices to the state of the consumer's mind, we understand that there is a deeper impact of the diet on our overall health—the food we eat defines our well-being, and the better dietetic choices we make, the better our bodies and minds are. Modern lifestyles increase the likelihood that people will eat in excess, consume foods high in sodium, added sugars, and saturated fat, and combine the intake of high-energy foods with reduced energy expenditure through physical activity [15-17]. This lifestyle leads to metabolic dysregulation, resulting in hypertension, hyperglycemia, hyperlipidemia, overweight or obesity, and other critical metabolic risk factors underlying the development of NCD [16, 18]. The World Health Organization considers a diet to be healthy if per day it provides less than 10% of total energy intake from added sugars, less than 30% of fats, and less than 5 g of salt, while containing legumes, whole grains, nuts, and at least 400 g of fruits and vegetables [15]. The preference for healthy, nutrient-dense foods like vegetables, fruits, and legumes is derived from the low energy density and the accompanying diversity of their macronutrients, minerals, vitamins, bioactive phytochemicals, as well as dietary fiber.

While the emphasis of current epidemiological investigations and food policy decision-makers is on foods and the pattern in which they are typically eaten [19, 20], the dietary guidelines, such as the U.S. Dietary Guidelines for Americans (DGA) and those published in other countries [21, 22], continue to identify nutrients and dietary factors of concern because they are typically either under- or overconsumed and are associated with disease risk [22-25]. Dietary fiber, alongside the milieu of chemicals with which it is associated, is a dietary factor of concern due to underconsumption in developed countries and in developing countries transitioning to Westernized food patterns [6,11,12]. Coincidentally, dietary fiber consumption shows inverse relationships with the development of MASLD [26, 27]. Dietary fiber is a type of complex carbohydrate whose chemical components vary among food categories and that is either slowly digested or indigestible by monogastric animals, including humans. Consequently, fiber-containing microbiota-accessible carbohydrates (MACs) are the main fuel source for the intestinal microbiota, and many of the health benefits associated with dietary fiber ingestion are attributed, in particular, to them. Several mediators of such benefits have been identified, including polyphenol derivatives, mucus layer protection, and especially the metabolites of bacterial fermentation, such as short-chain fatty acids (SCFAs) [28-30]. Nevertheless, dietary fiber encompasses various compounds with different functionalities, and the food source thereof plays an important role as well. As recently noted in the 2020–2025 DGA [22], and underscored by us [31, 32], one particular category of foods rich in dietary fiber that was once widely consumed yet drastically declined, especially in developed countries, is *pulses*.

Pulses are grain legumes rich in both protein and fiber, with a concomitant negligible content of fat [32]. On a per 100 kcal edible portion basis, whole pulses provide more dietary

fiber than any other food category. Given the substantial body of evidence and the immense diversity of health benefits they confer [33-40], pulses *de facto* should be designated as "superfoods" [41]. Thus, the increased consumption of pulses, such as chickpea, dry pea, lentil, and the most commonly consumed among them—the common bean, has the potential to close the currently observed dietary fiber gap in addition to improving dietary quality while decreasing the energy density of a food pattern [42, 43]. Perusal of the scientific literature reveals a growing number of systematic reviews and meta-analyses describing inverse relationships between pulse consumption and incidence of NCDs [34, 37, 39]. Our own research further supports that cooked pulse consumption improves metabolic dysregulation in genetic and dietary rodent models, including effects on gut microbial changes [44-49].

Common bean (*Phaseolus vulgaris* L.) is the most widely eaten type of pulse and consumed in the greatest quantities globally, and thus, it was chosen to study protective pulse effects in an obesogenic environment in a diet-sensitive model—the C57BL6/J mice. In Chapter II, the gut microbial response of female and male mice consuming increasing doses of common bean for 12 weeks is addressed. Chapter III reveals the impact of bean on the hepatic lipid levels, as well as providing molecular insight into the underlying effects of bean in the liver. RNA-seq analysis is complemented with metabolomic profiling from liver and plasma, including the cecal content samples in Chapter IV. Altogether, Chapters III and IV address the impacts of bean consumption on lipid metabolism. Finally, Chapter V summarizes the findings of the current work and provides limitations as well as implications for future work to continue investigating the health benefits of bean consumption.

CHAPTER II. Relandscaping the Gut Microbiota with Bean[1]

1. Introduction

Chronic non-communicable diseases, such as obesity, type-2 diabetes mellitus, cardiovascular disease, and cancer, account for greater than 70% of global deaths per annum [50]. Among the risk factors associated with their intricate and multifaceted etiology, poor diet has long been considered to play a role in these disease processes [51, 52]. While the emphasis of current epidemiological investigations and of food policy decision-makers is on foods and the pattern in which they are typically eaten [19, 20], dietary guidelines, such as U.S. Dietary Guidelines for Americans (DGA), as well as those published in other countries and by various organizations therein [21, 22], continue to identify nutrients and dietary factors of concern because they are typically either underconsumed, or are consumed in excess, and are therefore associated with disease risk [22-25].

Fiber, and the milieu of chemicals with which it is associated, is a dietary factor of concern due to underconsumption in developed countries and in developing countries transitioning to Westernized food patterns [6,11,12]. Dietary fiber is a type of carbohydrate whose chemical components vary among food categories and that is either slowly digested or is indigestible by monogastric animals including humans. Consequently, dietary fiber is a fuel source for the intestinal microbiota, and many of the health benefits associated with dietary fiber ingestion are attributed, in particular, to them. Several mediators of such benefits have

[1] The content of this chapter is based on our research article published in an open-access journal *Foods* from MDPI. References to tables, figures, and supplementary materials have "II" appended to them. Citation information is as follows: *Lutsiv, T., McGinley, J.N., Neil-McDonald, E.S., Weir, T.L., Foster, M.T. and Thompson, H.J., 2022. Relandscaping the gut microbiota with a whole food: dose–response effects to common bean. Foods, 11(8), p.1153.*.

been identified, including metabolites of bacterial fermentation, such as short-chain fatty acids, polyphenol derivatives, lower pH, and mucus layer protection [28-30]. However, dietary fiber encompasses various compounds with different functionality, and the food source thereof plays an important role as well. As recently noted in the 2020–2025 DGA [22], and as underscored by us [31, 32], one particular category of foods rich in dietary fiber that was once widely consumed and that has essentially disappeared from the food patterns typical of developed countries is pulses.

Pulses are grain legumes unique in their high content of both fiber and protein, as well as concomitant absence of fat [32]. On a per 100 kcal edible portion basis, whole pulses provide more dietary fiber than any other food category. Thus, the increased consumption of pulses, such as chickpea, dry pea, lentil, and the most commonly consumed among them—common bean, has the potential to close the dietary fiber gap by improving dietary quality while decreasing the energy density of a food pattern [42, 43]. Food guidelines on legume consumption differ across the countries: while Europe recommends over 450 g of legumes per week, the United States recommends less than 45 g total weekly [21]. Perusal of the scientific literature reveals a growing number of systematic reviews and meta-analyses describing inverse relationships between pulse consumption and incidence of chronic non-communicable diseases [34, 37, 39]. These reports are consistent with our findings that pulse consumption has anti-obesogenic activity in a rat model of polygenic obesity and in a mouse model of dietary-induced obesity where it also confers microbiota-modulating effects [44-49]. However, what is missing from the literature is an assessment of how the gut bacteria respond to increasing amounts of pulse in the diet and whether the biological sex of the organism has any effect on the observed responses.

Common bean, or *Phaseolus vulgaris* L., is the most widely eaten type of pulse along with being consumed in the greatest quantities globally, and therefore was chosen to study effects on the cecal microbial composition of mice. Our main objectives were: (1) to analyze changes to cecal bacteria composition with an increasing dose of common bean in the diet; and (2) to determine whether the biological sex of the mice has an effect on those changes. Following the recent changes in the nomenclature of bacterial taxonomy [53], we adopted herein the new names of phyla, e.g., Firmicutes were renamed to Bacillota, Bacteroidetes—to Bacteroidota, Verrucomicrobia—to Verrucomicrobiota, etc.; as well as updated names since the last version (13_8) of Greengenes reference database, such as family S24-7 was updated to name Muribaculaceae [54]. Despite translatability issues of the gut microbiota studies in the murine models [55, 56], our focus was the scope of the effects of bean consumption on shifts in the bacterial populations in the cecum. Since the intestinal microorganisms comprise only one of the elements of systemic physiologic changes induced by the diet, the findings obtained in the current study correspond to previous and future studies on mice in the realm of dietary effects on the etiology of chronic diseases.

2. Materials and Methods

2.1. Study Design

All animal-related work was performed in compliance with the Colorado State University Institutional Animal Care and Use Committee (protocol 18-7746A-KP 1431). Eighty female and eighty male wildtype C57BL6/J mice (stock# 000664) were purchased from The Jackson Laboratory (Barr Harbor, ME, USA) at 20 days of age. Mice were housed in solid-bottomed polycarbonate rodent cages and maintained on a 12 h light/dark cycle at

27.5 ± 2°C with 30% relative humidity and *ad libitum* access to distilled water. As a model for obesity, mice were adapted to a purified rodent diet formulation (with 32.5% dietary kcal derived from fat) and animal husbandry routine until they reached 8 weeks of age. This approach promotes dysbiosis that is associated with the obesity phenotype, which manifests beginning at 8 weeks of age [57]. At that time, animals were randomized based on their body weight to experimental diet groups (n = 20 of each sex per diet group) and fed their respective experimental diet formulations for 12–14 weeks (see Section 2.2.). Animals were euthanized by cervical dislocation following isoflurane-induced anesthesia. The cecum was harvested, cut open, and contents gently mixed with a clean spatula to produce a homogeneous mixture, which was placed in a sterile cryovial and snap-frozen in liquid nitrogen for subsequent DNA extraction. Cecal samples from animals within each diet group with a similar weight gain pattern were pooled (n = 2 per pool). Thus, each diet group was comprised of 10 pooled cecal samples total.

2.2. Experimental Diets

Purified diets were formulated to provide 32.5% of dietary kcal from fat to induce excessive weight gain in C57BL6/J mice [58]. Freeze-dried powder from whole cooked white kidney bean was incorporated into the diet by substituting casein with 0%, 17.5%, 35%, and 70% of the protein derived from bean. Despite increasing doses of the bean, adjustments were made in other components so that macronutrient content was similar across diet groups (**Table II.1**).

Table II.1. Experimental diets formulations.

Ingredient	0% Bean (g/100g)	17.5% Bean [1] (g/100g)	35% Bean [1] (g/100g)	70% Bean [1] (g/100g)
Solka-Floc	7.5	4.0	2.0	1.0
White Kidney Bean [2]	0.0	10.2	20.4	40.8
Corn Starch	15.9	15.2	12.1	2.0
Casein (≥85% protein)	23.5	19.4	15.3	7.0
Cerelose (Dextrose)	7.2	7.2	7.2	7.2
Sucrose	25.0	23.0	22.0	21.0
Vitamin mix [3]	1.1	1.1	1.1	1.1
DL-Methionine	0.3	0.3	0.3	0.3
L-Tryptophan (Sigma T0254-25G)	0.00	0.02	0.03	0.06
Choline bitartrate (41% choline)	0.2	0.2	0.2	0.2
Mineral mix [4]	3.8	3.8	3.8	3.8
Corn Oil	11.3	11.3	11.3	11.3
Anhydrous Butter Fat	4.2	4.2	4.2	4.2
Total (g)	***100.0***	***100.0***	***100.0***	***100.0***

[1] Experimental diet modified from the original (bean-free control) diet formulations; all formulations were formulated to be 58.6% carbohydrate, 15.5% fat and 20 % protein, *w/w*. [2] For the bean-fed groups, the whole bean was cooked and processed with the leachate, freeze-dried, and homogenized into a fine powder; total dietary fiber concentration of white kidney bean was 23.5 g/100g; [3] Dyets Inc: #310025 AIN-93G vitamin mix; [4] Dyets Inc: #210025 AIN-93G mineral mix.

2.3. 16S rRNA Gene Library Preparation, Sequencing, and Processing

From the cecal content, DNA was extracted with the QIAamp PowerFecal DNA kit (Qiagen, Germantown, MD, USA) according to the manufacturer's protocol, and its purity and concentration were determined by NanoDrop (Thermo Fisher Scientific, Waltham, MA, USA). The V4 region of the 16S rRNA gene was amplified and sequenced to construct paired-end sequencing libraries using the 515F-806R primer set following the Earth Microbiome Project protocols [59], followed by sequencing using the MiSeq Reagent Kit v2 2 × 250 bp on an Illumina MiSeq instrument housed at the Next-Generation Sequencing Facility at Colorado State University.

Bioinformatic processing of the obtained forward and reverse paired-end sequence reads was performed with QIIME 2 platform, version 2021.8 [60]. Raw sequence data were demultiplexed and quality-filtered via q2-demux plugin. Denoising was performed with the DADA2 pipeline (q2-dada2) [61]: each sequence pair was truncated from 225 bp (forward) and 155 bp (reverse), checked for chimeras, and filtered for quality control. Taxonomy was assigned to the resulting amplicon sequence variants (ASVs) using a Naive Bayes classifier (via q2-feature-classifier plugin [62]) pre-trained on Greengenes (16S rRNA, version 13_8)—a marker gene reference database trimmed to the V4 domain (bound by the 515F/806R primer pair) with a 99% sequence identity threshold [63]. The dataset was filtered to remove all features annotated as "mitochondria" and "chloroplast." A rooted phylogenetic tree was built using FastTree [64] and MAFFT [65] alignment via q2-phylogeny plugin.

2.4. Statistical and Bioinformatic Analyses

Further analysis was conducted in QIIME 2, MicrobiomeAnalyst (Marker-gene Data Profiling module) [66, 67], and *R* (version 4.1.1, R studio version 2021.09.0) on two output datasets: the ASVs abundance dataset and their taxa-assigned abundance dataset. The latter comprised a list of identified bacteria mapped to the lowest possible taxonomic level. Certain bacteria were underclassified and thus marked "I" if there was insufficient resolution to annotate to species (indicated with "s_" in the Greengenes database); or marked "II" if it was impossible to classify the ASVs to a deeper level (indicated as "_" in the Greengenes database). Features (ASVs or taxa) with less than two counts were automatically removed by pre-processing steps of MicrobiomeAnalyst's integral Sanity Check. As a result, the female cohort dataset consisted of 233 ASVs, whereas the male cohort dataset included 220 ASVs.

Using q2-diversity plugin in QIIME 2, the samples were rarefied (subsamples without replacements) to 21,418 (female cohort) and 23,617 (male cohort) sequences per sample, retaining 74.23% and 78.93% features (the maximally available option), respectively. Two samples from each sex cohort did not meet the sampling depth threshold and were excluded. Richness and evenness were analyzed using Observed Features, Faith's phylogenetic diversity, and Shannon's diversity index metrics, then statistically compared between the diet groups via the Kruskal-Wallis non-parametric test (both in QIIME 2) and visualized using R. Principal coordinates analysis (PCoA) of β-diversity matrices was based on Jaccard dissimilarity as well as phylogeny-based Weighted and Unweighted UniFrac distances, and were assessed using permutational multivariate analysis of variance (PERMANOVA) with 999 permutations in QIIME 2, and the results were visualized in MicrobiomeAnalyst.

For compositional analyses, the taxa-assigned datasets were further subjected to quality filtering and normalization in MicrobiomeAnalyst. Taxa were filtered for low abundance—a minimum of 10% samples with at least four counts were retained—as well as for the low variance—less than 5% based on the inter-quantile range were removed. Total sum scaling (TSS) was performed to normalize the data.

The Heat Tree Analysis was used to utilize the hierarchical structure of taxonomic classifications to quantitatively (using the median abundance) and statistically (using the non-parametric Wilcoxon Rank Sum test) depict taxonomic differences between microbial communities between the sex cohorts via Reingold-Tilford layout using *R* metacoder package in MicrobiomeAnalyst [68].

Bacterial biomarkers were discovered using the linear discriminant analysis (LDA) effect size (LEfSe) method [69]. This algorithm allowed detection of differentially abundant

taxa among the experimental groups using the Kruskal-Wallis test and then evaluated their relevance via an LDA score. LEfSe was performed on the phylum and the feature levels of the taxa-assigned dataset using cutoffs of <0.05 for the FDR-adjusted *p*-value and >2.0 for the logarithmic LDA score. Analyses were performed within sex cohorts as well as in the pairwise comparison setting to assess differences between the diet groups.

Variation of taxonomic abundance related to the diet group was visualized on a heatmap in MicrobiomeAnalyst after Ward's hierarchical clustering algorithm based on Minkowski distances. Feature level was used for the analysis of the taxa-assigned dataset.

Correlation analysis was performed to build correlograms between bacterial relative abundance pairs and the bean dosage using Spearman's rank-order correlation testing. Correlations with a *p*-value < 0.05 were included in the results.

Functional attributes of the identified microbial communities were predicted using Phylogenetic Investigation of Communities by Reconstruction of Unobserved States 2 (PICRUSt2) pipeline, version 2.4.1 [70]. With the ASV dataset as an input, PICRUSt2 performs phylogenetic placement by aligning ASVs to the reference 16S sequences (HMMER, www.hmmer.org, accessed on 1 December 2021) and incorporating them into the reference tree evolutionary placement algorithm (EPA)-NG and genesis applications for phylogenetic placement analysis (GAPPA) [71, 72], followed by the hidden-state prediction of gene families (*castor R* package [73]) and, finally, generation of metagenomic predictions and tabulation of pathways' inferences and abundances (Minimal set of Pathways (MinPath)) [74] and MetaCyc [75]. Statistical analysis of taxonomic and functional profiles (STAMP) software, version 2.1.3 (Robert Beiko, Halifax, NS, Canada), was used to analyze and visualize PICRUSt2 output data [76]. In brief, the pulse-free Control group and samples from

pulse-based diet groups were compared using Welch's two-sided *t*-test with 0.95 Welch's inverted CI method and the Benjamini-Hochberg FDR multiple test corrections method.

3. Results

3.1. Overview of the Bean-Induced Microbial Community in the Cecum

Analysis of bacteria at the phylum level allows for the detection of the most marked statistical differences between the experimental groups. Overall, six phyla were identified in the ceca of mice fed with or without increasing amounts of common bean. In light of recent changes in microbiological nomenclature [53], new phyla names are reported here. Each diet group demonstrated a distinct microbial profile (**Figure II.1**). Across all samples, the most prevalent phyla were the Gram-positive Bacillota (formerly Firmicutes) and the Gram-negative Bacteroidota (formerly Bacteriodetes); however, there is a significant increase in Bacteriodota and subsequent decrease in Bacillota and Actinomycetota (formerly Actimomycetes) with increasing bean dose.

Although the dose response trends were similar across male and female mice, there were some sex-specific changes. In the female cohort, the bean-free control diet exhibited the Bacillota:Bacteroidota ratio (a Firmicutes:Bacteroidetes ratio) of 1.154, with Bacillota being the most abundant phylum (43.03%), followed by Bacteroidota (37.3%), Verrucomicrobiota (15.4%), and Actinomycetota (2.72%). As bean was introduced to the diet, the Bacillota:Bacteroidota ratio decreased with the increasing dose (0.421–0.232), with Bacteroidota dominating in the cecum (56.65–74.12%), followed by Bacillota (23.85–17.23%), Verrucomicrobiota (16.95–4.94%), and Pseudomonadota (formerly Proteobacteria; 1.77–3.14%) as the bean dose increased.

In contrast, the Bacteroidota was dominant in male mice prior to the introduction of bean, with a Bacillota:Bacteroidota ratio of 0.922 in the control group and a range of 0.528–0.360 as the bean dose increased. The most abundant phyla were Bacteroidota (39.35–63.47%), Bacillota (36.29–22.88%), Verrucomicrobiota (18.02–9.62%), and Pseudomonadota (3.83% in the control and bean dose-dependent decrease from 5.24% to 3.81%). Therefore, despite similar patterns of change in phyla abundance, the male mice were less impacted by bean introduction than female mice.

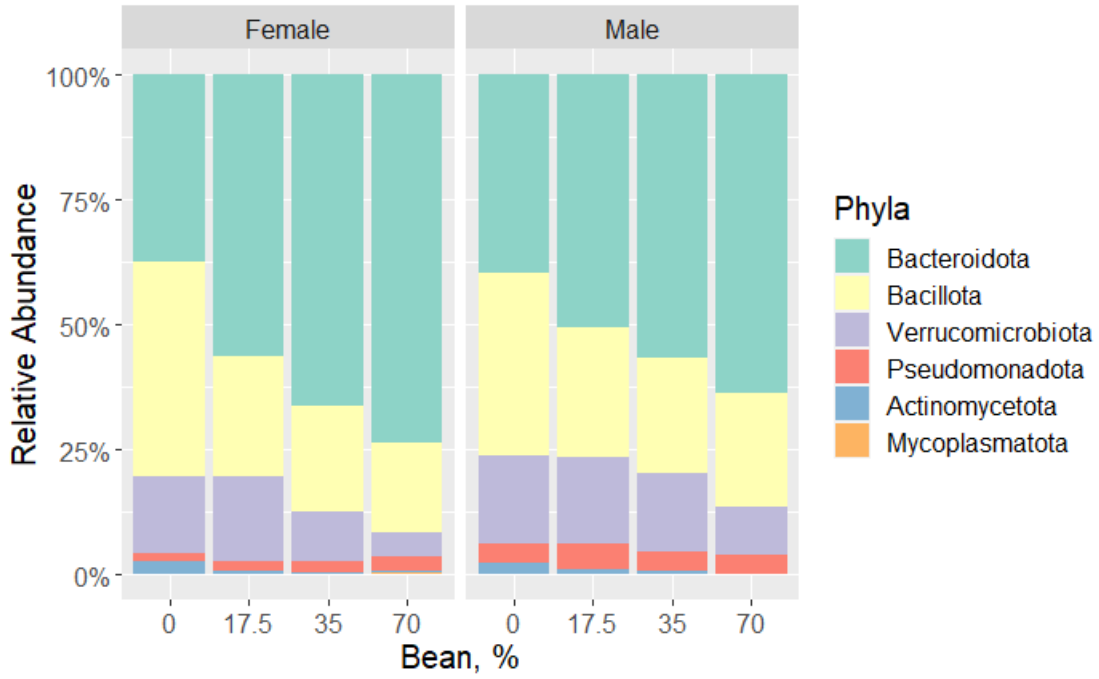

Figure II.1. Relative abundance of identified phyla across the diet groups of each sex cohort.

For more quantitative analyses of differences in bacterial communities across the diet groups, the relative abundances were subjected to Kruskal-Wallis testing with a *post hoc* Dunn test for pairwise comparisons, and the results are summarized in **Table II.2**. Starting at the 17.5% bean group, the relative abundance of Bacillota decreased by 19.18%, and then by 22.26% and 25.8% in the 35% and 70% groups, respectively, among the female cohort. Less drastically in males, Bacillota decreased by 10.14%, 12.74%, and 13.41% along with

the increasing bean dose in the diet groups. Starting at 35% bean, Actinomycetota decreased by 2.56% and 2.63% compared with the control group in females, and by 1.96% and 2.39%, respectively, in males. An increase in Bacteroidota upon bean consumption is observed starting at 35% bean in both sex cohorts (by 29.17–36.82% increase in females and 16.97–24.12% increase in males).

Table II.2. Relative abundances of phyla per each sex cohort and diet group.

Phyla / Bean dose	Female				Male			
	0%	***17.5%***	***35%***	***70%***	***0%***	***17.5%***	***35%***	***70%***
Actinomycetota	2.72	0.61	0.16 [1,***]	0.09 [1,***; 2,*]	2.48	1.05	0.52 [1,***]	0.09 [1,***; 2,***]
Bacteroidota	37.30	56.65	66.47 [1,***]	74.12 [1,***; 2,**]	39.35	49.52	56.32 [1,**]	63.47 [1,***; 2,**]
Bacillota	43.03	23.85 [1,**]	20.77 [1,***]	17.23 [1,***]	36.29	26.15 [1,*]	23.55 [1,**]	22.88 [1,**]
Pseudomonadota	1.52	1.77	2.21	3.14 [1,**; 2,**]	3.83	5.24	3.99	3.81
Mycoplasmatota	0.02	0.17	0.25 [1,*]	0.47 [1,***; 2,*]	0.04	0.03	0.11 [1,**; 2,**]	0.13 [1,**; 2,**]
Verrucomicrobiota	15.40	16.95	10.13	4.94 [1,*; 2,***; 3,*]	18.02	18.01	15.50	9.62 [2,*]

[1] Significantly different from the 0% group; [2] Significantly different from the 17.5% group; [3] Significantly different from the 35% group; Statistically significant phyla were determined by the Kruskal-Wallis testing of the relative abundances with * p-value < 0.05; ** p-value < 0.01; *** p-value < 0.001. p-values adjusted for multiple comparisons with the Benjamini-Hochberg method.

3.2. Analysis of α- and β-Diversity among the Diet Groups

Bean incorporation into the diet decreased the diversity of the cecal microbiota within samples. Observed richness, as well as Faith's phylogenetic diversity, were significantly higher in the bean-free control group compared with each bean-containing diet, but this was not observed in their male counterparts (**Figures II.S1–S2**). When α-diversity was assessed using the Shannon index (**Figure II.2**), which accounts for both ASVs richness and evenness within samples, the 70% bean diet group was statistically lower than the control diet in male mice, whereas all bean-based diet groups had significantly reduced diversity from the control diet in female animals. Looking at the uncorrected p-values, the males fed the 35% bean group also differed from the control with p-value = 0.034 (correction for multiple comparisons showed only a statistical trend, q-value = 0.052). Females responded to changes in their gut

microbiome at the lowest dose of bean compared to their male counterparts in terms of Shannon's indices. Each diet group was also assessed for α-diversity differences in female versus male cohorts (**Figure II.S3**). Only Faith's phylogenetic richness was higher in males compared to the female sample cohort, while according to the other metrics, there were no statistically significant differences despite the tendency for higher intra-sample diversity in males.

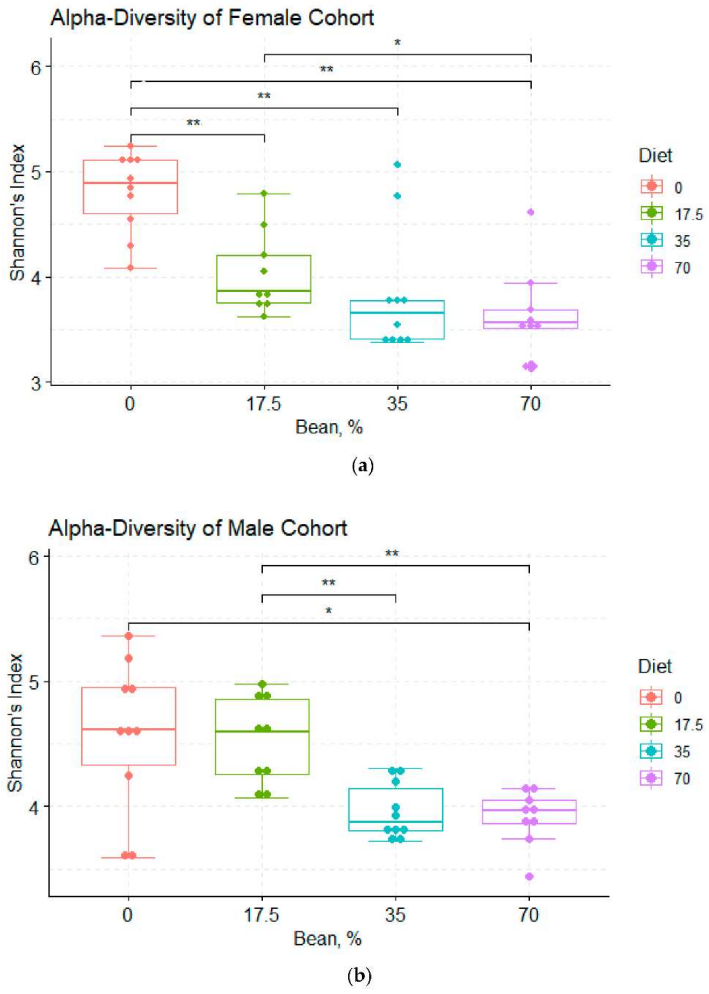

Figure II.2. (**a**) Shannon's indices of α-diversity of the female cohort. Statistically significant differences were determined by the Kruskal-Wallis test (p-value < 0.001) with * q-value < 0.05; ** q-value < 0.01; (**b**) Shannon's indices of α-diversity of the male cohort. Statistically significant differences were determined by the Kruskal-Wallis test (p-value = 0.002) with * q-value < 0.05; ** q-value < 0.01.

Several measures of β-diversity also suggested that the control diets resulted in a microbial profile distinct from the microbiota of the bean-containing diet groups. As the bean dose increased in the diet, the samples localized further away from the control group in the PCoA matrix. Pairwise PERMANOVA analysis indicated that all bean-based diets significantly differed from the bean-free control ($p < 0.01$). All diet groups significantly differed from one another when Jaccard distances were subjected to PCoA (**Figure II.S4**), highlighting the qualitative absence and presence of unique ASVs in both sex cohorts. Similar results were obtained when phylogenetic relationships were used to generate the distance matrices. There was a clear separation of diet groups in ordinations of both weighted (**Figure II.3**) and unweighted (**Figure II.S5**) UniFrac distance matrices. Therefore, bean-induced differences in the cecal microbial communities among the samples were detected even at the lowest tested dose (17.5%).

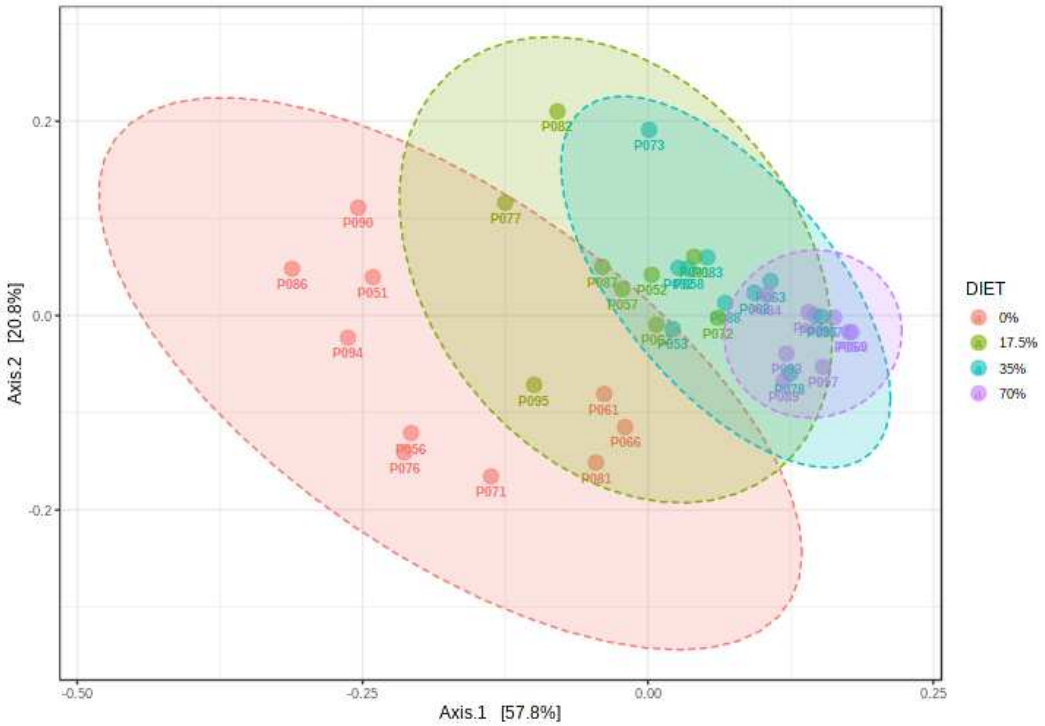

(a)

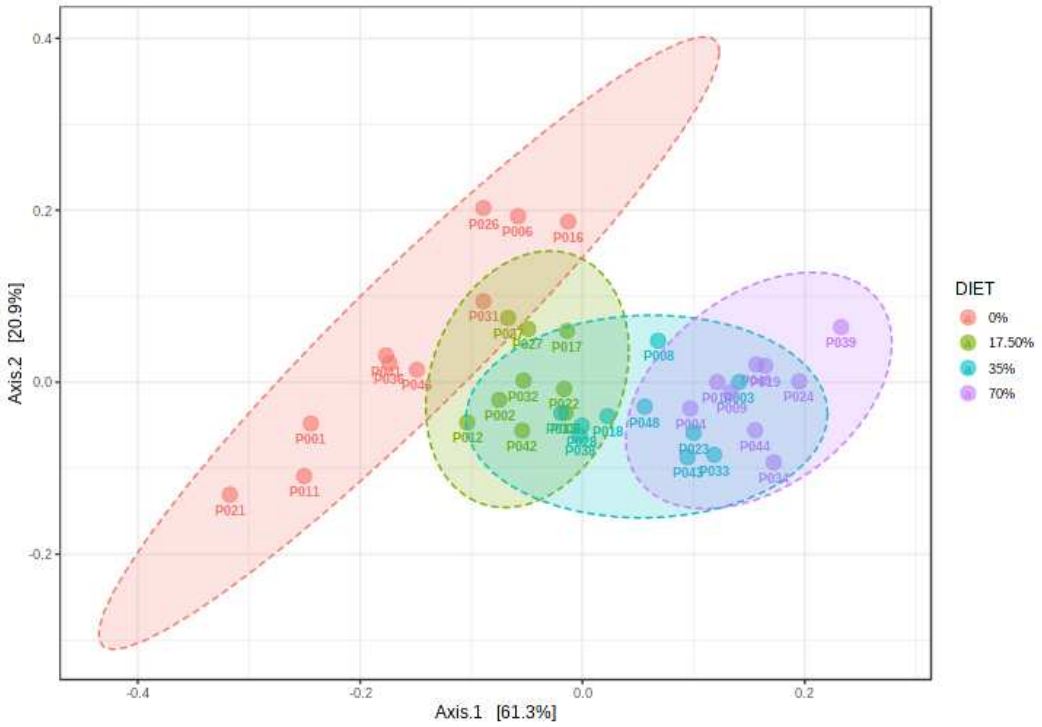

(**b**)

Figure II.3. Phylogenetic Weighted UniFrac distances were used to explain β-diversity across diet groups. Differences between the samples were tested by the permutational multivariate analysis of variance (PERMANOVA): samples are colored and grouped by their corresponding diet group into ellipses representing 95% confidence intervals. (**a**) in the female cohort, pseudo-*F*-value = 12.845; *p*-value < 0.001. All diet groups were statistically different from one another; (**b**) in the male cohort, pseudo-*F*-value = 14.751; *p*-value < 0.001. All diet groups were statistically different from one another.

3.3. The Differential Abundance Analyses

Observed changes in the cecal microbiota from the aforementioned analyses revealed that female and male mice respond differently to the introduction of whole beans into the dietary formulation. **Figure II.4** displays the relative abundance (post filtering) of detected cecal bacteria at their lowest possible taxonomic level across all tested diet groups. Muribaculacease, *Akkermansia muciniphila*, Rikenellaceae (I), *Bacteroides (II)*, Clostridiales (II) comprised on average the top 5 most abundant bacterial taxa. To better visualize the distribution of the microbiota in our samples, we constructed a hierarchical clustering heatmap. **Figure II.S6** displays that, regardless of sex, the bean-free control samples cluster

distinctly from the bean-fed diet groups in a similar pattern. Differences between the sex cohorts are evident in each diet as well. Next, all bean-containing diet groups were subjected to the Heat Tree analysis (**Figure II.5**) to show group-wise changes in relative abundances of the bacteria that drive sex-dependent differences upon bean consumption. Overall, Bacilli were more abundant in the female mice, as well as *Turicibacter, Lactococcus, Lactobacillus, Ruminococcus*, Muribaculaceae, and RF39, whereas Christensenellaceae, Peptostreptococcaceae, Clostridiaceae, *Bacteroides, Coprococcus, Sutterella*, *Allobaculum*, *B. pseudolongum*, and *A. muciniphila* were more representative of the male cohort. These sex-dependent biomarkers across all the diet groups were further confirmed via pairwise LEfSe setting (**Figure II.S7**).

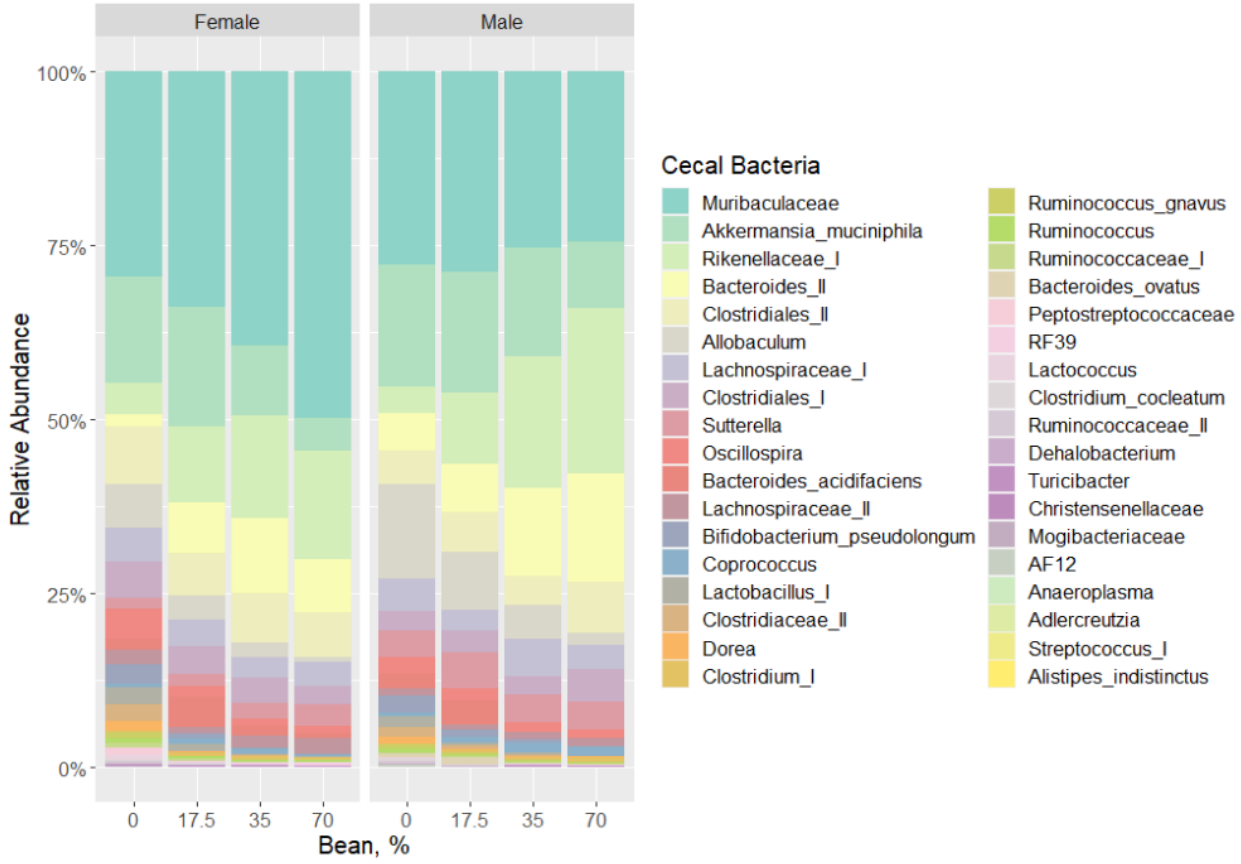

Figure II.4. Relative abundance of cecal bacteria at their lowest level of identified taxonomy across the diet groups of each sex cohort.

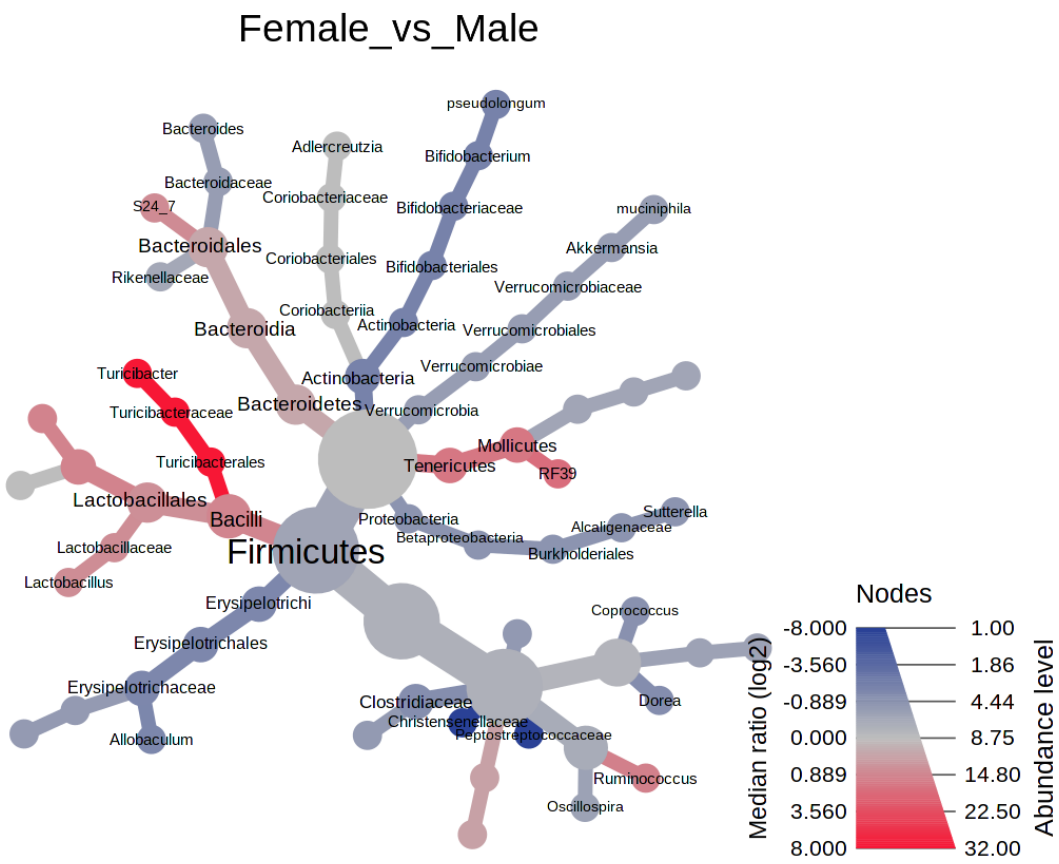

Figure II.5. The Heat Tree analysis of taxonomic changes in the female versus male cohorts. The color corresponds to the log2 ratio of median proportions of taxa observed in each cohort across only bean-containing diet groups. Only significant differences are colored according to the Wilcoxon rank-sum testing. Nomenclature used herein is according to the Greengenes database.

To determine which bacteria are the most influential in driving the differences across the diets in each sex cohort, LEfSe was performed. LEfSe indicated that 25 microbiota were statistically differential biomarkers of diet groups in the female cohort (**Figure II.6a,b**). According to the pairwise LEfSe analyses, Rikenellaceae (I), *Bacteroides (II)*, and *Clostridium (I)* significantly increased compared with the control in all bean-based diets, whereas higher counts of Muribaculaceae, *Sutterella*, and RF39 were observed starting from the 35% dose of bean. These 6 bacterial groups comprise a bean-enhanced eco-group in the female mice (**Figure II.6a**). Interestingly, *Coprococcus* was statistically enhanced in

the 17.5% bean group versus bean-free control, but not in the higher bean dose groups. Similarly, *Anaeroplasma* was significantly different from the control only in the 35% bean group. In the male cohort, there were 28 differential bacterial biomarkers across the diet groups (**Figure II.6c,d**). Among them, Rikenellaceae (I) and *Clostridium (I)* steadily increased in all bean-based diets compared with the control group; *Bacteroides (II)* and *Coprococcus* were enhanced starting from 35% bean dosage, whereas unclassified Clostridiales (I) and RF39 were significantly enhanced compared to the bean-free control only in the 70% bean group. These taxa form a bean-enhanced eco-group in the male mice (**Figure II.6c**). Interestingly, in the 35% bean diet group, *Turicibacter* was also statistically different from the control and 17.5% bean groups, but not in the higher 70% dose group.

The bean-suppressed eco-group in the male samples was comprised of *Allobaculum, B. pseudolongum, Parabacteroides*, Clostridiaceae (II), *Lactobacillus (I), Dorea, R. gnavus, Ruminococcus, AF12, C. cocleatum, Lactococcus,* Ruminococceae (II), and *Dehalobacterium*, which decreased in all bean-based groups versus the control; as well as *B. acidifaciens, Oscillospira*, and *B. ovatus*, the abundance of which declined starting from 35% bean dosage; lastly, *Adlercreutzia* were statistically different from the control only in the male 70% bean group (**Figure II.6d**). In contrast, in the female mice, *Oscillospira, B. pseudolongum*, Clostridiaceae (II), *Lactobacillus (I), Dorea*, Peptostreptococcaceae, *R. gnavus, Lactococcus, Ruminococcus,* Ruminococcaceae (II), *Clostridium (II), Dehalobacterium*, Mogibacteriaceae, *Streptococcus (I), Adlercreutzia, Enterococcus*, as well as—starting from 35% bean dose—*C. cocleatum*, Ruminococcaceae (I), Clostridiales (I), and *Allobaculum* create the bean-suppressed eco-group (**Figure II.6b**). Additionally, *Turicibacter, Coprococcus*, and *A. muciniphila* were significantly decreased in the 70% bean group compared with both the 0% and 17.5% bean groups.

Coprococcus was not included in the bean-suppressed female eco-group due to its significantly increased abundance in the 17.5% versus 0% bean group comparison.

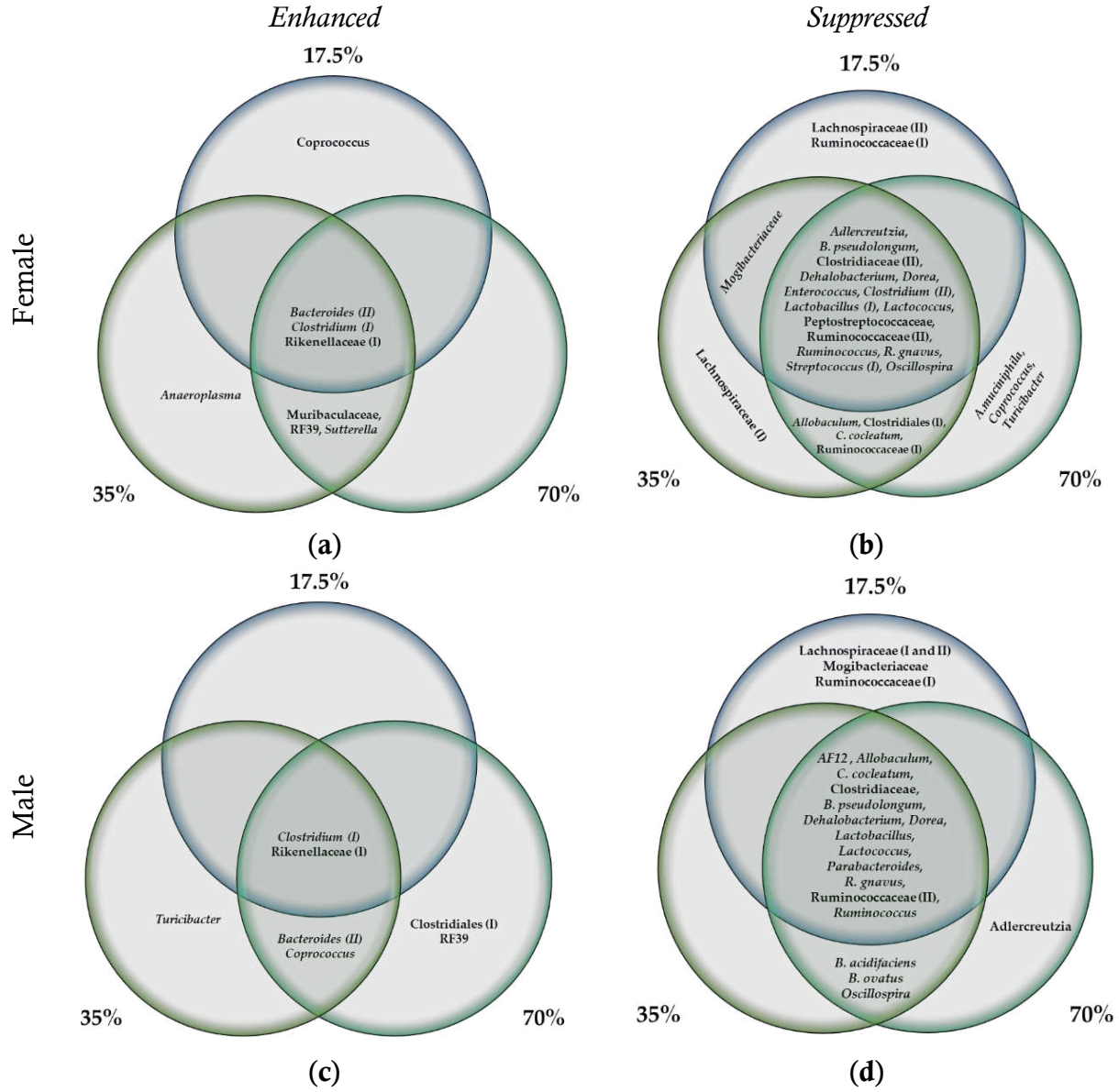

Figure II.6. Bean-induced bacterial biomarkers of the (**a**, **c**) female and (**b**, **d**) male cohorts according to the pairwise linear discriminant analysis (LDA) of effect size (LEfSe) at the feature level. Panels (**a**, **b**) exhibit bean-enhanced, whereas (**c**, **d**) exhibit bean-suppressed bacterial biomarkers. All represented bacteria were statistically significant (LDA score > |2.0|, FDR-adjusted p-value < 0.05).

Finally, the identified bacteria of the bean-induced ecosystem were confirmed in Spearman's rank-order correlation (**Figure II.7**). Interestingly, the same bacteria identified in

the LEfSe runs correlated positively with their respective eco-groups and the bean dose. Muribaculaceae, RF39*, Sutterella*, Rikenellaceae (I), and *Bacteroides (II)* positively correlated with the bean dose, whereas *Lactococcus*, *Lactobacillus (I)*, Peptostreptococcaceae, *Allobaculum*, and *B. pseudolongum* displayed a strong negative association in the female cohort. In the male cohort, the most positively correlated bacteria with the bean dose were Rikenellaceae (I), *Bacteroides (II)*, *Clostridium (I),* and RF39*,* whereas *B. pseudolongum, Allobaculum, R. gnavus, Lactococcus*, *Lactobacillus (I)*, *C. cocleatum*, and Ruminococcaceae (II) were the most negatively correlated with the bean dose.

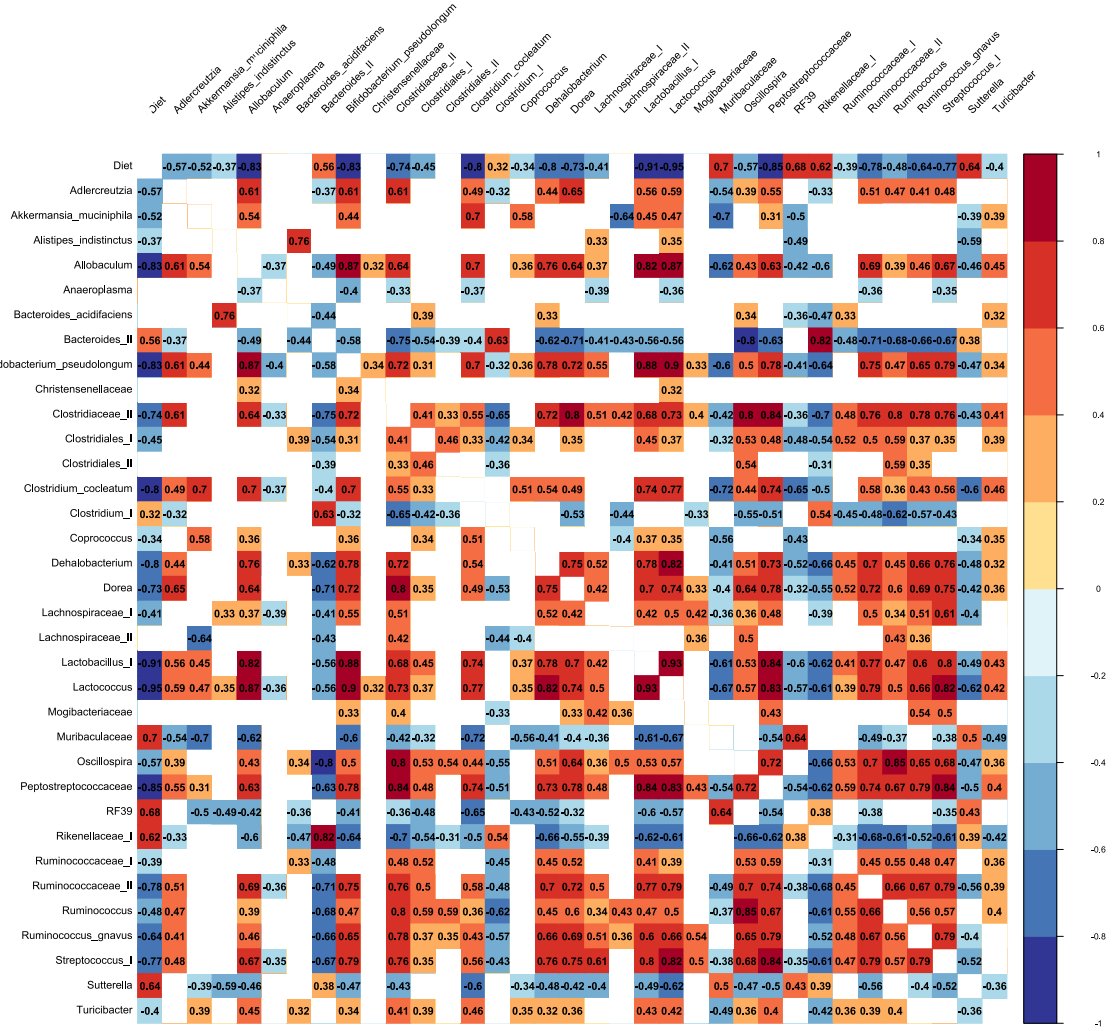

(a)

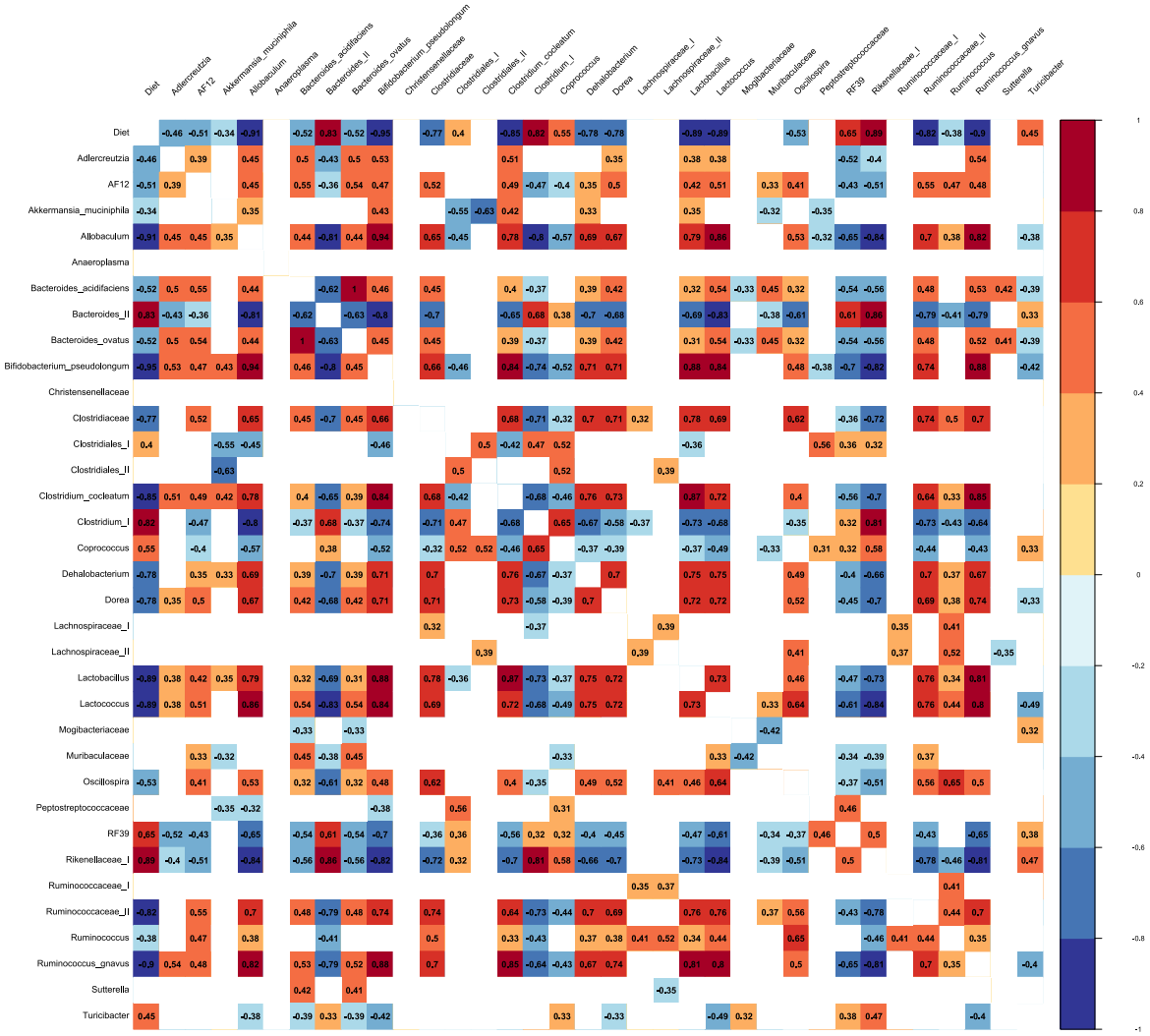

(**b**)

Figure II.7. Spearman's rank-order correlation analysis of the relative abundances of the cecal bacteria identified in the (**a**) female and (**b**) male cohorts. Heatmap represents power of correlation: from the red indicating positive to the blue indicating negative correlation coefficient values. Only correlations with the *p*-value < 0.05 were included in the correlogram.

3.4. Predicted Functional Differences of the Microbial Communities

PICRUSt2 assessment of the predicted metagenomic functions overall showed that females displayed significantly more differentially represented pathways between the bean-free and bean-based diets compared to their male counterparts (**Figures II.8, II.9, II.S8,** and **II.S9**). Increasing doses of the dietary bean increased the number of differences in

the bacterial metabolic pathways from 152 to 198 compared with the control. Out of these, 12–45 pathways had an effect size of over 20% difference in proportions. The male cecal microbiota responded more modestly upon the introduction of bean: from 95 to 160 differential pathways. There were 11 to 32 pathways with over 20% difference in proportions in the male cohort. Interestingly, males showed no predicted metabolic pathway differences between 0% and 17.5% diet groups, with over 20% difference in proportions. Overall, increasing bean dose in the diet predictably increased the amount of differential microbial functional pathways.

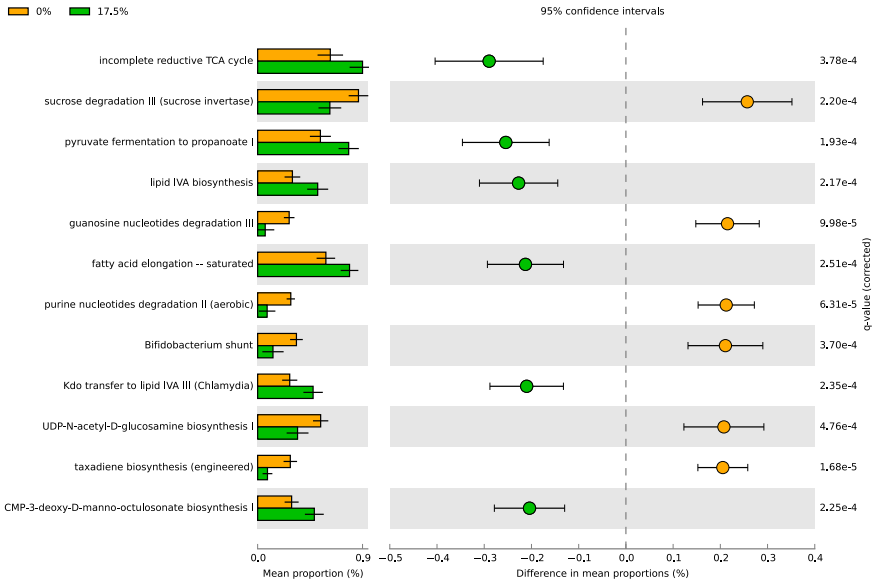

(a)

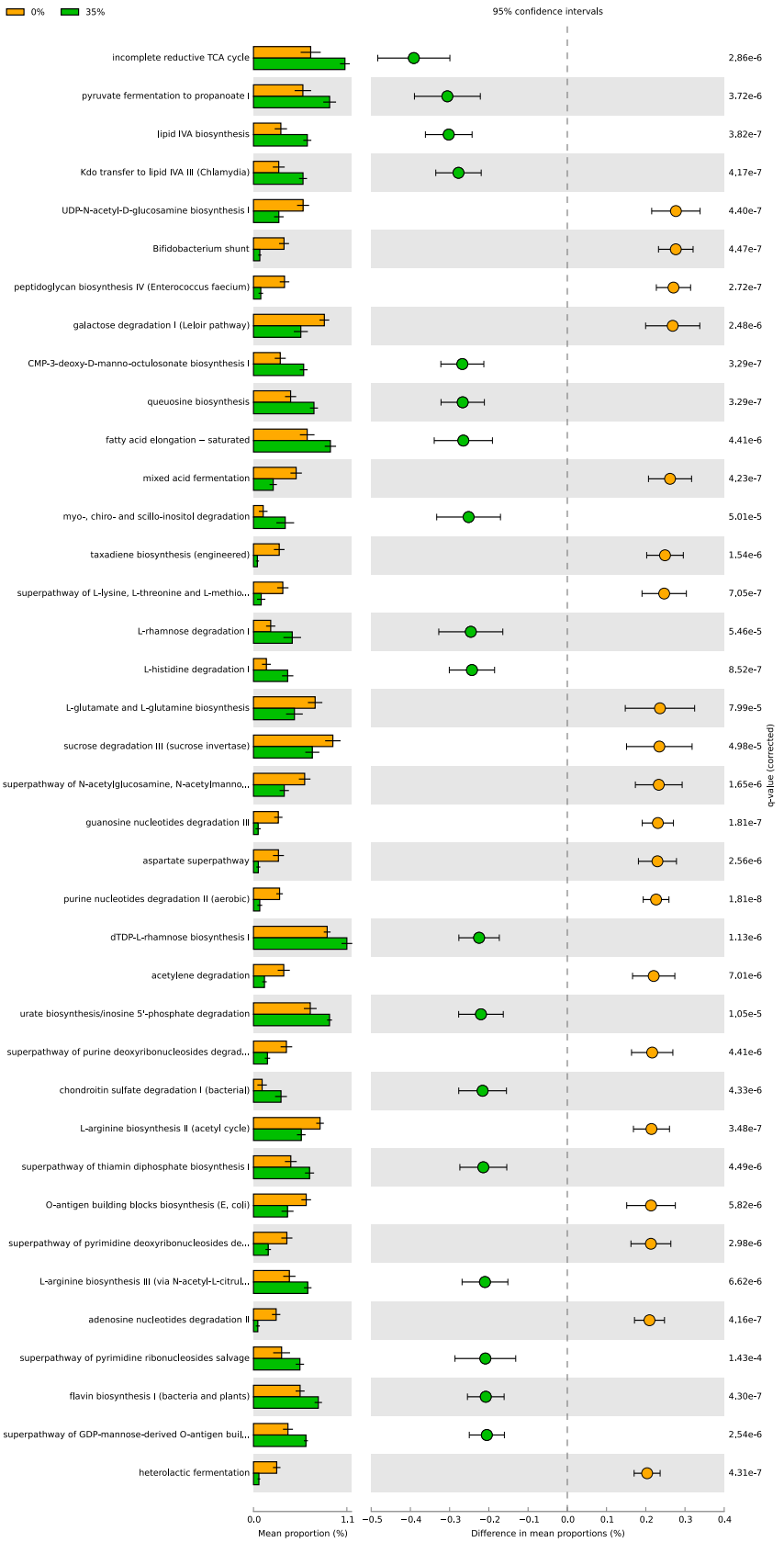
0%
35%
95% confidence intervals
incomplete reductive TCA cycle
pyruvate fermentation to propanoate I
lipid IVA biosynthesis
Kdo transfer to lipid IVA III (Chlamydia)
UDP-N-acetyl-D-glucosamine biosynthesis I
Bifidobacterium shunt
peptidoglycan biosynthesis IV (Enterococcus faecium)
galactose degradation I (Leloir pathway)
CMP-3-deoxy-D-manno-octulosonate biosynthesis I
queuosine biosynthesis
fatty acid elongation − saturated
mixed acid fermentation
myo-, chiro- and scillo-inositol degradation
taxadiene biosynthesis (engineered)
superpathway of L-lysine, L-threonine and L-methio...
L-rhamnose degradation I
L-histidine degradation I
L-glutamate and L-glutamine biosynthesis
sucrose degradation III (sucrose invertase)
superpathway of N-acetylglucosamine, N-acetylmanno...
guanosine nucleotides degradation III
aspartate superpathway
purine nucleotides degradation II (aerobic)
dTDP-L-rhamnose biosynthesis I
acetylene degradation
urate biosynthesis/inosine 5'-phosphate degradation
superpathway of purine deoxyribonucleosides degrad...
chondroitin sulfate degradation I (bacterial)
L-arginine biosynthesis II (acetyl cycle)
superpathway of thiamin diphosphate biosynthesis I
O-antigen building blocks biosynthesis (E. coli)
superpathway of pyrimidine deoxyribonucleosides de...
L-arginine biosynthesis III (via N-acetyl-L-citrul...
adenosine nucleotides degradation II
superpathway of pyrimidine ribonucleosides salvage
flavin biosynthesis I (bacteria and plants)
superpathway of GDP-mannose-derived O-antigen buil...
heterolactic fermentation
2,86e-6
3.72e-6
3.82e-7
4,17e-7
4.40e-7
4,47e-7
2.72e-7
2.48e-6
3,29e-7
3.29e-7
4.41e-6
4,23e-7
5.01e-5
1,54e-6
7,05e-7
5.46e-5
8,52e-7
7.99e-5
4.98e-5
1,65e-6
1.81e-7
2,56e-6
1,81e-8
1.13e-6
7.01e-6
1,05e-5
4.41e-6
4,33e-6
3.48e-7
4.49e-6
5,82e-6
2.98e-6
6.62e-6
4,16e-7
1.43e-4
4,30e-7
2,54e-6
4,31e-7
q-value (corrected)
0.0
1.1
Mean proportion (%)
−0.5
−0.4
−0.3
−0.2
−0.1
0.0
0.1
0.2
0.3
0.4
Difference in mean proportions (%)

(**b**)

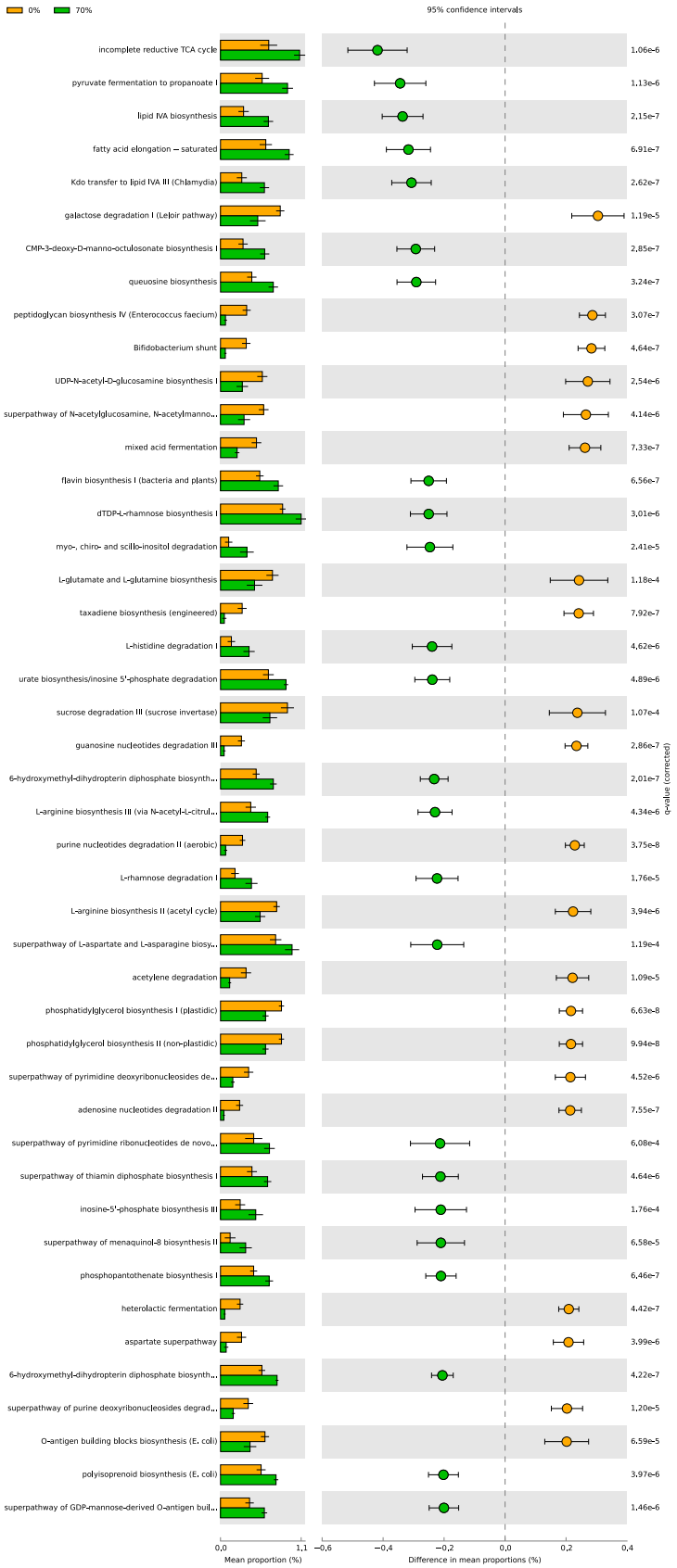
0%
70%
95% confidence intervals
incomplete reductive TCA cycle
pyruvate fermentation to propanoate I
lipid IVA biosynthesis
fatty acid elongation -- saturated
Kdo transfer to lipid IVA III (Chlamydia)
galactose degradation I (Leloir pathway)
CMP-3-deoxy-D-manno-octulosonate biosynthesis I
queuosine biosynthesis
peptidoglycan biosynthesis IV (Enterococcus faecium)
Bifidobacterium shunt
UDP-N-acetyl-D-glucosamine biosynthesis I
superpathway of N-acetylglucosamine, N-acetylmanno...
mixed acid fermentation
flavin biosynthesis I (bacteria and plants)
dTDP-L-rhamnose biosynthesis I
myo-, chiro- and scillo-inositol degradation
L-glutamate and L-glutamine biosynthesis
taxadiene biosynthesis (engineered)
L-histidine degradation I
urate biosynthesis/inosine 5'-phosphate degradation
sucrose degradation III (sucrose invertase)
guanosine nucleotides degradation III
6-hydroxymethyl-dihydropterin diphosphate biosynth...
L-arginine biosynthesis III (via N-acetyl-L-citrul...
purine nucleotides degradation II (aerobic)
L-rhamnose degradation I
L-arginine biosynthesis II (acetyl cycle)
superpathway of L-aspartate and L-asparagine biosy...
acetylene degradation
phosphatidylglycerol biosynthesis I (plastidic)
phosphatidylglycerol biosynthesis II (non-plastidic)
superpathway of pyrimidine deoxyribonucleosides de...
adenosine nucleotides degradation II
superpathway of pyrimidine ribonucleotides de novo...
superpathway of thiamin diphosphate biosynthesis I
inosine-5'-phosphate biosynthesis III
superpathway of menaquinol-8 biosynthesis II
phosphopantothenate biosynthesis I
heterolactic fermentation
aspartate superpathway
6-hydroxymethyl-dihydropterin diphosphate biosynth...
superpathway of purine deoxyribonucleosides degrad...
O-antigen building blocks biosynthesis (E. coli)
polyisoprenoid biosynthesis (E. coli)
superpathway of GDP-mannose-derived O-antigen buil...
1.06e-6
1.13e-6
2.15e-7
6.91e-7
2.62e-7
1.19e-5
2.85e-7
3.24e-7
3.07e-7
4.64e-7
2.54e-6
4.14e-6
7.33e-7
6.56e-7
3.01e-6
2.41e-5
1.18e-4
7.92e-7
4.62e-6
4.89e-6
1.07e-4
2.86e-7
2.01e-7
4.34e-6
3.75e-8
1.76e-5
3.94e-6
1.19e-4
1.09e-5
6.63e-8
9.94e-8
4.52e-6
7.55e-7
6.08e-4
4.64e-6
1.76e-4
6.58e-5
6.46e-7
4.42e-7
3.99e-6
4.22e-7
1.20e-5
6.59e-5
3.97e-6
1.46e-6
q-value (corrected)
0,0
1,1
Mean proportion (%)
−0,6
−0,4
−0,2
0,0
0,2
0,4
Difference in mean proportions (%)

(c)

Figure II.8. PICRUSt2 results indicating differential predicted functional pathways with 20% of the difference in the mean proportions between the bean-free and the bean-containing diet groups in the female cohort: bean-free diet (0%) is indicated in beige, while bean-based diet samples (**a**–17.5%; **b**–35%, and **c**–70%)—in green. Extended error bar plot indicating the mean proportion of pathways assigned to each group, difference between them, and corrected *p*-value (*q*-value) of each.

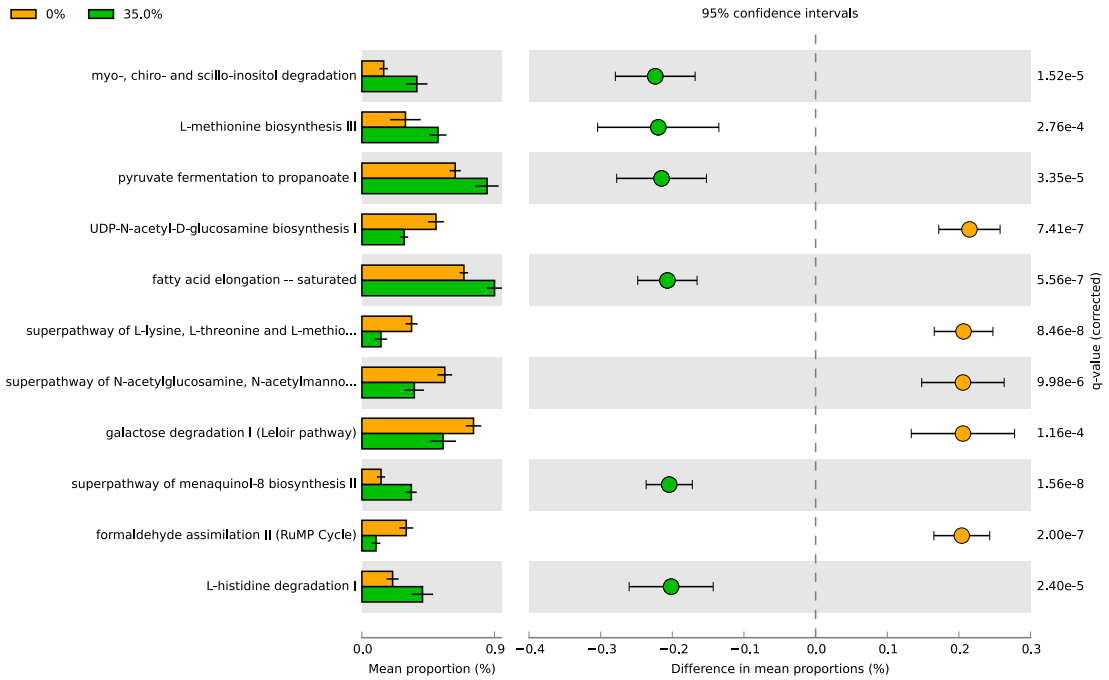

(a)


0%
70.0%
95% confidence intervals
myo-, chiro- and scillo-inositol degradation
pyruvate fermentation to propanoate I
L-rhamnose degradation I
L-histidine degradation I
formaldehyde assimilation II (RuMP Cycle)
peptidoglycan maturation (meso-diaminopimelate con...
superpathway of L-lysine, L-threonine and L-methio...
incomplete reductive TCA cycle
L-lysine biosynthesis II
fatty acid elongation -- saturated
L-methionine biosynthesis III
dTDP-L-rhamnose biosynthesis I
cis-vaccenate biosynthesis
superpathway of menaquinol-8 biosynthesis II
aspartate superpathway
inosine-5'-phosphate biosynthesis III
gondoate biosynthesis (anaerobic)
6-hydroxymethyl-dihydropterin diphosphate biosynth...
superpathway of L-phenylalanine biosynthesis
reductive TCA cycle I
superpathway of L-tyrosine biosynthesis
galactose degradation I (Leloir pathway)
6-hydroxymethyl-dihydropterin diphosphate biosynth...
superpathway of N-acetylglucosamine, N-acetylmanno...
1,4-dihydroxy-6-naphthoate biosynthesis II
queuosine biosynthesis
lipid IVA biosynthesis
flavin biosynthesis I (bacteria and plants)
S-adenosyl-L-methionine cycle I
UDP-N-acetyl-D-glucosamine biosynthesis I
Kdo transfer to lipid IVA III (Chlamydia)
Bifidobacterium shunt
1.24e-9
1.22e-8
2.30e-8
8.22e-9
5.77e-8
1.45e-6
8.02e-9
1.29e-6
1.94e-8
1.04e-9
9.93e-5
1.00e-8
2.78e-7
9.61e-11
7.62e-9
7.26e-9
7.21e-7
5.26e-7
1.72e-7
3.27e-6
1.68e-7
1.78e-4
1.50e-9
7.37e-6
3.72e-8
1.04e-7
1.75e-6
4.44e-8
4.51e-8
1.29e-6
1.26e-6
9.49e-9
q-value (corrected)
0.0
1.1
Mean proportion (%)
−0.4
−0.3
−0.2
−0.1
0.0
0.1
0.2
0.3
0.4
Difference in mean proportions (%)

(b)

Figure II.9. PICRUSt2 results indicating differential predicted functional pathways with 20% of the difference in the mean proportions between the bean-free and the bean-containing diet groups in the male cohort: bean-free diet (0%) is indicated in beige, while bean-based diet samples (**a**–35% and **b**–70%)—in green. Extended error bar plot indicating the mean proportion of pathways assigned to each group, difference between them, and corrected *p*-value (*q*-value) of each.

4. Discussion

The diets used in this study were formulated to maintain equivalent macronutrient content—i.e., the percent (weight/weight) of protein, carbohydrate, and fat across the four diet groups. What varied were the qualitative characteristics of the dietary carbohydrate and protein components and the content of bean-associated bioactive compounds. The bean-free diet provided macronutrients from highly refined sources, whereas the common bean diets contained their dose-respective fraction derived from the cooked bean powder. In addition, these diets containing the whole food cooked beans provided a high variety of dietary phytochemicals such as polyphenols among others, exerting additional effects. Diet formulations were adjusted according to the proximate analysis of the nutritional composition of the cooked bean [33, 77-79]. Considering that common bean is generally consumed as a whole food, even when used as a recipe ingredient, the diet formulations investigated mimicked the manner in which human populations consume common bean [33].

4.1. Bean Effects on the Overall Diversity of the Cecal Microbiota

The assessment of microbial diversity under bean consumption indicated that increasing bean dose reduced the variety of bacterial species within samples and that the reduction was more robust in females than in male mice. The decrease in species richness was not expected in the bean-fed groups given that a complex mixture of carbohydrate in common bean replaced refined carbohydrate sources. Thus, this observation may reflect

either the presence of bacteriostatic factors in the common bean powder and/or that the bacterial taxa induced by feeding bean suppressed the growth of a broad range of co-occurring taxa. The observed differences in sex-associated responses were also unexpected and merit further investigation.

PCoA of three distance matrices (Jaccard, weighted/unweighted UniFrac) showed gradual and statistically significant distancing of the bean-containing samples with each increasing dose away from the bean-free control group. Each diet group was also significantly different between males and females. Samples of the 17.5% bean group localized in a transitioning ellipse between bean-free and bean-based groups of higher doses. Consistent with our findings, recently reported data in humans indicate sex differences in the ratio of total human-associated bacteria, dominated by the colonic microbiota, to the total cell count of referenced humans: 1.3:1 in males and 2.2:1 in females [80]. In mice, sex-dependent as well as sex-by-diet-dependent changes in the gut microbiota composition have been reported and attributed predominantly to hormonal effects, especially that of testosterone [81, 82].

4.2. Biomarkers of the Bean-Induced Ecosystem

Consumption of common bean induced an increase in *Bacteroides (II), Clostridium (I),* Rikenellaceae (I), and RF39, as well as a reduction in counts of *Adlercreutzia, Allobaculum, B. pseudolongum, C. cocleatum,* Clostridiaceae (II), *Dehalobacterium, Dorea, Lactococcus, Oscillospira,* and *R. gnavus, Ruminococcus,* Ruminococceae (II) (**Figures II.S6** and **II.S7**). These effects, which were dose-dependent and observed in both sexes, parallel observations from studies in humans and are also consistent with other studies in mice. Obese humans were reported to exhibit lower abundances of Rikenellaceae [83-85], and so did mice [86-88]. In mice fed isocaloric yet different types of fiber-based diets, the Rikenellaceae were enhanced

under dietary cellulose, inulin, and pectin [89], i.e., either insoluble or soluble types of dietary fiber that are also included in the dietary formulations studied here. Unclassified order RF39 was also detected by LEfSe as enhanced by the bean diets. RF39 was deemed as one of the major gut lineages of the human gut that showed the potential to produce acetate and hydrogen but lacked the capacity for other numerous highly conserved metabolic pathways [90, 91].

Some dose-dependent biomarkers of the bean-induced changes in the cecal microbiota composition differed between male and female cohorts. The bean-induced changes in the female cohort were distinguished from those in the male one by representatives of Muribaculaceae and *Sutterella*, which were enhanced upon a 35% and higher bean doses (Figure S6a), as well as by the suppressed *A. muciniphila*, unclassified Clostridiales (I), Clostridiaceae (II), *Clostridium (II)*, *Enterococcus,* Mogibacteriaceae, Peptostreptococcaceae, Ruminococcaceae (I), *Streptococcus (I),* and *Turicibacter* (**Figure II.S7a**). When LEfSe was set to determine the sex-dependent biomarkers of each diet group, only Muribaculaceae were also statistically more abundant in females versus males, whereas abundances of *A. muciniphila, Sutterella,* Mogibacteriaceae, Peptostreptococcaceae, and Ruminococcaceae (I) were significantly higher in the male cohort (**Figure II.6**). Muribaculaceae are one of the dominant gut bacteria engaged in degradation of dietary carbohydrates and whose abundance is decreased by high-fat diet conditions [54, 92] and obesity resistance [93], yet increased upon bean consumption [94-96]. Research on *Sutterella* reported in the literature is equivocal in the context of dietary responses and health impacts. Several studies showed increased *Sutterella* in mice fed low-fat diets [97, 98], while others showed decreased abundance under similar conditions [98, 99]. Interestingly, in our previous report,

Muribaculaceae and *Sutterella* were also members of the pulse-enhanced eco-group, but in the male mice, including those fed 35% of bean [44]. The unclassified *Clostridium* mapped to two different species (marked I and II). In our experiments, bean dose-dependently enhanced *Clostridium (I)* but suppressed the abundance of *Clostridium (II)* (**Figures II.S6a** and **II.S7a**). Additionally, unclassified Clostridiales (I) were suppressed by bean consumption in the female mice's cecal microbiota starting at the 35% dose (**Figure II.S7a**), but were then enhanced in the male cohort upon a 70% dose of bean (**Figure II.S6b**). Clostridia, in general, are associated with various functions as commensal bacteria, ranging from their potential as probiotics to their role in a number of human diseases [100, 101].

On the other hand, the male cohort contrasted to the female cohort with the bean-enhanced *Coprococcus* and *Clostridiales (I)* (**Figure II.S6b**) as well as the suppressed *Parabacteroides, Lactobacillus (I), AF12, B. acidifaciens,* and *B. ovatus* (**Figure II.S7b**) in their bean-induced microbial ecosystem. *B. ovatus* counts were statistically higher in male compared with female mice, yet *Lactobacillus (I)* were more abundant in the female cohort. *Bacteroides spp.* are obligate anaerobes, found solely in the gastrointestinal tract of mammals, showing great plasticity and adaptability in their commensalism and mutualism [102]. They have received mixed associations with obesity [85, 103-105] but were shown to utilize and respond positively to dietary fiber, such as inulin and xyloglucan, by *B. acidifaciens* and *B. ovatus*, in particular [106-108]. *B. acidifaciens* has also been shown to decrease upon feeding of the insoluble high-fiber diet [109].

4.3. Potential Impact of the Bean Macronutrients

4.3.1. Protein

Diets with an increased intake of protein, such as the Paleolithic and ketogenic diets, have increased in popularity in recent years [110]. However, several studies have shown quantitatively different effects on the microbiota with consumption of animal versus plant proteins [111]. This study was controlled for total protein in the diet and, therefore, was designed to evaluate how the source of dietary protein affects the gut microbiota. The quality (biological value) of protein from plant sources is well-known to be lower than that from animal sources [112]. For pulses in general, and for common bean in particular, sulfur-containing amino acids and tryptophan are the first and second most limiting amino acids [113], and they were provided in the diet formulation. In addition, the digestibility of bean protein has been reported to be lower than many protein sources, presumably because of the presence of trypsin and chymotrypsin inhibitors. However, these antinutrient factors are eliminated when bean is soaked and cooked before eating [114, 115], which is how the bean was prepared in this study. PICRUSt2 analysis of the predicted microbial function herein demonstrated that bean consumption was not dominated by pathways associated with protein fermentation, aside from significant L-histidine degradation (I), nor branched short-chain fatty acid production. This finding is not surprising given that we have previously reported that mice and rats have the same growth efficiency when pair-fed the highest bean dose studied herein, suggesting similar utilization of dietary protein [46, 47]. Additionally, dietary fiber is known to reduce fermentation of protein in the gut of monogastric species [116, 117]. Thus, these findings fail to indicate that consuming up to 70% of dietary protein from common bean, when properly processed, would result in negative metabolic effects associated

with excessive protein fermentation in the gut [117, 118]. However, bean-containing diets were also distinguished by L-arginine biosynthesis (III) via *N*-acetyl-L-citrulline, whereas the bean-free group upregulated L-arginine biosynthesis (II) via acetyl cycle. The bean-free group was also distinguished with significant increases in superpathways of L-lysine, L-threonine, L-methionine biosynthesis (I), L-phenylalanine biosynthesis, L-tyrosine biosynthesis, aspartate superpathway, L-lysine biosynthesis (II), and S-adenosyl-L-methionine cycle (I), and this was more evident in male than female mice. This is consistent with the fact that common bean is rich in the levels of lysine, tyrosine, and phenylalanine [53,96,97]. Interestingly, despite the inclusion of methionine in their diet formulations, bean-based groups were still marked with L-methionine biosynthesis (III) pathway upregulation.

4.3.2. Carbohydrate

Early reports underestimated the total amount of dietary fiber in common bean and other pulses. However, the adoption of an internationally accepted consensus definition of dietary fiber and of a method for its measurement has revealed that the amount of dietary fiber and protein is similar on the basis of the percent of dry matter [119]. Moreover, we have reported how pulse consumption in both the U.S. and Canada has the potential to close the dietary fiber gap [120]. What this study did was to afford an opportunity to understand how a change in carbohydrate quality from refined to increasing amounts of whole food-derived carbohydrate, that is particularly rich in its fiber content, impacted commonly studied characteristics of the gut microbiota.

Common bean is a rich source of carbohydrates (60–70% of dry weight) [35]. Among these, the most prevalent prebiotic components are resistant starch, sugar alcohols (such as

mannitol, sorbitol, and xylitol), raffinose oligosaccharides (stachyose, raffinose, verbascose), fructose oligosaccharides (kestose and nystose), and long-chain oligosaccharides (inulin) [97,100,101]. The functional profile of the bean-induced ecosystem was, in part, characterized by an incomplete reductive TCA cycle and pyruvate fermentation to propanoate I. Propanoate, or propionate, is one of the main short-chain fatty acids produced by the gut microbial metabolism and is associated with hepatic gluconeogenesis and glucose metabolism, adipocyte leptin signaling and reduced fat accumulation, reduced inflammation via HDAC inhibition, and overall health-promoting properties [121-124].

A particularly interesting observation was that incorporation of bean into the diet reduces the abundance of Actinomycetota, predominantly represented by *Bifidobacterium pseudolongum.* A characteristic feature of these bacteria is the *Bifidobacterium* shunt that ferments glucose to lactate—also downregulated compared with the bean-free control group. *B. pseudolongum* showed a similar pattern of change together with other lactic acid-producing bacteria, such as *Lactobacillus*, *Lactococcus*, and *Streptococcus.* These bacteria, in particular, are associated with the galactose metabolism [125, 126], and we report a concomitant downregulation of the Leloir pathway of galactose degradation (I), homo- and heterolactic fermentation, and others. Interestingly, these bacteria can also metabolize partially hydrolyzed proteins, including casein [87, 126-128], producing bioactive peptides. In diets with increasing bean doses, casein proportionally declines, which might have contributed to reductions in the abundance of these bacteria. However, metabolizing dietary protein by the gut microbiota generally has a negative connotation [117, 129-131], and *Bifidobacterium*, *Lactobacillus*, *Lactococcus*, and *Streptococcus* can produce toxic compounds upon metabolizing proteins [94,110,113], including biogenic amines, ammonia, phenol/indoles, etc.

Considering our results, bean may protect the mice from fermentation of proteins due to its high content of dietary fiber [117].

4.3.3. Bioactives

Pulse bioactives, some of which have been referred to as antinutrients, may be involved in mediating effects on the gut microbiota [132]. For example, phenols are often poorly absorbed and thus reach the large intestine, where they interact directly with the gut microorganisms. Common bean has been reported to contain various phenolic acids (chlorogenic acid, gallic acid, p-hydroxybenzoic acid, caffeic acid, protocatechuic acid, p-coumaric acid, rosmarinic acid, ferulic acid, sinapic acid, and ellagic acid) and flavonoids (epicatechin, catechin, gallocatechin gallate, epigallocatechin gallate, quercetin, hesperidin, and rutin), as well as various polyphenols [77]. These compounds may simultaneously induce duplibiotic effects, i.e., antimicrobial and prebiotic activities [133]. This could explain the relandscaping of gut bacterial composition that we observed upon increasing the dietary bean dose: fewer taxa were enhanced than suppressed. Metabolomic and metametabolomic studies are needed to further elucidate the role that these low molecular compounds and their microbiota-generated derivatives play in accounting for bean-induced effects on the gut microbial composition.

5. Summary and Implications

This is a deep, comprehensive analysis of the sex- as well as dose-dependent differences in the cecal bacteria composition of mice upon consumption of cooked whole-food bean in the diet when overall macronutrient content was held constant across

the treatment groups. Identified eco-groups provide insight into the generalized effects of bean consumption as a whole food on the gut microbiota.

The impact of biological sex on the composition of the bacterial ecosystem that persisted despite an increase in the amount of bean consumed has not been, to our knowledge, reported previously. Our data suggest that females will be more responsive to bean consumption than males at any dose consumed. Given that there are many noted weaknesses in the clinical and population studies of the consumption of common bean and other pulse crops on disease risk, the recognition of potential biological sex differences to pulse consumption in both study design and data analysis has the potential to improve the sensitivity and statistical power of studies in humans. Investigation of the origins of the biological sex differences may also provide insights about common bean-gut microbiota-host interactions important to developing precision approaches to chronic disease prevention and control.

This investigation also has implications for the dose of common bean and other pulses that is required to improve health and well-being as well as mitigate disease risks. Current recommendations appear to be based less on scientific evidence and more on what it is presumed that consumers will eat [21]. The science reported herein indicates the potential value of levels of consumption typical of high pulse consumers identified in both NHANES and its Canadian equivalent [43, 134]. Moreover, even higher levels of consumption may hold benefits if mediation is via the gut microbiota. Clearly, more work on target levels of consumption is required, and this must include well-designed and controlled clinical investigations.

Using mice as a preclinical animal model to study the effects of diet on gut microbial composition has both strengths and limitations [31,32,117,118]. This work differs from other reports in that animals were received from the same vendor and housed in the same animal room so that reported differences that can arise from vendor, shipment, and animal husbandry practices were minimized. Consequently, the likelihood that all mice had similar species richness within the gut at the beginning of feeding of the test diet formulations was maximized. We acknowledge that the composition of these eco-groups may change among studies, but, in our judgment, this type of assessment redirects focus towards collective changes in the microbial groups rather than the solitary differences in each. Clearly, the next step in advancing understanding of the diet-microbiota-host paradigm requires extension of the research approach beyond the question of defining "who's home" to determining what the microbial ecosystem is doing and where within the gut the microbiota are exerting effects via yet-to-be-identified chemical mediators that impact the host.

CHAPTER III. Thwarting Metabolic Dysfunction-Associated Fatty Liver Disease (MAFLD) with Common Bean[2]

1. Introduction

The 21st century is distinguished by globalization of sedentary lifestyle (owing to mechanization, automation, and computerization of labor), dietary patterns (especially the unbalanced Western-type), and the consequential upsurge in the burden of non-communicable diseases (such as obesity, type II diabetes mellitus, cardiovascular diseases, and cancer) which account for more than 70% of deaths per annum globally [11, 13, 14]. Despite their multifactorial etiology, disrupting the organism's metabolic homeostasis is fundamental to their pathogenesis [11, 12]. The liver plays a central role in regulating whole-body metabolism in mammals, and the diet-induced chronic liver disorder is referred to as metabolic dysfunction-associated fatty liver disease, or MAFLD—formerly known in the biomedical literature as "non-alcoholic fatty liver disease" (NAFLD). In 2020, an international group of experts from 22 countries reached a consensus to adopt the new terminology—MAFLD—thereby emphasizing dysregulation of metabolism as the leading pathophysiological mechanism of the disease [9, 135, 136]. This terminology will be used henceforth.

As it progresses, MAFLD encompasses a broad continuum of chronic and heterogeneous liver comorbidities. Phenotypically, hepatic steatosis [137]—the abnormal intrahepatic retention of lipids in the cytoplasm of hepatocytes—is observed. Approximately

[2] The content of this chapter is based on our research article published in an open-access journal *Foods* from MDPI. References to tables, figures, and supplementary materials have "III" appended to them. Citation information is as follows: *Lutsiv, T., McGinley, J.N., Neil, E.S., Foster, M.T. and Thompson, H.J., 2023. Thwarting metabolic dysfunction-associated fatty liver disease (MAFLD) with common bean: Dose-and sex-dependent protection against hepatic steatosis. Nutrients, 15(3), p.526.*

1 in 5 individuals with hepatic steatosis progress to ectopic lipid deposition with concurrent hepatocyte damage, inflammation, and early-stage fibrosis, which signifies metabolic dysfunction-associated steatohepatitis (MASH) [10]. In turn, 20–25% of people with MASH within ten years develop advanced fibrosis with severely impaired liver function termed cirrhosis, the end-stage liver disease, markedly increasing the probability of hepatocellular carcinoma (HCC) development [9, 10]. By 2030, MAFLD-induced HCC will be the leading reason for liver transplantation, exceeding hepatitis C [138, 139]. Today, the overall prevalence of MAFLD worldwide is 32.4% (with a 95% confidence interval of [29.9%, 34.9%]) [140]. Around 70–90% of overweight or obese individuals as well as people with type II diabetes also suffer from MAFLD and exhibit dyslipidemia, lipotoxicity, insulin resistance, and hypertension as features of MAFLD [137, 141]. Therefore, to tackle such a complex systemic challenge such as MAFLD, there is an urgent need for effective preventative strategies, such as adopting food patterns to improve whole-body health status.

Pulses are dry seeds of grain legumes unique in their content of small molecules, dietary fiber, and protein and their negligible content of lipids [32]. Owing to their profile of nutrients and bioactive compounds, pulses can be termed *superfoods*. However, their regular consumption has practically disappeared from the dietary patterns of developed countries and beyond—a change that has occurred concomitantly with the global increase in chronic disease burden. As discussed in [31], incorporating pulses into the diet can improve the quality of food patterns, and population data have reported reduced occurrences of diseases associated with metabolic dysfunction in high pulse consumers [34, 37, 39]. These reports are consistent with our findings that pulse consumption has an anti-obesogenic activity in rodent models of polygenic and dietary-induced obesity, including effects on liver

lipid metabolism [44-49]. However, the minimal pulse dose required to elicit discernible effects on the hepatic phenotype, the impact of biological sex, and underlying molecular mechanisms have not been extensively elucidated.

Therefore, we focused on the most consumed type of pulse—common bean, *Phaseolus vulgaris* L., to assess its effects on the development of high fat diet induced MAFLD. The objectives of this study were: (1) to quantify hepatic lipid content and determine the liver histopathological response to increasing dose of dietary bean consumption; (2) to characterize the impact of the biological sex on the bean-induced outcomes; and (3) to analyze the liver transcriptomic signature to deduce candidate molecular mechanisms underlying observed bean-induced phenotypes.

2. Materials and Methods

2.1. Animal Feeding Study

C57BL6/J female and male mice (stock #000664) were obtained from the Jackson Laboratory (Barr Harbor, ME, USA) at twenty days of age. Standard husbandry conditions were applied: polycarbonate rodent cages with a solid bottom, *ad libitum* access to distilled water and food, a 12-h light/dark cycle, 27.5 ± 2°C room temperature. Adaptation to the housing routine and a purified diet containing 32.5% kcal fat based on the formulation D12266B (Research Diets Inc., New Brunswick, NJ, USA), as described in [46], continued until eight weeks of age, after which 20 animals were assigned by staggered randomization by body weight to each experimental diet group and fed their respective experimental diet formulations for 12–14 weeks (see Section 2.2). Animals were euthanized by cervical dislocation following isoflurane-induced anesthesia. Liver was excised, snap-frozen in liquid

nitrogen, and samples stored at -70°C until evaluated. All the procedures performed on animals complied with the Colorado State University Institutional Animal Care and Use Committee guidelines (protocol KP 1431).

2.2. Diet Formulations

Experimental diets were formulated so as to remain equal in total dietary energy content enabling evaluation of the direct effects from the bean. All diets were composed of equal macronutrient proportions weight by weight, i.e., 58.6% total carbohydrate, 15.5% total fat, 20% total protein, and 5.9% micronutrients, according to the AIN-93G recommendations. Mice received 32.5% kcal derived from fat, which is within the range for both total lipid dietary practice in humans [22] and simultaneously for obesogenic studies using the C57BL6/J animal model [57]. Diet containing 11% dietary fat energy was used as a low-fat and bean-free control. All diets were comprised of purified ingredients, with the exception of bean. White kidney beans were cooked as a whole food, processed with leachate, freeze-dried, and then homogenized into a fine powder. Bean doses were calculated as 0% (bean-free control), 17.5%, 35%, and 70% of total dietary protein derived from bean. Total dietary fiber concentration of bean was 23.5 g/100 g bean powder [142]. The formulation of the experimental diets is shown in **Supplemental Table III.S1**.

2.3. Histopathology

A small portion of frozen liver from each animal (n = 2 per group) was embedded in Tissue-Tek OCT compound (Sakura Finetek, Torrance, CA, USA) on a cryostat chuck and quickly frozen in the cryostat (Leica Biosystems, Deer Park, IL, USA) using a heat sink. Frozen sections of liver were cut at 10 μm, mounted on Histobond slides (Statlab Medical

Products, McKinney, TX, USA), placed in pre-cooled plastic slide boxes, and stored at -70°C until ready for staining.

2.3.1. Fixation

Frozen section slides were removed from the -70°C freezer, one stain set at a time, placed in a vertical slide rack and allowed to thaw at room temperature for 5 min prior to immersion in fixative, 10% neutral buffered formalin for 5 min.

2.3.2. Hematoxylin and Eosin (H&E) Staining

Formalin-fixed slides were rinsed in deionized water, stained with Harris hematoxylin for 2 min, rinsed in deionized water, and counterstained in eosin Y for 1 min. Slides were dehydrated in a series of graded ethanols, starting with two changes of 95% ethanol, two changes of 100% ethanol, and one change of isopropanol, then cleared in four changes of xylene before mounting with MM24 mounting media (Leica Biosystems, Deer Park, IL, USA) and glass coverslips.

2.3.3. Trichrome Staining

Formalin-fixed slides were rinsed in deionized water and stained using the Gomori one-step aniline blue trichrome stain kit (Newcomer Supply, Middleton, WI, USA). Briefly, slides were immersed in Bouin's solution and incubated at 60°C for 1 h. Slides were allowed to cool to room temperature for 10 min, rinsed well in running tap water, and rinsed in deionized water. Slides were immersed in freshly prepared Weigert's iron hematoxylin for 10 min, washed in running tap water, and rinsed in deionized water. Slides were immersed in the Gomori one-step aniline blue trichrome solution for 20 min followed by differentiation

in 0.5% acetic acid for 2 min and quickly rinsed in deionized water before dehydration, clearing, and mounting, as listed above.

2.3.4. Oil Red O (ORO) Staining

Formalin-fixed slides were rinsed in deionized water. Excess water was blotted from each slide prior to being immersed in 100% propylene glycol on a shaker with gentle, continuous agitation for 5 min. Slides were transferred directly to Oil Red O propylene glycol solution (Newcomer Supply, Middleton, WI, USA) and stained with gentle, continuous agitation for 1 h. Slides were differentiated in 85% propylene glycol with gentle, continuous agitation for 3 min followed by gentle rinsing in two changes of deionized water. Slides were counterstained in hematoxylin for 2 min, gently washed in tap water, blued in Scott's tap water for 1 min, gently rinsed in two changes of deionized water, and mounted with Gel/Mount aqueous mounting media (Biomeda, San Jose, CA, USA) and a glass coverslip. Edges of the glass coverslip were sealed with clear fingernail polish to prevent evaporation of the aqueous mounting media.

2.4. Quantification of Liver Lipid Content

Lipid was isolated from the dried liver samples (n = 10 per group) using a methyl tert-butyl ether (MTBE) biphasic extraction method [143]. Weights collected throughout sample processing (fresh tissue, desiccation, extraction, lipid isolation, and dry matter) were used to quantify lipid content expressed as mg of lipid per mg of dry liver weight.

2.5. RNA Isolation and RNA-Seq Analysis

Frozen liver samples (n = 10 per group) were ground to a fine powder using ceramic pestles in ceramic mortars filled with liquid nitrogen. RNA samples were extracted using

the RNeasy mini-kit (QIAGEN, Inc., Germantown, MD, USA) according to the manufacturer protocol. RNA integrity was determined with Experion automated electrophoresis station (Bio-Rad Laboratories, Inc., Hercules, CA, USA). Samples were diluted to a concentration of 4 ng/μL in the 50 μL of RNase-free water and under dry ice shipped to the Genomics and Microarray Core at the University of Colorado Anschutz Medical Center (Aurora, CO, USA) for the cDNA library construction and preparation using Nugen Universal mRNA kit (Tecan Genomics, Inc., Redwood City, CA, USA) and subsequent paired-end (2 × 150 bp) RNA sequencing (RNA-Seq hereafter) using a NovaSEQ 6000 sequencer (Illumina, Inc., San Diego, CA, USA). The sequencing data were further processed using QIAGEN CLC Genomics Workbench, version 21.0.3 (QIAGEN, Redwood City, CA, USA), https://digitalinsights.qiagen.com (accessed on April 24th, 2021). Raw reads were trimmed using quality scores (quality limit = 0.05) for removal of ambiguous nucleotides and read-through adapters. The resulting high-quality reads were mapped to *Mus musculus* genome reference, version GRCm38, using gene ontology associations to generate transcript-level expression tracks. The transcript expression data containing 66,624 genes were subjected to the differential abundance analysis (see Section 2.6) producing output datasets of pairwise comparison pairs (35% vs. 0%, 70% vs. 0%, and 70% vs. 35% bean diet groups). Differentially expressed genes (DEGs), their *p*-values, *p*-values corrected for multiple comparisons using Bonferroni method and Benjamini–Hochberg procedure controlling the false discovery rate (FDR; *q*-values), expression fold change, expression $\log_2$ ratios, and the values for the maximum of the two average reads per kilobase million (RPKMs) per diet group in a comparison pair comprised each comparison table. DEGs containing at least 10 RPKMs for each comparison pair were uploaded to

QIAGEN Ingenuity Pathway Analysis (IPA) software, v81348237 (QIAGEN, Redwood City, CA, USA), https://digitalinsights.qiagen.com/IPA (accessed on July 13th, 2022) [144], for further analysis.

Within IPA, each comparison dataset was subjected to the Core Analysis with Ingenuity Knowledge Base (Genes only) as a reference set and relaxed integral filters for species, tissues, and cell lines. Expression $\log_2$ ratio was selected as a measurement to calculate directionality in the analysis. To maximize the biological interpretation, the list of DEGs was further quality-filtered by the *p*-value < 0.05 to keep each comparison pair dataset within recommended by IPA limits (**Table III.1; Supplemental Table III.S2**). IPA mapped DEGs to identifiers (IDs); 9 IDs in each group were unmapped and discarded. Identifiers that mapped to the same molecule were resolved to one data measurement by the expression *p*-value.

Table III.1. IPA analysis-ready identifiers mapped to DEGs within each comparison group pair.

Group	**35% vs. 0% Bean**	**70% vs. 0% Bean**	**70% vs. 35% Bean**
Cohort	***DEGs*** [1]	***DEGs*** [1]	***DEGs*** [1]
	Pre-filtered Mapped IDs [2]		
Females	3547	3579	3541
Males	3539	3539	3497
	Core Analysis-ready IDs [3]		
Females	461	966	389
Males	394	1130	535
TOTAL DEGs [4]		*66,624*	

[1] Differentially expressed genes; [2] All mapped to DEGs and duplicate-resolved identifiers; [3] Filtered by *p*-value < 0.05. [4] Total amount of observed DEGs from CLC Genomics Workbench output dataset.

Canonical Pathways, Upstream Analysis, and Diseases and Functions engines were used to analyze DEGs. Briefly, expression patterns of the DEGs were cross-referenced with the published studies worldwide from the QIAGEN Ingenuity Knowledge Base, and *p*-values of overlap between the observed DEGs patterns and their associations were calculated. Activation *z*-scores measuring the prediction strength of the DEGs effects (activation or inhibition) were calculated based on direction of DEGs expression changes. Mapped functional associates were deemed significant with the $|z|$-score ≥ 2 and the *p*-value < 0.05 of the overlap (B-H *p*-value < 0.1) between our experimentally observed dataset and the QIAGEN Ingenuity Knowledge Base.

2.6. Statistical Evaluation

Hepatic lipid quantification data (expressed as milligrams per dry liver tissue weight) were analyzed and visualized in *R* (v4.2.2) using *FSA*, *rstatix*, and *gpubr* packages.

Statistical differential expression analysis of RNA-Seq data in CLC Genomics Workbench was conducted through the Differential Expression for RNA-Seq tool via generalized linear modeling for each gene assuming the negative binomial distribution of read counts and subsequent Wald testing for all group pairs to generate the expression track tables. In IPA, *p*-values of overlap were calculated using a right-tailed Fisher's exact test and further adjustment for multiple hypothesis testing applying Benjamini–Hochberg correction method (B-H *p*-values). At times, *p*-values were reported in their negative logarithmic format ($-\log_{p\text{-value}}$; $-\log_{\text{B-}}$ as provided by IPA. *z*-scores were calculated using internal IPA algorithms.

Selected DEGs were visualized in *R* in counts per million (CPMs) normalized for the library sizes with the trimmed mean of M values (TMM) method using *ggpubr* package.

3. Results

3.1. Livers Accumulate Less Lipid upon Increasing Consumption of Bean

MAFLD onset is grossly identified by excessive accumulation of lipid in the liver. Consumption of bean markedly reduced the lipid content per g liver dry weight in both females and males (**Figure III.1**). Regression analysis indicated that the reduction was linear across increasing bean doses in both sexes (regression coefficient, -35.3, $p < 0.001$ and -90.3, $p < 0.001$ in female and male mice, respectively). Pairwise comparisons revealed that females exhibit less hepatic lipid at the 35% dose without any statistical distinction with the higher bean dose, whereas males had a significant effect only in the 70% group which statistically differed from both 0% and 35% bean doses (**Figure III.1a**). The 70% bean dose nullified sex-dependent differences in hepatic lipid levels (**Figure III.1b**).

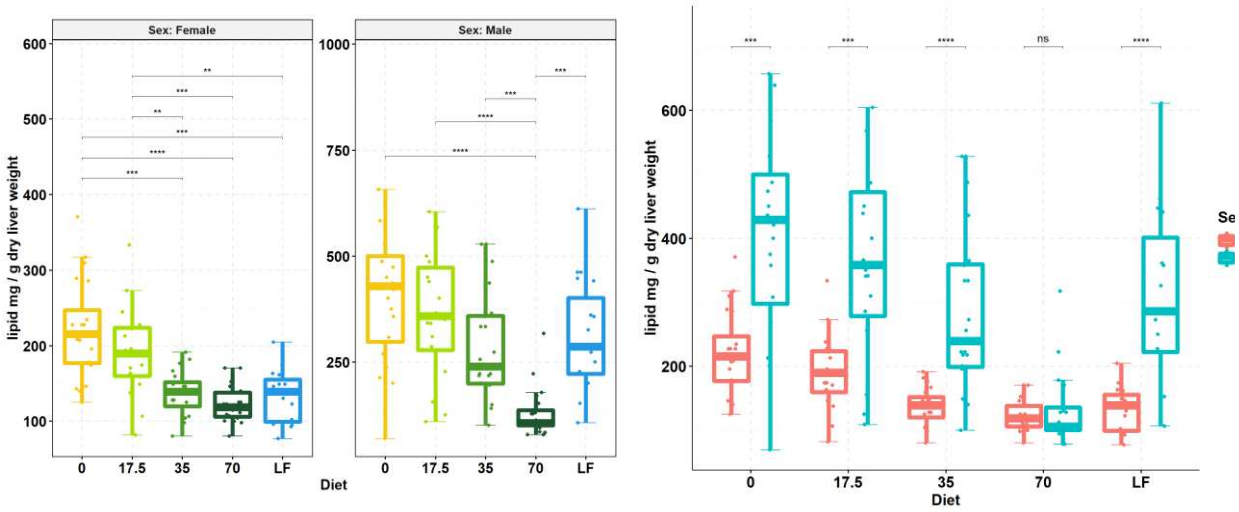

(**a**) (**b**)

Figure III.1. Effect of dietary bean on the liver lipid content. Box plots report amount of hepatic lipid (in mg) normalized to g of dry liver weight across the diet groups and sex cohorts. Diets are indicated by the percent (%) of dietary protein provided by bean, including a low-fat (LF) diet as a negative control. Kruskal–Wallis testing showed significant differences by the diet effect ($\chi^2 = 41.598$, p-value = 2.021e-08 in the female cohort; $\chi^2 = 40.15$, p-value = 4.029×10^{-8} in the male cohort). (**a**) Pairwise comparisons between the diet group were conducted using the post-hoc Dunn test; (**b**) Pairwise comparison between sex cohorts were tested with the Mann-Whitney *U* test. The Benjamini–Hochberg method was used for

the multiple testing correction of *p*-values. * *p*-value < 0.05; ** *p*-value < 0.01; *** *p*-value < 0.001; **** *p*-value < 0.0001.

3.2. Dietary Bean Visually Reduces Steatosis Severity in the Liver Tissue

To determine the phenotypic liver response to consumption of increasing doses of bean, frozen sections of liver were stained for histological evaluation. The H&E-stained sections (**Figure III.2**) showed that livers from male and female 0% bean-fed mice displayed the classic features of hepatic steatosis, i.e., extensive accumulation of lipid droplets, heterogenous in size and shape, in the cytoplasm and the consequential ballooning [137]. However, only focal areas of lymphocyte accumulation were detected, and no evidence of fibrosis was observed. These changes were not observed in mice fed the 70% bean diet, and lipid accumulation was similar to that observed in the low-fat-fed group of mice. To confirm these effects, sections were subjected to ORO staining (**Figure III.3**) and to trichome staining. The ORO staining confirms the results of the H&E stain relative to lipid accumulation. The trichrome stain (data not shown) confirmed the lack of collagen accumulation in any of the animals evaluated.

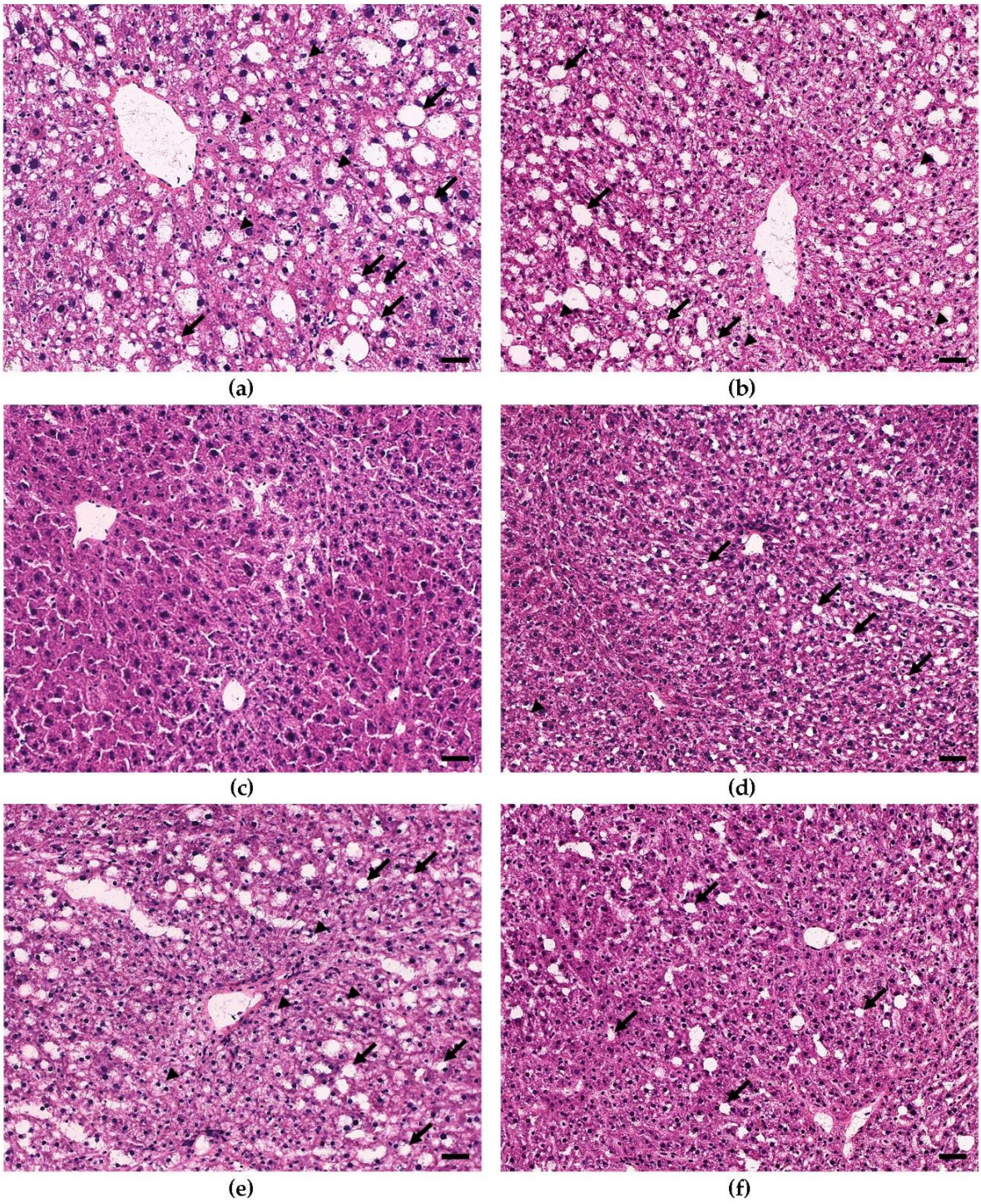

Figure III.2. Comparison of lipid accumulation in male and female H&E-stained liver sections across different diets. (**a**) Male 0%; (**b**) Female 0% bean; (**c**) Male 70% bean; (**d**) Female 70% bean; (**e**) Male low fat; (**f**) Female low fat. Steatosis (arrows); hepatocyte ballooning (arrowheads); magnification 200×; bars = 40 μm.

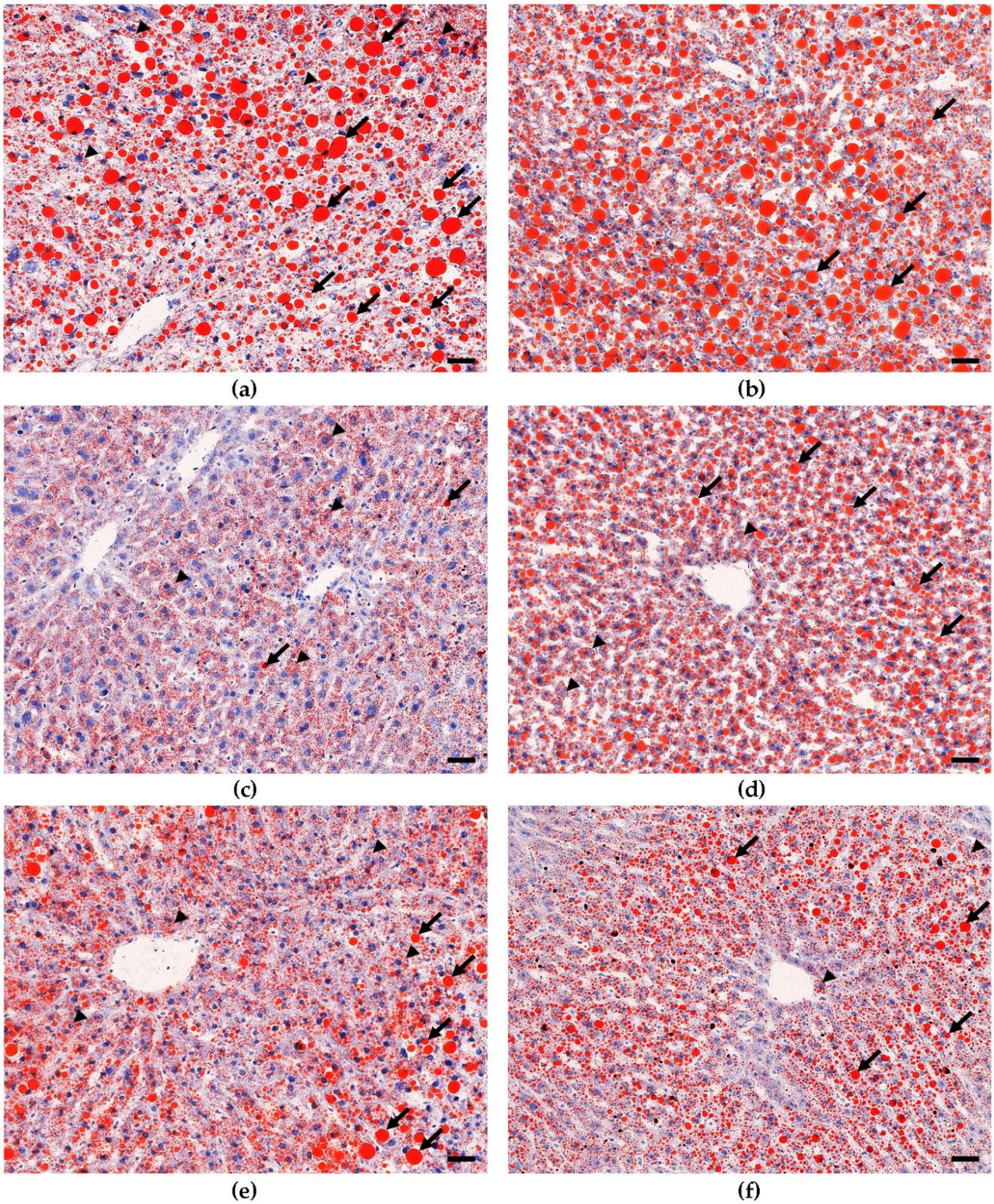

Figure III.3. Comparison of lipid accumulation in male and female Oil Red O-stained liver sections across different diets. (**a**) Male 0%; (**b**) Female 0% bean; (**c**) Male 70% bean; (**d**) Female 70% bean; (**e**) Male low fat; (**f**) Female low fat. Extracellular lipid (arrows); intracellular lipid (arrowheads); magnification 200×; bars = 40 μm.

3.3. Liver Transcriptomic Signature upon Consumption of Bean Indicates Protection from Hepatotoxicity

To infer the underlying molecular mechanisms that may explain the effects on liver lipid content and histology (**Figures III.1–3**), total RNA was isolated from liver samples and subjected to the RNA-Seq. Only 0%, 35%, and 70% bean-containing diet groups were selected as the most prominently responsive to dietary beans. The Tox Functions engine within the IPA Core Analysis was used to provide an overview of the toxicity endpoints associated with the bean-induced liver within the Hepatotoxicity category as a focus. Accordingly, bean-induced DEGs patterns revealed significant suppression of hepatic steatosis, inflammation, and necrosis, and upregulation of bile acid secretion in both female and male mice (**Figure III.4a**). Suppression of hepatic steatosis was significant in the 70% compared to both the 0% (z-score = -2.549) and the 35% (z-score = -2.195) bean groups in females (**Figure III.4b**). In contrast, the bean-stimulated expression patterns in the male cohort did not reach statistically significant z-score values but the trend was similar to the females (**Supplementary Table III.S3**).

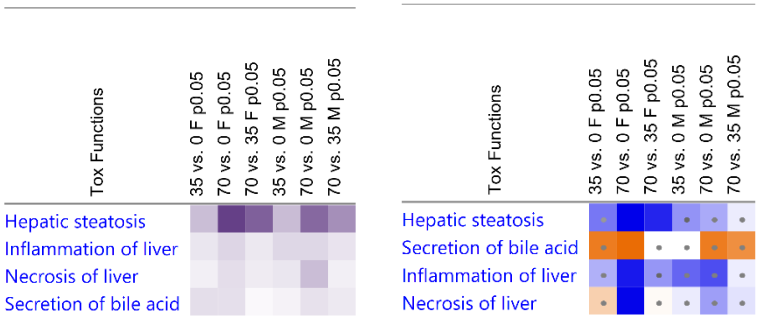

(a) **(b)**

Figure III.4. Heatmap of the Hepatotoxicity Functions based on the differentially expressed gene patterns in the liver tissue samples of female (F) and male (M) mice. Functions were organized by the collective score values. Pairwise comparisons are indicated in the column headers with first three from the left for the females and the other three columns for the males. Significant functions were filtered by B-H p-values < 0.1 and $|z|$-scores > 2, (**a**) shades of

purple indicate -$\log_{B\text{-}}$; (**b**) blue shades indicates inhibition, orange—activation, for 70% diet group in at least one sex cohort. Dots denote insignificant $|z|$-scores < 2.

Collectively, hepatotoxicity analysis of global bean-induced liver transcriptomes indicates that consumption of bean altered expression of hepatic genes predominantly related to the lipid metabolism, and it was more pronounced in female than male mice—an observation consistent with hepatic lipid content in the bean-fed animals (**Figure III.1**) and the histopathologic changes shown in Figures 2 and 3. Therefore, we next focused on the key mechanisms regulating hepatic FA metabolism involving the observed bean-induced DEGs.

3.4. Bean Consumption Maps to Hepatic Fatty Acid Metabolic Pathways and Regulators

Hepatic fat is stored as lipid droplets which consist predominantly of triacylglycerols (TAGs) formed by esterification of free fatty acids (FAs) with glycerol [145]. Considering the central role of FAs to MAFLD progression [146, 147], we performed IPA Canonical Pathways analysis with a particular focus on metabolic signaling associated with FAs. Consumption of beans significantly upregulated TAG degradation and downregulated TAG biosynthesis (**Figure III.5a**). The FA β-oxidation was upregulated in the 70% dose compared to the 0% and 35% bean groups in females, albeit the FA activation and the mitochondrial L-carnitine shuttle pathway had significant overlaps with the observed DEGs in both cohorts but insufficient *z*-scores to infer their activation (**Figure III.5a; Supplementary Table III.S3**). Similarly, β-oxidation of unsaturated/odd-number FAs and the FA α-oxidation also displayed only significant overlap with bean-induced DEGs (**Figure III.5a; Supplementary Table III.S3**). Finally, biosynthetic pathways of long-chain FAs conjugates oleate, stearate, and γ-linoleate indicated a pattern of inhibition, which corresponds to suppression of lipogenesis upon consumption of beans for both sex cohorts (**Figure III.5a**).

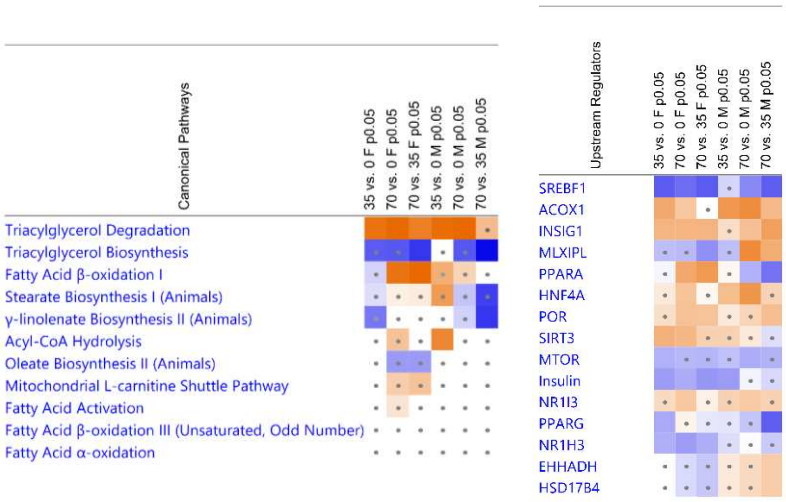

(**a**) (**b**)

Figure III.5. Canonical pathways and upstream regulators associated with fatty acid metabolism in liver upon consumption of common bean. (**a**) Canonical pathways; (**b**) upstream regulators. Pairwise diet comparison groups are indicated in the columns. Heatmap colors and their intensity indicate activity status according to the *z*-score values direction: orange signifies activation and blue—inhibition. Dots denote insignificant $|z|$-scores < 2. Indicated pathways had a significant *p*-values of overlap < 0.05 (B-H *p*-values < 0.1) and are organized by the collectively largest absolute *z*-score values across the comparisons.

To identify the most significant potential regulators of bean effects in the context of lipid metabolism, we subjected the observed DEGs to the Upstream Analysis in IPA. The sterol regulatory element-binding transcription factor 1 (SREBF1; also known as sterol regulatory element-binding protein 1c, SREBP1c) and MLX-interacting protein-like (MLXIPL; also known as the carbohydrate regulatory element-binding protein, ChREBP) are the key transcriptional regulators of *de novo* lipogenesis in liver. SREBP1 was predicted to be inhibited in all but the lowest bean dose groups. MLXIPL showed a trend of inhibition in the female cohort; however, in males, was upregulated in the 70% versus 0% and 35% bean diets (**Figure III.5b**). While SREBF1 is stimulated by insulin (even under conditions of insulin resistance) via mammalian target of rapamycin (mTOR) and by liver X receptor α (LXRα, encoded by *Nr1h3*), MLXIPL signaling is induced by dietary glucose (even more potently by dietary fructose) independently of insulin or dietary fat [148-150]. Accordingly,

we observed inhibition of insulin and its receptor INSR and insulin receptor substrate 1 (IRS-1) based on bean-induced downstream DEGs indicative of improved insulin sensitivity. To support the trend, mTOR complex 2 partner and regulator RICTOR (rapamycin-insensitive companion of mTOR) displayed inhibition, whereas negative regulators of mTOR complex 1, tuberous sclerosis proteins TSC1/2, were upregulated (**Supplementary Table III.S4**). SREBF cleavage-activating protein (SCAP) promoting SREBF1 activity is counteracted by insulin-induced genes INSIG-1/2—also in accordance with our data (**Figure III.5b**). LXRα belongs to the nuclear receptors [151], and bean-induced DEGs predict its inhibition, consistent with upregulation of nuclear receptor co-repressor N-Cor (**Figure III.5b**), which also suppresses their target genes [152]. Another nuclear receptor group, peroxisome proliferator-activated receptors (PPARs) are involved in regulation of majority of genes involved in lipid metabolism as nutrient sensors activated by FA derivatives [149, 151]. Hepatic PPARα (*Ppara*) stimulates expression of genes associated with mitochondrial and peroxisomal FA β-oxidation, whereas PPARγ (*Pparg*) is associated adipose tissue and lipid droplet regulation but shows strong responsiveness to MAFLD in liver. Bean suppressed PPARγ, but PPARα was predicted to be upregulated in females yet downregulated in males based on their downstream DEGs. Progression of MAFLD to MASH involved regulatory network of upregulated SREBF1, PPARγ, and disrupted activity of hepatocyte nuclear factors HFN1A, HFN4A, and ONECUT1 [153, 154], which were predicted to be upregulated upon bean consumption (**Figure III.5b, Supplementary Table III.S4**). Finally, sirtuin 3 (SIRT3) improves metabolic dysfunction, and its activation has been associated with beneficial caloric restriction and exercise [148]; however, here, an

isocaloric diet containing even 35% protein deriving from bean was sufficient to arrange DEGs patterns predicting activation of SIRT3 in females (**Figure III.5b**).

Taken together, dietary bean dose-dependently affects key regulatory nodes of TAG metabolism associated with MAFLD, and such effects differ between females and males.

3.5. Consumption of Beans Reduces Uptake and de novo Lipogenesis of Free Fatty Acids and Differentially Affects Transport, Oxidation, and Incorporation into Lipid Droplets

TAGs serve as both the source and preferred anabolic end-point of intracellular FAs [145, 149]. Corresponding to Canonical Pathways analysis results in **Figure III.5a**, dietary bean increased expression of TAG hydrolases, such as hepatic lipase C (*Lipc*) and several carboxylesterases *Ces1d*, *Ces2a*, *Ces2e*, *Ces3a*, *Notum*, etc., which signify greater capacity for lipolysis in the liver in female and male livers. Upstream analysis indicated that males' DEGs predicted activation of hormone-sensitive lipase (*Lipe*) and monoacylglycerol lipase (*Mgll*), despite observed reduced expression of *Mgll* and *Pnpla2*—lipolysis-initiating lipase which was slightly expressed more in females fed beans, instead (**Figure III.5b; Supplementary Figure III.S1**). TAGs can also undergo lipophagy via formation of autolysosomes [149, 155]. While both cohorts had reduced expression of lysosomal acid lipase A (*Lipa*), females also increased expression of microtubule-associated protein 1 light chain 3 (LC3; encoded by *Map1lc3a;* **Supplementary Figure III.S1**), one of the markers of lipophagy (autophagic degradation of lipid droplets) in liver [155-158]. Nevertheless, bean-induced DEGs showed inhibition of upstream transcription factor EB (TFEB; **Figure III.5b**), which regulates lipophagy and drives expression of LIPA, serving as another piece of evidence that lipophagy is hardly mediating dietary bean effects [157, 159]. Finally, bean-fed females increased expression of LDLR-related protein 1 (*Lrp1*) and apolipoprotein E (ApoE), which are

involved in uptake of dietary TAG-rich chylomicron remnants and improved MAFLD (**Figure III.6; Supplementary Figure III.S1** and **Table III.S4**) [160].

Lipolysis leads to intracellular FA flux, which in MAFLD patients is predominantly driven by uptake of free non-esterified FAs [161]. Consuming increasing doses of beans reduced expression of the plasma membrane FA-binding protein (FABPpm, encoded by *Fabp2*) and FA translocase/cluster of differentiation 36 (CD36)—higher levels of which are a biomarker of high-fat diet-induced hepatic steatosis [149] and whose reduction had a larger magnitude in males than in females (**Figure III.6**). Expression of *Cd36* is regulated by PPARγ, aryl hydrocarbon receptor (AHR), LXRα, mTOR [149, 162], and even SREBF1 and MLXIPL [149, 163], all of which were affected by dietary bean based on their downstream DEGs (**Figure III.5b; Supplementary Table III.S6**). Females also slightly increased expression of the very long-chain FA transport proteins 2 and 5 (FATP2/5, also known as very long-chain acyl-CoA synthetases and solute carrier family 27A members 2/5, encoded by *Slc27a2/5*), despite significant downregulation of SLC27A2 in upstream analysis (**Figures III.5b–6**). However, *Slc27a5*, which was the only upregulated FATP in males, has been reported to be rather associated with the conjugation of bile acids than FAs uptake (**Supplementary Figure III.S2** and **Table III.S4**) [164].

Once inside the cells, FAs are transported by cytosolic FA-binding proteins (FABPs), acyl-CoA-binding domain-containing proteins (ACBDs), and others [149]. Males exhibited reduced expression of *Fabp4/5* and *Acbd4*, whereas females decreased expression of *Fabp5* and *Acbd5* with a slight increase in *Fabp1* levels (**Supplementary Figure III.S2** and **Table III.S4**). While all these FABPs correlate with the hepatic fat content [165], FABP1 was also

associated with protective role by redirecting intracellular FAs towards oxidation, energy utilization, and disposal [148, 166, 167].

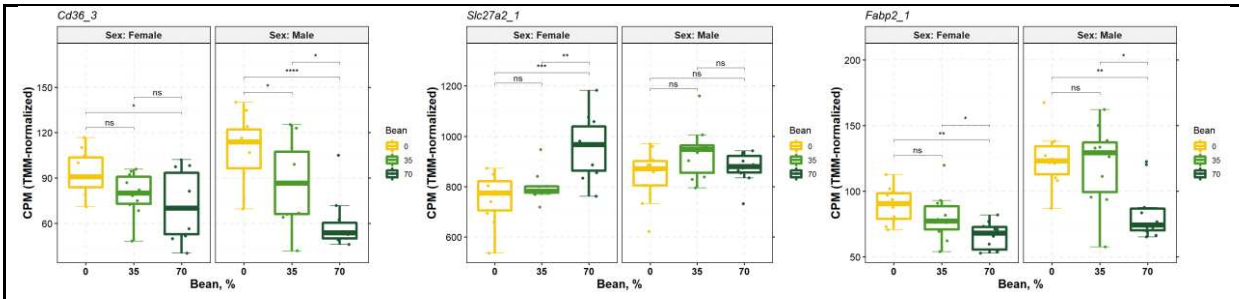

Fatty Acid Uptake

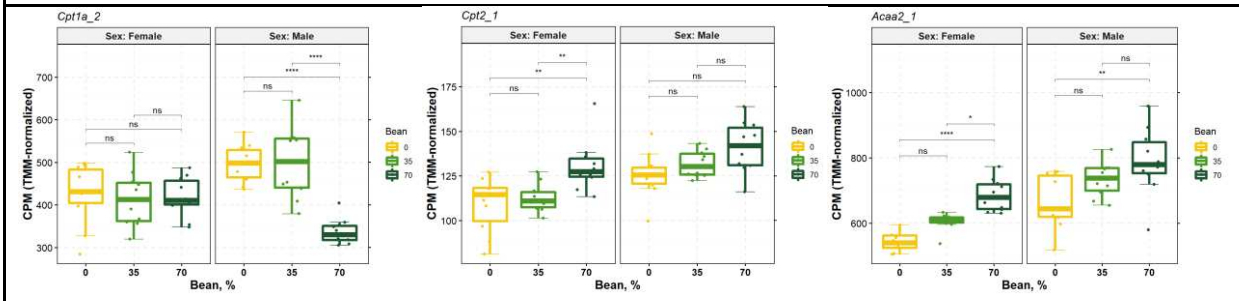

Mitochondrial β-oxidation of Fatty Acids

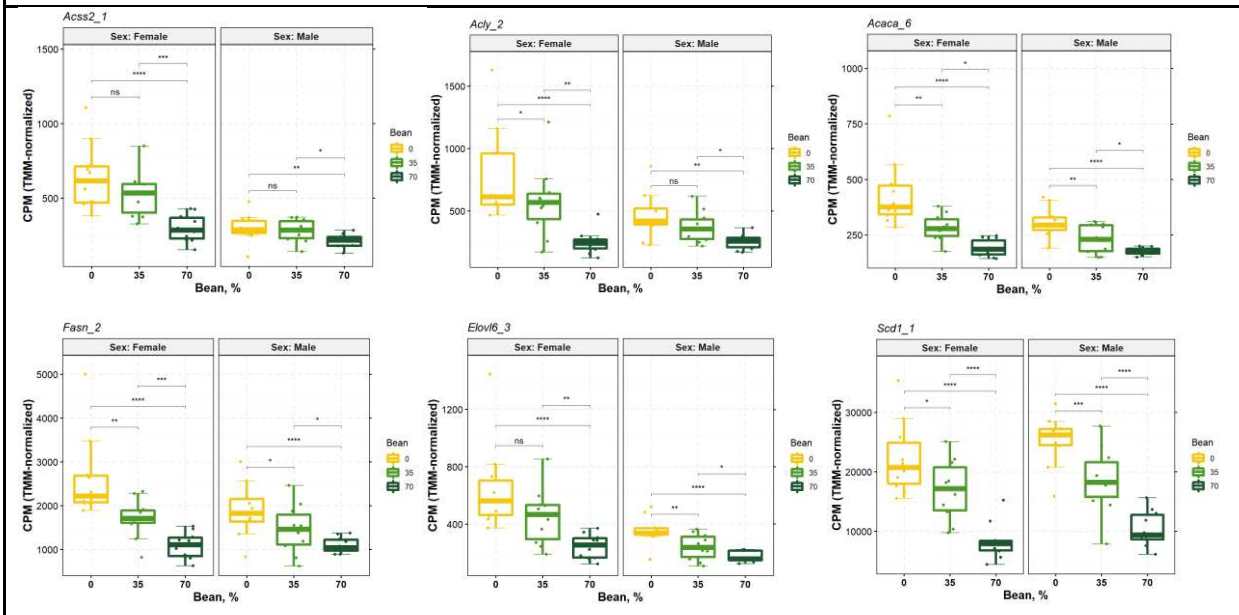

***de novo* Lipogenesis**

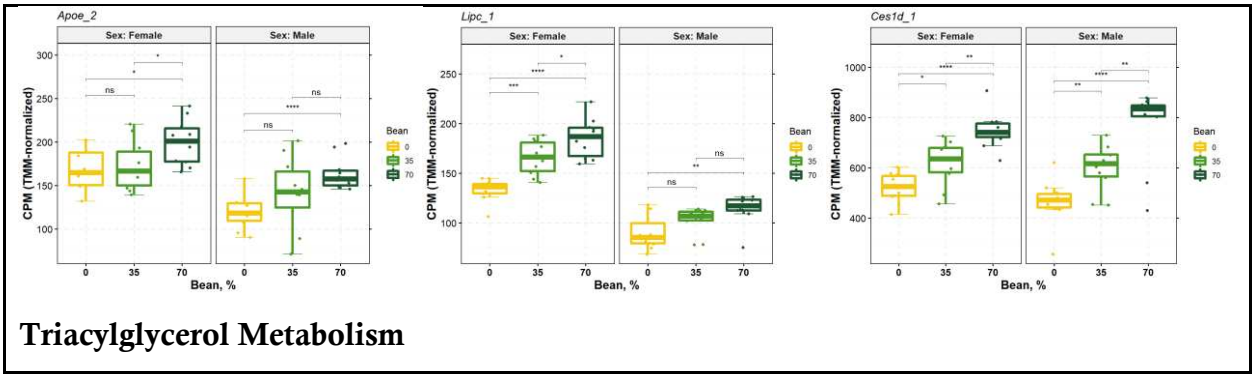

Figure III.6. Expression of genes involved in lipid metabolism in the livers of female and male mice upon consumption of beans. Differential expression analysis performed in CLC Genomic Workbench. * p-value < 0.05; ** p-value < 0.01; *** p-value < 0.001; **** p-value < 0.0001.

FAs enter metabolic pathways following activation by acyl-CoA synthetases (ACSs) as respective acyl-CoA molecules [168]. Consumption of beans suppressed short-chain ACS *Acss2* and long-chain ACS *Acsl5* in both sex cohorts (females also reduced levels of ER-based *Acsl3*). In contrast, bean increased propionyl-CoA ACS *Acsf*, medium-chain ACSs *Acsm1/5* (however, *Acsm3* was reduced in females), and expression of long-chain *Acsl1*. While *Acsl1* is associated with oxidation of long-chain FAs, *Acsl3/5* are mainly connected to thioesterification of *de novo* synthesized FAs for lipogenic pathways (**Supplementary Figure III.S3** and **Table III.S4**) [149, 167].

Oxidation is the main mechanism of FAs utilization, which occurs predominantly in mitochondria (β-oxidation), but also can take place in peroxisomes (α-oxidation of branched-chain FAs and β-oxidation of very long-chain FAs) and in the endoplasmic reticulum (ER; ω-oxidation of FAs via cytochrome P450 enzymes, CYPs) [168]. The 70% of bean sample compared to the bean-free control and lower bean dose in males significantly reduced expression of carnitine palmitoyltransferase CPT1 (*Cpt1a*)—the rate-limiting step of mitochondrial β-oxidation—regulating long-chain FAs transfer across mitochondrial outer membrane. In contrast, females elevated carnitine-acylcarnitine translocase (CACT, *Slc25a20*)

and CPT2 levels mediating transport of CPT1-derived acyl-carnitines across the inner mitochondrial membrane and conversion thereof back to acyl-CoAs, respectively [163, 168]. CPT2 also showed a trend of increase in the male cohort, but without a significant *p*-value (**Figure III.6**; **Supplementary Table III.S4** and **Figure III.S4**). CPT1 is regulated by MLXIPL, PPARα, and PPARγ coactivator-1 (PGC-1), and the subunit and stabilizer of the latter, *Ppargc1b*, showed inhibited trend in upstream analysis (**Supplementary Table III.S6**) [149, 166, 169]. Subsequently, bean consumption differentially affected enzymes involved in the course of FA β-oxidation in mitochondria with a noticeable trend towards an increased acyl-CoA dehydrogenases (ACADs) for short-chain FAs *Acadsb*, medium-chain FAs *Acadm*, and long-chain FAs *Acadl*, *Acadvl*, and *Acad11* in females, whereas males upregulated only short-chain FAs mitochondrial ACADs *Acadsb* and *Acad8*. Females also upregulated 3-hydroxyacyl-CoA dehydrogenase *Hadh*, including hydroxyacyl-CoA dehydrogenase-α (*Hadha*) and hydroxyacyl-CoA dehydrogenase-β (*Hadhb*)—units of the mitochondrial trifunctional protein degrading long-chain FAs [170]; as well as final thiolase (*Acaa2*) producing acetyl-CoA and shorter by two carbons acyl-CoA molecules [168]. Additionally, enoyl-CoA isomerase (*Eci2*) and 2,4-dienoyl-CoA reductase (*Decr1*), both of which handle unsaturated FAs, were induced in females (**Supplementary Figure III.S4** and **Table III.S4**). In contrast, males upregulated only mitochondrial short-chain FAs ACADs (*Acadsb* and *Acad8*), *Acaa2*, and *Eci2*. Such a transcriptomic signature implies that despite a greater capacity of female livers to β-oxidize various FAs, males rather target short-chain FAs in mitochondria (**Supplementary Figure III.S2**).

Long- and very long-chain acyl-CoAs canonically undergo initial catabolism via peroxisomal β-oxidation which consists of essentially the same reactions as the mitochondrial

one but catalyzed by different enzymes [168, 171, 172]. Consumption of beans induced expression of peroxisomal acyl-CoA oxidase (*Acox1* for females and *Acox2* for males) mediating rate-limiting initial dehydrogenation. Upstream analysis indicated that ACOX1 was predicted to be upregulated in both sex cohorts upon bean consumption with higher *z*-score in males than females (**Supplementary Figure III.S5** and **Tables III.S4** and **III.S6**). L-bifunctional protein (LBP, encoded by *Ehhadh*) and D-bifunctional protein (DBP, encoded by *Hsd17b4*) mediating hydration and subsequent dehydrogenation of FAs were upregulated (**Figure III.5b**) in males, but peroxisomal 2,4-dienoyl-CoA reductase *Decr2* expression was reduced. Subunits of final thiolases in peroxisomes *Acaa1a/b* were increased only in female cohort. Finally, there was a slight decrease in peroxisomal FAs transporter—ATP-binding cassette (ABC) protein of subclass D *Abcd1* in both sex cohorts under bean-containing diets. This is in contrast to increased *Slc27a2* and *Acbd5* associated with peroxisomal import of long- and very-long chain FAs in females (**Supplementary Figure III.S5**) [171].

Imbalanced hepatocytes upon MAFLD counterintuitively respond to systemic lipid overload with enhanced *de novo* lipogenesis of new FAs [148, 149, 165]. Bean consumption incrementally reduced expression of key enzymes in this process: aforementioned *Acss2* and ATP-citrate lyase (ACLY), both cytosolic and mitochondrial acetyl-CoA carboxylases I and II, respectively (ACC1/2, *Acaca/b*), fatty acid synthase (FASN), including elongases *Elovl2/5/6* and desaturases *Fads1/2*, *Scd1* in both sex cohorts. Males additionally decreased levels of *Elovl1* transcripts but increased such of *Elovl3*, whereas females reduced expression of lipogenic *Slc25a1* (**Figure III.6; Supplementary Figure III.S6** and **Table III.S4**). Expression of these lipogenic genes is regulated mainly by SREBF1, especially when

stimulated by postprandial circulating insulin, and by MLXIPL induced by dietary carbohydrates [137, 150].

Newly synthesized long-chain FAs are in the form of acyl-CoAs which can enter TAGs biosynthetic pathways or be first transformed to free FAs by acyl-CoA thioesterases (ACOTs). The glycerol-3-phosphate (G3P) pathway (also termed the Kennedy pathway; involves G3P- (GPATs) and acyl-G3P acyltransferases (AGPATs)), while 2-monoacylglycerol pathway consists of mono- (MGATs) and diacylglycerol acyltransferases (DGATs). Both are connected by lipins-mediated production of diacylglycerol [149, 163]. Bean consumption reduces expression of lipins *Lpin2*, a GPAT encoded by *Gpam*, AGPATs *Agpat2* (females) and *Agpat3* (males) [149]. Males also reduce glycerol kinase *Gk* that generates G3P from glucose and glycerol but upregulate *Dgat2*. Additionally, bean induced significant downregulation of *Lpcat3* (both sex cohorts) and *Pnpla3* (females only) that possess acyl-G3P acyltransferase activity within TAGs biosynthesis pathway according to IPA Canonical Pathways (**Figure III.5a; Supplementary Figure III.S7**). Finally, packaging of newly made TAGs into lipid droplets also involves DFF45-like effector proteins (CIDE group) together with abovementioned ACSL3/5 [149], and consumption of beans reduced their expression in males (**Supplementary Figure III.S7**), while females' DEGs indicated downregulation of CIDEC in the upstream analysis (**Figure III.5b**). CIDE proteins, ACSL3, DGAT2, including perilipins (PLINs), PNPLA3, and apolipoproteins are packaged into lipid droplets for storage and very low-density lipoproteins (VLDLs) for export [173]. Consumption of bean reduced expression of *Plin3* (males also reduced *Plin2*), apolipoproteins ApoA4 and ApoC2 (females also reduced ApoA5), but increased levels of *Plin5* as well as aforementioned ApoE (females also elevated ApoA2, while males increased ApoH; (**Supplementary Figure III.S7**).

The upstream analysis also indicated that bean-upregulated FOXA1 (**Figure III.5b; Supplementary Table III.S6**) which suppresses multiple target genes involved in TAGs synthesis, such as GPAM, DGAT2, and some apolipoproteins [174].

Ultimately, increasing dose of consumed beans significantly affected genes involved in every key mechanism of hepatic FAs metabolism, enabling its effective regulation of hepatocellular FAs and TAGs levels. These findings were consistent with results of IPA Canonical Pathways analysis, whereas IPA Upstream analysis revealed similar patterns of bean-induced DEGs and their functional association.

4. Discussion

MAFLD is a global public health concern rooted at the crossroads of metabolically dysregulated chronic non-communicable diseases and the respective detrimental economic, societal, and environmental consequences [175-177]. Effective care of MALFD patients is limited by the affordability, accessibility, and safety of interventions for the public and depends on the stage of disease progression. Nevertheless, even if better treatment measures are developed, modifying lifestyle risk factors remains central in MAFLD management, therapy, and prevention, according to consensus statements and recommendations for the public health agenda from the multidisciplinary group of experts [9]. Within lifestyle, chronic positive energy balance, particularly in adults, is a strong driver of MAFLD, but the global trends have been opposite and highly refractory to change [178]. This reality drives attention toward global food patterns and food types therein.

Given that the Mediterranean-type food pattern is reported to be protective against metabolic disorders, such as MAFLD, whereas the Western-type pattern is a major risk factor for the disease, a category of foods discriminating the two patterns are pulses. Moreover,

dietary guidelines, such as The Dietary Guidelines for Americans [32], inadvertently support the consumption of pulses as a vegetable side dish rather than as a staple food. We argue that as a consequence of such exclusion, dietary quality and associated health benefits are markedly reduced. This dilemma is partly due to a lack of clinical or population data that inform what dose/dietary concentration of pulse is needed to secure protection against fatty liver disease and whether biological sex plays a role. These issues are directly addressed by the work reported herein.

4.1. Dietary Bean-Induced Liver Phenotype

The design of this study used *ad libitum* feeding of a recognized obesogenic diet formulation that induces both MAFLD as well as obesity in C57BL6/J mice since that is the human context in which our study questions are most appropriately considered. Figures 1–3 clearly show that excessive hepatic steatosis—a hallmark of MAFLD [137, 142, 179]—is prevented by common bean consumption regardless of sex. Such an effect only becomes uniform enough to achieve statistical significance in female mice when ≥ 35% of dietary protein is derived from bean. In male mice, 70% dose is required to render an effect statistically distinct from the bean-free control. Implication of hepatic steatosis in the response to the dietary bean was consistent with the results of the bean-induced DEGs that mapped to this hepatotoxicity with the highest *p*-values (**Figure III.4**). The magnitude of bean required relative to the amount currently consumed in populations such as those in developed countries such as the USA, Canada, and many countries in Europe, underscores the critical importance of understanding the metabolic pathways through which common bean exerts these effects.

4.2. Triacylglycerol as the Main Chemical Form of Hepatic Lipid

Hepatic steatosis develops as acquisition and biosynthesis of intrahepatic lipids surpass the limits of their catabolism, utilization, and export such that excess fat is stored in intracellular vacuoles as lipid droplets [150]. The latter consist of neutral lipids, e.g., TAGs and cholesterol esters, surrounded by a phospholipid monolayer carrying proteins involved in synthesis, degradation, and trafficking of those lipids [173]. There is a fine-tuned balance between formation and degradation of TAGs within lipid droplets. TAGs are the preferred form of energy storage in the liver as they are biochemically inert [145] and, thus, serve as both the source and anabolic end-point of hepatocellular FAs [149]. In contrast, diacylglycerols, acyl-carnitines, ceramides, glycerophospholipids, sphingolipids, free cholesterol, and especially free FAs are associated with severe lipotoxicity [146, 147, 180]. About 15% of MAFLD-associated TAGs in the liver originate from the diet [161]. Females upregulate *Lrp1* expression, indicative of greater uptake of chylomicron remnants but, simultaneously, of improved MAFLD state [160]. Transcriptomic analysis revealed that the consumption of beans significantly upregulates canonical degradation of TAGs with the concomitant pattern of TAGs biosynthesis inhibition (**Figure III.5a**). Therefore, the expected reduction in hepatic TAGs content based on such a transcriptomic signature is also observed in the lipid quantification and liver histopathology (**Figures III.1–3**).

4.3. Contribution of Extracellular Free Fatty Acids Uptake

Excessive caloric intake renders adipose tissue and skeletal muscle (the primary destinations of dietary fat in the postprandial state) overloaded with intestinally derived chylomicrons so that their remnants and their spillover-derived non-esterified FAs are cleared from circulation by the liver [149]. Moreover, the accompanying dysfunction of adipose tissue

increases its rates of lipolysis [147, 181], releasing non-esterified free FAs into circulation. These free FAs are the primary source for 59% of TAGs in MAFLD livers. MAFLD-compromised hepatocytes upregulate the uptake of free FAs [149, 166, 180]. While short- and medium-chain FAs diffuse across hepatocyte plasma membrane due to their lipophilicity [182], long-chain FAs entry is mediated mostly by the membrane-bound proteins [149]. Higher levels of respective CD36 are a biomarker of high-fat diet-induced hepatic steatosis [149], and its reported knockdown improved insulin sensitivity and steatosis owing to observed decrease in FA uptake and TAGs concentration [149, 166, 183]. CD36, which was dramatically reduced more in males than females upon dietary bean, is considered the most contributing factor in FA-induced lipotoxicity in MALFD [180]. Its expression is regulated by PPARγ and LXR [149], whose downregulation, according to upstream analysis, was consistent with CD36 suppression (**Figure III.5b**). Therefore, upon bean consumption, females show a greater response in mediating uptake of lipoproteins and their degradation, whereas males rather downregulate FAs transport mechanisms.

4.4. Hepatocellular Oxidation of Fatty Acids

Analysis of intracellular FAs transport proteins and FABPs, ACSs, and ACOTs, as well as transcripts of FA oxidation enzymes indicated: a) bean consumption generally exerted a pro-catabolic profile in both sex cohorts; b) females displayed more evidence for enhanced mitochondrial β-oxidation of long-chain FAs and peroxisomal β-oxidation of very long-chain FAs; and c) males' DEGs patterns connect more to mitochondrial β-oxidation of short-chain, odd-number, and unsaturated FAs and peroxisomal β-oxidation of long-chain FAs. AMP-activated protein kinase (AMPK) suppressing mTOR, SREBP1, and ACC1/2 in favor of FAs β-oxidation [166, 184] showed patterns of bean-induced activation (**Supplementary**

Table III.S6), which is in accordance with the sex-dependent signature of bean consumption that significantly mapped FAs β-oxidation to females. Taken together, this points to *a priori* differential dietary challenges and sex-dependent differences in hepatic lipid catabolism which accordingly result in differential effects of dietary beans. While females exhibit a more pronounced increase in capacity for FA oxidation in livers than males, the latter demonstrate differential effects of bean consumption on hepatic FA β-oxidation.

4.5. Bean Effects Shared by Both Sex Cohorts

A dramatic reduction in the capacity to drive *de novo* lipogenesis in hepatocytes of mice was more uniform between females and males. Considering that mice fed bean-containing diets also reduced body adiposity [47], the contribution of adipose tissue-derived free FAs would be markedly reduced. Furthermore, under the MAFLD conditions, 26% of hepatic TAGs originate from *de novo* lipogenesis of new FAs in hepatocytes [161]. Thus, the suppression of lipogenic genes we demonstrate herein, including upstream regulators assessment indicating significant and dose-dependent inhibition of lipogenic SREBF1, potentially resembles the primary mechanism of bean-induced protection. After all, bean-promoted health benefits were potent enough to reduce expression of genes driving the obesogenic phenotype in C57BL6/J mouse model, such as *Acss2*, *Acly*, *Elovl6*, *Scd1*, *Acaca*, and *Slc25a1* [57]. Therefore, consumption of beans induces sex-dependent effects on improving hepatic FA oxidative capacity but not on the suppression of *de novo* lipogenesis. This is consistent with the observed transcriptomic trend of TAGs biosynthesis inhibition (**Figure III.5a**).

4.6. Differential Sex-Dependent Effects of Common Bean

The multi-omics integrative studies determined that males exhibit more MAFLD-associated hepatic genes than females, especially those associated with lipid metabolism, and identified key genes driving MAFLD in the livers of female and male mice, including but not limited to *Insig1*, *Acss2*, *Acot/4*, *Pnpla3* shared by both sexes; female-specific *Lipc*, *Srebf1*, *Slc27a5*; male-specific *Cidec*, *Mogat1*, *Cd36*, *Fasn*, *Cpt2* [185, 186]. Consistently, all these genes were detected among observed DEGs or their predicted upstream regulators, including the observation that males displayed more hepatic DEGs upon bean consumption than females. Observation that bean-induced protective effects from hepatic steatosis were qualitatively observed at the lower dose in females compared to males indicates that there are sex-dependent differences in MAFLD etiology and that males overall exhibit greater susceptibility to MAFLD comorbidities [185-188]. We report that female and male mice responded to dietary beans with opposite effects on PPARα and MLXIPL, and males exhibited steatogenic associations (**Figure III.5b; Supplementary Table III.S4** and **III.S6**). Levels of PPARα and PPARγ are increased upon a high-fat diet; however, knockout studies indicated that PPARα ablation exacerbates MAFLD, and PPARγ ablation protects mice from its development [151]. MLXIPL contribution to MAFLD development stems from obesogenic effects of dietary carbohydrates [189]. We report, however, that primary lipogenic targets of MLXIPL signaling, such as key genes of *de novo* lipogenesis, show a significant reduction in transcript expression in males. Taken together, these could indicate less efficient FA oxidation as well as the effects of dietary carbohydrates may be in the way of bean-induced protective health benefits for the liver in males.

4.7. Translational Considerations

In many respects, a vegan food pattern is a predominant type practiced globally. The significance of this is that it is well established that human health and well-being are maintained when all protein is obtained from plant sources. Moreover, globally, a substantial amount of plant protein is consumed from the botanical family Fabaceae. Within that family, the foods contributing to the protein are primarily either oilseed legumes (soy and peanut) or grain legumes, i.e., pulses (common bean, chickpea, lentil, and dry pea). Oilseed legumes predominate in economically developed countries, while pulses—in the remainder of the world. There, pulses are treated as a staple food crop, not a vegetable side dish. By definition, a staple food crop is eaten daily in large amounts as a primary source of energy and protein, and they are affordable and accessible. As such, pulses, with common bean as an example, could be leveraged to reduce the prevalence of fatty liver disease in developed countries featuring low levels of pulse consumption and in developing countries where the public health trends indicate that fatty liver disease is increasing in segments of the population with improving economic status, preferring highly processed convenience foods. Collectively, this raises the important question: *is increased pulse consumption feasible given the amounts needed to secure disease preventive effects, e.g., on MAFLD?*

In our judgment, the answer is yes, but it will require increased prominence of stealth health approaches. Specifically, flours of each pulse can be prepared as minimally processed whole food ingredients and incorporated into foods for which consumers in various populations show a preference. As witnessed by the rapid increase in the release of pulse-containing food products, it is feasible. Beyond this, the effort will gain credibility in the biomedical community by identification of the specific gene/protein targets by which

bean inhibits the development of a disease such as MAFLD and the specific chemical(s) that alters gene expression or protein activity. Whether the chemicals are an intrinsic component of bean and other pulses or are produced by interacting pulse food components with the gut microbiome and its associated immune component remains to be determined. Once that chemistry is understood, pulses can be processed to ensure that their use as food ingredients maintains the amount and form necessary to secure health benefits.

4.8. Limitations and Strengths

Our primary goal in the present study was to determine dose- and sex-dependent effects of bean consumption on liver protection from the obesogenic dietary environment and both quantitative chemical analyses and qualitative histopathology provide strong evidence of dose and biological sex dependent effects of bean consumption on diet-induced MAFLD. In addition, a secondary objective was to deduce potential molecular mechanisms underlying these observed phenotypes. Considering the multifaceted nature of hepatic lipid metabolism, the results we report herein are only the tip of the iceberg and provide an initial overview of dietary bean effects on MAFLD prevention. Recognizing that transcriptional signatures are only one step in the regulatory cascade that determines protein activity and metabolite patterns, this work will serve to direct detailed analyses of the effects of bean consumption on the phosphoproteome that are focused and guided by metabolomic analyses of plasma and liver. However, those analyses are considered beyond the scope of this investigation.

The translation of preclinical data to potential human relevance must always be done bearing in mind the limitations of each animal model. In the work reported herein, the model is well established for its value in studying metabolic dysfunction and the underlying findings have been demonstrated in two rodent species. This work was done in a preclinical model

rather than in human subjects because of the paucity of information available about dose or the effect of biological sex. Additionally, a specific bean cultivar and a dose response design were used in male and female animals. Ultimately, mechanistic studies using genetically engineered mouse (GEM) methodology, e.g., knock-out strategies, will be required to establish causality. The work reported herein constitutes a foundation for in-depth, targeted analyses upon which genetic manipulations can be designed.

5. Conclusions

We demonstrate that consumption of common bean under isocaloric and obesogenic dietary conditions exerts potent protection from lipid accumulation in the liver in a dose- and sex-dependent manner. In particular:

- females exhibited lower hepatic lipid content at the 35% dose, whereas males achieved a similar reduction with the 70% dose of bean;
- common bean dose-responsively inhibited *de novo* lipogenesis in both sex cohorts;
- additionally, females showed greater capacity for FA oxidation, whereas males significantly reduced uptake of extracellular free FAs;
- bean consumption significantly affected genes involved in TAGs metabolism consistent with enhanced hydrolysis and diminished biosynthesis;
- bean-induced DEGs patterns indicated that reduced PPARα signaling and activated by dietary carbohydrates MLXIPL signaling may be at the core of lower susceptibility of male mice to dietary bean protection from hepatic steatosis;
- hepatic CYPs-regulated FA oxidation, oxidative stress, cholesterol metabolism, bile acid metabolism, and inflammation appear to also be significantly affected by

increasing doses of beans in the diet and will be assessed in further communications.

Collectively, we provide strong evidence that incorporating common bean into the diet dose dependently protects both female and male mice from the diet-induced onset of MAFLD.

CHAPTER IV. Consumption of Bean alters Bile Acid Metabolism[3]

1. Introduction

In the age of rapidly rising metabolic dysfunction-associated co-morbidities, metabolic dysfunction-associated steatotic liver disease (MASLD) is of particular concern. Currently, over 30% of adults are affected by MASLD, with a significant economic burden worldwide, exceeding USD 100 billion in the U.S. alone [190]. The term "MASLD" has recently replaced the literature-rich non-alcoholic fatty liver disease (NAFLD) [6, 191, 192]. MASLD is associated with a wide range of diseases involving dysregulated metabolism, including more severe pathologies of the liver (metabolic dysfunction-associated steatohepatitis (MASH), cirrhosis, hepatocellular carcinoma), albeit the leading cause of mortality in patients with MASLD remains cardiovascular disease (CVD), accompanied by dyslipidemia [193]. Lifestyle interventions, such as regular intake of high-quality diets (adherent to the Dietary Guidelines [194]) and increased physical activity to achieve weight loss and maintenance, remain central to the management of MASLD and point to the predominant culprit in its incidence—excess caloric intake. Therefore, switching from Westernized dietary patterns to the consumption of plant-based protein and increased dietary fiber and whole foods rather than ultra-processed foods is the first line of recommendation for preventing and controlling MASLD [195, 196].

Consumption of common bean, the most consumed representative of grain legumes, i.e., pulses, has been reported to have beneficial effects on multiple chronic diseases [197,

[3] The content of this chapter is based on our research article published in an open-access journal *Nutrients* from MDPI. References to tables, figures, and supplementary materials have "IV" appended to them. Citation information is as follows: *Lutsiv, T., Fitzgerald, V.K., Neil, E.S., McGinley, J.N., Hussan, H. and Thompson, H.J., 2025. Cooked Bean (Phaseolus vulgaris L.) Consumption Alters Bile Acid Metabolism in a Mouse Model of Diet-Induced Metabolic Dysfunction: Proof-of-Concept Investigation. Nutrients, 17(11), p.1827.*

198]. Though acknowledged as a concentrated source of dietary protein, bean also provides equivalent amounts of dietary fiber [199]. While dietary fiber is not considered a nutrient, it is well established that its presence in the diet has marked effects on health, especially via effects on intestinal microbiota [200, 201]. The chronic diseases impacted, in addition to MASLD, include obesity, type 2 diabetes, CVDs, and several types of cancer; however, the mechanism(s) underlying these effects has not been fully elucidated [41]. While a number of pathways have been implicated, e.g., hepatic *de novo* lipogenesis [202], ceramide-mediated signaling [203], and mTOR network signaling [204], limited effort has been directed to linking such effects to bile acids.

The role of bile acids in host metabolism extends far beyond lipid digestion and absorption, to physiologic and pathophysiologic effects encompassing inflammatory responses, effects on vasculature, glucose metabolism, insulin sensitivity, energy expenditure, and other mediators of metabolic health [205, 206]. Bile acids are produced from cholesterol and conjugated with amino acids (e.g., taurine in mice) to form bile salts in the liver. The bile acids synthesized in the liver are deemed primary and comprise cholic and chenodeoxycholic acids in humans [207]. Murine livers additionally synthesize hyocholic, ursodeoxycholic, and α-/β-muricholic acids [207-209]. Those bile acids are then secreted into the gallbladder and released into the small intestine within bile, aiding in dietary lipid emulsification/absorption. Most bile acids are reabsorbed via enterohepatic circulation in the lower ileum, while the remaining bile acids interact with intestinal microorganisms in the colon. Microbiota deconjugate and re-conjugate bile acids, conduct their dehydroxylation/hydroxylation, dehydrogenation, oxidation, epimerization, and other modifications [209], producing secondary bile acids, such as deoxycholic, lithocholic, hyodeoxycholic, ω-muricholic acids,

etc. Further biotransformation of secondary bile acids also takes place, seldom distinguished in the scientific literature as tertiary bile acids [210-212]. Enterohepatic circulation continues along the large intestine, and unabsorbed bile acids/salts are excreted with feces. Some primary and secondary bile acids also reach the systemic circulation, extending their function as signaling molecules beyond the gastrointestinal tract and liver. Patients with metabolic diseases, like MASLD and obesity, often exhibit hypercholesterolemia and elevated bile acid levels (especially conjugated primary species), so among therapeutic approaches, complementing dietary modifications and exercise, prescription of bile acid sequestrants is common [206, 213]. Drugs such as cholestyramine bind bile acids in the gastrointestinal tract and eliminate them with feces, resulting in greater redirection of hepatic cholesterol to bile acid synthesis to compensate for bile acid loss. First- and second-generation bile acid sequestrants are based on plant-derived polysaccharides. Importantly, polysaccharide and protein biopolymers in common bean have been reported to act as bile acid sequestrants [214].

The functional repertoire of bile acids is enhanced by the gut microbiota, which show bidirectional effects as bile acids affect intestinal bacterial communities and the latter metabolize and alter bile acid composition and concentration in the gut [212, 215]. Common bean is an abundant source of total dietary fiber as assessed by the integrated method of analysis [216]. In fact, to our knowledge, the common bean has one of the highest concentrations of total dietary fiber per 100 kcal edible portion of any category of whole food [217]. Not only does this indicate that bean consumption has strong potential to exert effects on the composition of the gut microbiome, as has been reported in humans and mice, but it is likely the lower digestibility of bean protein in conjunction with its dietary fiber content will exert unique effects on the composition and function of the colon microbiome [218].

The work reported herein is a proof-of-concept investigation. Conceptualization was prompted by several clinical/feeding studies' observations in which the consumption of common bean renders an organism resistant to severe complications from obesogenic lifestyles, particularly related to dyslipidemia [202-204, 219]. Biospecimens from previous studies were interrogated to discern whether sufficient evidence exists to support hypothesis testing in prospective preclinical and clinical investigations.

2. Materials and Methods

2.1. Experimental Design

Experiments were conducted in male and female C57BL6/J mice (cat. 000664) from the Jackson Laboratory (Barr Harbor, ME, USA) at 20-day-old age in multiple studies. Mice had *ad libitum* access to food and filtered water in solid-bottom polycarbonate mouse cages with a 12 h light/dark cycle at 27.5 ± 2°C ambient temperature. Prior to eight weeks of age, animals were adapted to husbandry conditions and diet, which was a purified powdered diet providing 32.5% kcal from fat. At 8 weeks of age, mice were assigned to experimental diet groups using staggered randomization by body weight and fed their respective diet for 12–14 weeks.

Experimental diets were isocaloric and formulated to maintain equal macronutrient proportions, weight by weight, according to the AIN-93G recommendations [220, 221]. The bean seed was cooked, processed with leachate, puréed, freeze-dried, and milled into a homogenous fine powder. In contrast, control contained only purified ingredients. For more information on the formulations of experimental diets, please refer to **Supplementary Table IV.S1**.

At necropsy, mice were anesthetized via isoflurane inhalation to a surgical plane of anesthesia, blood was collected via cardiac puncture using a 25 or 26 g needle and 1 cc syringe, and transferred into an EDTA-coated microtainer tube. The animals were then euthanized by cervical dislocation. The blood was spun at 2000× *g* for 10 min, the plasma was collected, transferred to a cryovial, and snap-frozen in liquid nitrogen. Liver was excised, placed in a sample bag, and snap-frozen in liquid nitrogen. The cecal contents were gently harvested and thoroughly mixed into a homogenous mixture, placed in a sterile cryovial, and snap-frozen in liquid nitrogen for subsequent DNA extraction. The liver, cecal contents, and plasma samples were stored at -70°C. All animal work was approved by the CSU IACUC (Colorado State University, Institutional Animal Care and Use Committee protocol number 1431).

2.2. Measurement of Total Bile Acids

Cecal contents, feces, liver tissue, and plasma samples were subjected to the colorimetric total bile acid assay using the Mouse Total Bile Acid kit (cat. 80471, Crystal Chem, Inc.; Elk Grove Village, IL, USA). Feces from 24 h collection were placed in 2 mL cryovials and stored at -70°C. Dry matter was performed on each sample in duplicate. Briefly, each sample was weighed out and dried in a 90°C oven for 24 h, the samples were removed and cooled for 30 min in a desiccator and weighed. This process was repeated until the samples were at a constant dry weight. From this, the percent dry matter was calculated and the average of the duplicates was used. Tissues were weighed out and 75% ethanol was added in a volume 10 times greater than the amount of material used for cecal and fecal material, and 5–8 times greater volume for ground frozen liver. Samples were sonicated for 2 h at 50±3°C, after which they were centrifuged at 4000×*g* for 10 min. EDTA-treated plasma

samples were used directly. The assay procedure was performed on a 96-well plate with each sample assayed in duplicate according to the manufacturer's protocol. In addition to the provided calibrator, a control of known bile acid concentration for mice was also used (cat. 80473; Crystal Chem, Inc.; Elk Grove Village, IL, USA). Deionized water was used as a blank. Samples were incubated with Reagent CC1 (nitrotetrazolium blue (NBT) solution) for 5 min at 37°C, after which absorbance was measured at 540 nm. Then, Reagent CC2, containing 3α-hydroxysteroid dehydrogenase, was added, and the mixture was incubated for 5 min at 37°C. 3α-hydroxysteroid dehydrogenase converts 3α-OH bile acids into 3-keto steroids in the presence of NAD^+, forming an equimolar quantity of NADH, which, in turn, reacts with NBT in the presence of diaphorase enzyme, forming a formazan dye. After adding the stop solution, absorbance measurement was conducted at 540 nm to detect the newly formed dye. Plates were run in the microplate reader (SpectraMax M5, Molecular Devices, LLC; San Jose, CA, USA), detecting formazan dye at 540 nm, which is proportional to the concentration of bile acids. Blank-corrected difference in two absorbances is proportional to the bile acid titer of the original sample, and using calibrator/control absorbance, values were extrapolated into μM levels of detected bile acids. The amount of bile acids detected was corrected for the percentage of dry matter in the cecal, fecal, and liver tissue samples, followed by the density correction of the volume of ethanol used. Values were normalized for the total percent dry matter of cecal and liver weights collected during necropsy.

2.3. Metabolomic Profiling

Samples of plasma, cecal contents, and liver were delivered to Metabolon Inc. (Morrisville, NC, USA) for metabolomic analysis using ultrahigh-performance liquid chromatography–tandem mass spectroscopy (UPLC-MS/MS). Given our previous findings

that females were more responsive to the bean effect [202], this study was originally designed to focus on 7 samples from males with female samples pooled into 1 sample per group for cost-effective purposes, resulting in $n = 8$ per experimental group (control and bean) per tissue. Metabolon used Waters ACQUITY ultra-performance liquid chromatography (UPLC) with a Thermo Scientific Q-Exactive high-resolution/accurate mass spectrometer interfaced with a heated electrospray ionization (HESI-II) source and Orbitrap mass analyzer operated at 35,000 mass resolution [222]. Samples were analyzed on Metabolon's global untargeted metabolomics platform (HD4) using their standard statistical approaches. Briefly, the resulting peak area-under-the-curve data were median-scaled (each compound across samples is corrected to have a median of 1.00, normalizing each data point proportionately). Then, missing values were imputed by replacing them with the respective compound's observed minimum value. For plasma samples, the resulting data were additionally normalized for the extracted volume differences and rescaled to have a median of 1.00. To determine the statistical differences between control and bean, Welch's two-sample *t*-test was performed with additional adjustment to decrease the false discovery rate using the Benjamini–Hochberg procedure. Separately, for compounds identified by Metabolon as bile acids, median-scaled imputed data were subjected to principal coordinates analysis (PCoA) using the Bray–Curtis dissimilarities and Jaccard distances. Visual separation or lack thereof was confirmed using permutational multivariate analysis of variance (PERMANOVA) to compare the variation between groups to the variation within groups (differences in the means/centroids) and a test for multivariate dispersion (PERMDISP) to check whether differences between groups arise from dispersion of the data.

2.4. RNA Isolation and RNA-Seq Analysis

Frozen liver tissue was ground to powder under liquid nitrogen to perform RNA extraction with the RNeasy mini-kit following the manufacturer's protocol (cat. 74104, QIAGEN, Inc., Germantown, MD, USA). Integrity of isolated RNA was determined using the Experion automated electrophoresis station (Bio-Rad Laboratories, Inc., Hercules, CA, USA). Liver RNA samples were then submitted for cDNA library construction and RNA sequencing (Illumina, Inc., San Diego, CA, USA) to the Genomics and Microarray Core at the University of Colorado-Anschutz Medical Campus (Aurora, CO, USA). Raw sequencing data were processed using CLC Genomics Workbench software, version 23 (QIAGEN, Redwood City, CA, USA), and resulting differentially expressed genes (DEGs) datasets were further evaluated with Ingenuity Pathway Analysis (IPA) software, v127006219, for subsequent analysis (QIAGEN, Redwood City, CA, USA). Out of 25,526 DEGs, 21,797 DEGs were protein-coded and used for the analysis. IPA's Core Analysis was performed on the dataset of DEGs with maximum mean between the groups greater than 10 TPM and p-value < 0.05. Multiple DEGs mapping to a single molecule in IPA were resolved by the highest mean TPM value between the groups. Thus, 2804 analysis-ready molecules were used for the IPA's Core Analysis. Briefly, expression patterns of the DEGs were cross-referenced with the published studies worldwide within the QIAGEN Ingenuity Knowledge Base, and p-values of overlap between the observed DEGs patterns and their associations were calculated. Similarly, activation z-scores measuring the prediction strength of the DEGs effects (activation or inhibition) were calculated based on the direction of DEGs expression changes. Mapped functional associates were deemed significant with the $|z|$-score ≥ 2 and

the p-value < 0.05 of the overlap between our experimentally observed dataset and the QIAGEN Ingenuity Knowledge Base.

2.5. Quantitative Real-Time PCR Analysis

An amount of 1 μg of total RNA isolated from liver tissue samples (see Section 2.4) was used for cDNA synthesis with Superscript II reverse transcriptase (Invitrogen, Carlsbad, CA, USA). DNA oligo-primers were previously synthesized (Integrated DNA Technologies, Coralville, IA, USA) [223]. Quantitative real-time PCR (qPCR) was performed on an iCycler iQ5 (Bio-Rad, Hercules, CA, USA) using optical-grade 96-well plates (Thermo Fisher Scientific, Waltham, MA, USA). As previously reported [224], each 20 μL PCR reaction was composed of 10 μL 2X SYBR green Supermix (Bio-Rad, Hercules, CA, USA), 1.5 μL of 4 μM forward and reverse primers, 2 μL synthesized cDNA, and 5 μL nuclease-free water. The PCR conditions were as follows: 95°C for 1.5 min, followed by 40 cycles of 95°C for 15 s and 56.5°C for 1 min. Fluorescent products were detected at the last step of each cycle. qPCR was followed by a melt curve analysis to verify primer specificity. Samples were run in triplicate, and the relative expressions of FXR and SHP were calculated by normalizing the threshold cycle (Ct) values to β-actin (*Actb*) gene expression. Expression of β-actin was set up in reactions that included 10 μL 2X TaqMan Fast Advanced Master Mix, 1 μL 20X TaqMan Gene Expression Assay (β-actin: Mm00607939; Thermo Fisher Scientific, Waltham, MA, USA), 2 μL synthesized cDNA, and nuclease-free water to 20 μL total volume. The TaqMan thermocycling conditions were 50°C for 2 min, 95°C for 2 min, followed by 40 cycles of 95°C for 3 s and 60°C for 30 s. The fold change in expression relative to the control-fed animals was computed by the negative value of the ΔΔCt method as previously described [225].

2.6. Western Blot Analysis

Frozen liver tissue samples were ground to a powder under liquid nitrogen, weighed into pre-cooled microcentrifuge tubes, and subjected to protein lysate extraction as previously described [226]. Protein lysate concentration was determined by the bicinchoninic acid assay (BCA) method [227]. Nanocapillary Immuno-electrophoresis was performed using the Jess instrument (ProteinSimple, San Jose, CA, USA) as previously described [228] with the following changes: final concentration of the protein lysates was 0.7 mg/mL when probed with anti-FGF15 and 0.2 mg/mL for all other targets, and each primary antibody was incubated for 120 min. The following primary antibodies were used: mouse monoclonal anti-FXR/NR1H4 (D-3; cat. SC-25309), mouse monoclonal anti-SHP (H-5; cat. SC-271511), mouse monoclonal anti-FGF-15 (D-9; cat. SC-514647), rabbit polyclonal anti-CYP7A1 (E-10; cat. SC-518007), and mouse monoclonal anti-CYP7B1 (WW-H9; cat. SC-134309) from Santa Cruz Biotechnology, Inc. (Dallas, TX, USA). Data were normalized by dividing the target protein peak area-under-the-curve by the corrected total protein area-under-the-curve within each sample capillary using the Compass Software for Simple Western (v6.1.0; ProteinSimple, San Jose, CA, USA).

2.7. Microbiome Analysis Using 16S rRNA Gene Amplicon Sequencing

Total DNA was extracted from cecal contents with the QIAamp PowerFecal DNA kit (cat. 51804, Qiagen, Germantown, MD, USA) according to the manufacturer's protocol, and its purity and concentration were determined by NanoDrop (Thermo Fisher Scientific, Waltham, MA, USA). The V4 region of the 16S rRNA gene was amplified and sequenced to construct paired-end sequencing libraries using the 515F-806R primer set following the Earth Microbiome Project protocols [59], followed by sequencing using the MiSeq Reagent Kit v2

2×250 bp on an Illumina MiSeq instrument (Illumina, Inc., San Diego, CA, USA) housed at the Next-Generation Sequencing Facility at Colorado State University.

Bioinformatic processing of the obtained forward and reverse paired-end sequence reads was performed with QIIME 2 platform, version 2024.10 [60]. Raw sequence data were demultiplexed and quality-filtered via q2-demux plugin. Denoising was performed with the DADA2 pipeline (q2-dada2) [61]. Taxonomy was assigned to the resulting amplicon sequence variants (ASVs) using a Naive Bayes classifier (via q2-feature-classifier plugin [62]) pre-trained on Greengenes2 (16S rRNA, version 2022.10) marker gene reference database trimmed to the V4 domain (bound by the 515F/806R primer pair) with 99% sequence identity threshold [63, 229]. The dataset was filtered to remove all features annotated as "mitochondria" and "chloroplast." A rooted phylogenetic tree was built using FastTree [64] and MAFFT [65] alignment via q2-phylogeny plugin. ASVs feature table was collapsed to the Genus taxonomy level and subjected to the differential abundance analysis using ANCOM-BC method [230] in QIIME 2.

Functional attributes of the identified microbial communities were predicted using Phylogenetic Investigation of Communities by Reconstruction of Unobserved States 2 (PICRUSt2) pipeline, version 2.4.1 [70]. With the ASV dataset as an input, PICRUSt2 performs phylogenetic placement by aligning ASVs to the reference 16S sequences (HMMER, www.hmmer.org) and incorporating them into the reference tree (evolutionary placement algorithm (EPA)-NG and genesis applications for phylogenetic placement analysis (GAPPA) [71, 72], followed by the hidden-state prediction of gene families (*castor R* package [73]) and, finally, generation of metagenomic predictions and tabulation of pathways' inferences and abundances (Minimal set of Pathways (MinPath) [74] and MetaCyc [75].

Differential abundance analysis of microbiome data was performed in QIIME 2 using ANCOM-BC method [230].

2.8. Microbiome Analysis Using Shotgun Metagenomic Sequencing

Whole-genome DNA sequencing was performed on total DNA extracted from cecal samples pooled from 20 animals total (n = 3 per experimental group). Libraries were prepared and sequenced on an Illumina NovaSeq 6000 system at the Genomics Shared Resource at the University of Colorado, Anschutz Medical Campus (Aurora, CO, USA). Specifically, 100 ng of genomic DNA was sonicated using an E220 focused ultrasonicator (Covaris, LLC; Woburn, MA, USA) to produce 200 bp fragments, which were purified using Agencourt AMPure XP beads (Beckman Coulter, Inc.; Indianapolis, IN, USA). Ovation Ultralow System V2 (Tecan Group Ltd.; Männedorf, Switzerland) was used to prepare Illumina libraries following the manufacturer's instructions. Libraries were quality-checked for size and concentration with electrophoresis using a high-sensitivity D1000 kit on a 4200 TapeStation (Agilent Technologies, Inc.; Santa Clara, CA, USA). Sequencing depth was at 60 million (2 × 150 bp) paired-end reads per sample.

Metagenome reconstruction and analysis were performed on the U.S. Department of Energy Systems Biology Knowledgebase (KBase) platform [231] following the published protocol [232] using default parameters unless otherwise specified. Briefly, after importing the data files to KBase, read quality was assessed using FastQC (v0.12.1), followed by data pre-processing steps: trimming Illumina adapters, trimming low-quality bases on both read ends, removing duplicate reads, and removing host sequences with the JGI RQCFilter pipeline (BBTools v38.22); then filtering out low-complexity reads (entropy filtering method with $0 \leq 70 \leq 100$ entropy threshold or $0 \leq 7 \leq 100$ dust threshold parameters) with PRINSEQ

(v0.20.4). Metagenome assembly was performed using MEGAHIT (v1.2.9 [233]) with meta-sensitive parameter preset and default contig length parameter in the $300 \leq 2000$ range. Resulting contigs were binned using three methods: MaxBin2 (v2.2.4 [234, 235] using 107 bacterial marker gene set), MetaBAT2 (v1.7 [236]), and CONCOCT (v1.1 [237] using BBMap mapping tool). Binned contigs from these three methods were optimized using DAS Tool (v1.1.2 [238] using blast [239] identification tool) to obtain consensus metagenome-assembled genomes (MAGs), which were evaluated with CheckM (v1.0.18 [240]) using a full reference tree for placement of each genome bin to a lineage clade for phylogenetic marker determination. The resulting data were filtered with CheckM to obtain medium-quality bin subsets with completeness $\geq 50\%$ and contamination $< 10\%$ to maximize our detection of bile acid metabolism-associated genes. Functional summaries for each MAG were annotated using DRAM (v0.1.2 [241]), and taxonomy was assigned with GTDB-Tk (v2.3.2 [242]) using The Genome Taxonomy Database (GTDB) [243].

2.9. Statistical Analysis

All statistical analyses were conducted using *R* (v4.4.3) [244], unless otherwise specified in the aforementioned sections. Results of the total bile acid assays, qPCR, and Western blot were analyzed by *t*-test within the rstatix package [245]. Significance was accepted at the level of $p < 0.05$ and $q < 0.05$. Respective visualizations were built using *ggpubr* [246] and *plotly* [247] packages.

3. Results

3.1. Bean Consumption Elevates the Excretion of Total Bile Acid Levels

To determine the effects of cooked bean consumption on the levels of bile acids, cecal and fecal material, plasma, and liver tissue, biospecimens were subjected to an enzymatic total bile acid analysis from female mice fed a diet with ~60% of total dietary protein derived from bean. Plasma samples contained bile acids below the detection level for the assay, so we could not quantify their amounts. In cecal contents, there was no statistical difference between bean and control groups in the amount of total bile acids per g of dry weight (**Figure IV.1a**). However, we observed larger ceca owing to a greater amount of cecal contents in the bean group compared to the control groups across our studies (**Supplementary Figure IV.S1**). Therefore, when we adjusted the values by the total cecal weights (bile acid concentration × cecum weight), we observed a statistically significant increase in total bile acid content in the bean group (**Figure IV.1a**). Consistent with this observation, bean consumption increased the amount of excreted bile acids compared to the control per g feces of dry weight (**Figure IV.1b**). These data indicate that bile acids are sequestered in the gut of bean-fed mice, and that a significant fraction of them escape enterohepatic circulation and are eventually excreted. In liver tissues, despite a trend of greater levels of total bile acids in the bean group, no statistical difference was observed (**Figure IV.1c**), indicating that the liver maintains homeostasis of bile acid content with no evidence of cholestasis.

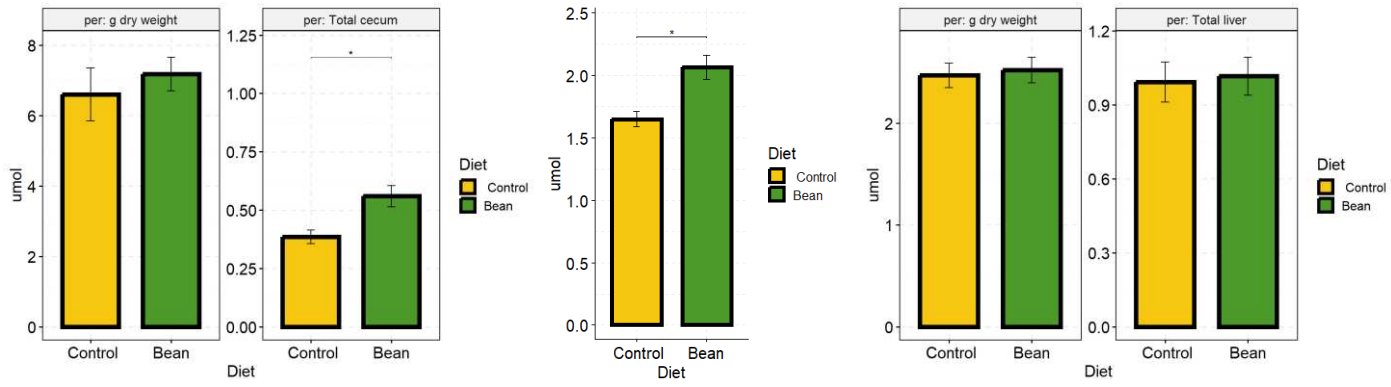

Figure IV.1. Bar plots of total bile acids in bean (green) and control (yellow) group in (**a**) cecal content, (**b**) feces, and (**c**) liver tissue samples. Left panel indicates amounts of total bile acids in µmol/g dry matter analyzed; right panel indicates µmol total bile acids in total tissue per animal (**a**,**c**). * indicates *p*-value < 0.05.

3.2. Global Metabolomics Indicate a Higher Variety of Bile Acids upon Bean Consumption

Cecal content, liver tissue, and plasma samples were subjected to untargeted metabolomics analysis to gain deeper insight into bile acid changes that occur upon bean consumption. The work shown below was performed in female and male mice fed the same dietary formulations as in the previous section: the experimental group contained ~60% of total dietary protein derived from cooked common bean. The first question addressed was whether differences in relative abundance of identified bile acids by diet group (control or bean) were sufficient for separation in principal coordinates analysis (PCoA) using Bray–Curtis dissimilarity ordination (**Figure IV.2**) and Jaccard distances (**Supplementary Figures IV.S3**).

Separation of liver samples was confirmed by PERMANOVA (Bray–Curtis: $R^2 = 0.243$, $F = 4.501$, p-value = 0.001; Jaccard: $R^2 = 0.225$, $F = 4.071$, p-value = 0.001). Similarly, differences were observed in the cecal metabolites (Bray–Curtis: $R^2 = 0.191$, $F = 3.306$, p-value = 0.015; Jaccard: $R^2 = 0.196$, $F = 3.421$, p-value = 0.003). Only plasma bile acids did not show a difference between control and bean (Bray–Curtis: $R^2 = 0.131$,

F = 2.108, p-value = 0.099; Jaccard: R^2 = 0.125, F = 2.007, p-value = 0.082), which might be due to missing values in a lot of plasma samples (on average, 32%). Separation of bean and control samples was also statistically observed when primary and secondary bile acids were analyzed separately in the liver and cecum, but not plasma (**Supplementary Figures IV.S3** and **IV.S4**). No differences according to PERMDISP tests were detected in the analyzed datasets, indicating that observed differences were not due to dispersion of data.

Collectively, these data signify marked differences in bile acid composition induced by bean consumption. Secondary bile acids may be of greater importance in driving these differences, judging by higher values of F-statistics compared with primary bile acid analysis in PERMANOVA. Global plasma metabolomics reflected our total bile acid assay results in plasma samples from a different study, indicating that bean effects on bile acids are more prominent within the gastrointestinal tract and liver rather than systemically.

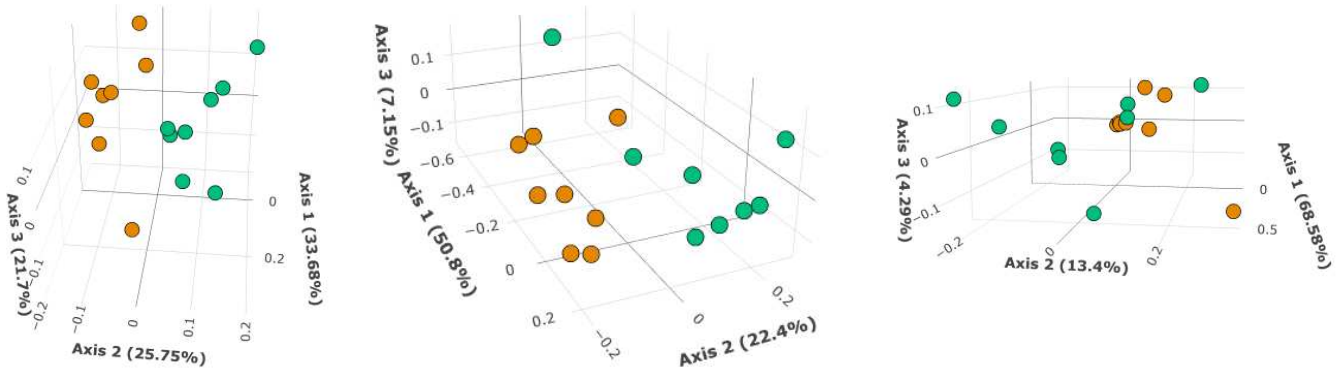

(a) **(b)** **(c)**

Figure IV.2. PCoA plots of bile acids in bean (green) and control (orange) samples using Bray–Curtis dissimilarity in (**a**) liver, (**b**) cecal, and (**c**) plasma samples. The 2D plots were adjusted to maximize visual separation of bean-fed and control samples.

Next, we calculated the statistical differences in bean versus control groups to elucidate particular bile acids driving the differences between the control- and bean-fed animals (**Figure IV.3; Supplementary Table IV.S2**). While metabolomics data of the liver tissue provide only a snapshot in time of bile acids produced and enterohepatically recirculated,

the data indicate that among 15 detected primary bile acids, levels of taurocholate were reduced, while taurohyocholate was increased in the bean-fed animals (**Figure IV.3a**). With $0.1 > p$-value > 0.05, glyco-β-muricholate tended to decrease, while taurochenodeoxycholic acid (7 or 27)-sulfate—to increase in livers of bean-fed animals (**Supplementary Table IV.S2**). Conversely, 10 secondary bile acids were identified: animals that were fed bean exhibited lower levels of 6β-hydroxylithocholate, hyodeoxycholate, and taurohyodeoxycholic acid, whereas taurolithocholate, 6-oxolithocholate, and 7-ketodeoxycholate were significantly increased compared to bean-free control in the liver tissue.

In the cecal contents (**Figure IV.3b**), out of 15 detected primary bile acids, 6 were significantly decreased compared to the bean-free control, namely tauroursodeoxycholate, α- and β-muricholates, glyco-β-muricholate, glycocholate sulfate, and chenodeoxycholic acid sulfate. Interestingly, glycine conjugation of bile acids is atypical for rodents, pointing to the potential effect of gut microbial metabolism and respective reconjugation of bile acids under bean consumption [207, 209]. Eighteen secondary bile acids (i.e., microbial metabolites) were identified in the metabolomics analysis of the cecal contents. Bean consumption significantly decreased levels of hyocholate derivatives: hyodeoxycholate and isohyodeoxycholate. Moreover, dehydrolithocholate and 3-dehydrodeoxycholate were elevated, indicating higher activity of bacteria harboring 3α-hydroxysteroid dehydrogenase activity metabolizing cholic acid. 6β-hydroxylithocholate, also known as murideoxycholate, was significantly reduced in the bean group, inferring either higher microbial 7α-dehydroxylation of β-muricholate, 6β-epimerization of hyodeoxycholate, or 6β-hydroxylation of lithocholate activities in control-fed animals [205, 248, 249]. Its reduction was also observed in the liver (**Figure IV.3a**). The reduction in taurodeoxycholate was

the greatest in effect size, albeit it did not reach a significant q-value (**Supplementary Table IV.S2**). With $p = 0.078$, 3-dehydrocholate showed a trend for an increase in bean-fed ceca.

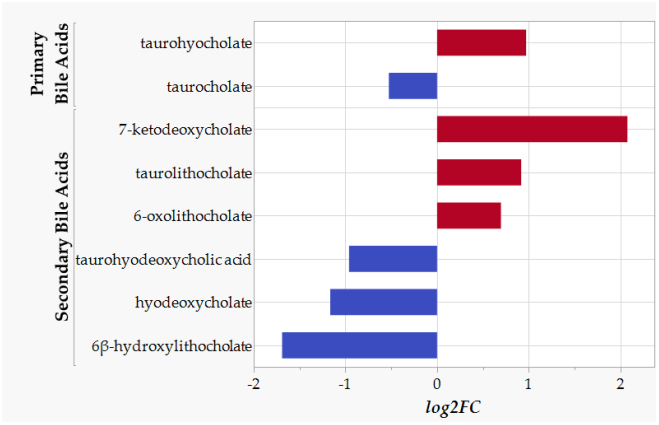

(**a**)

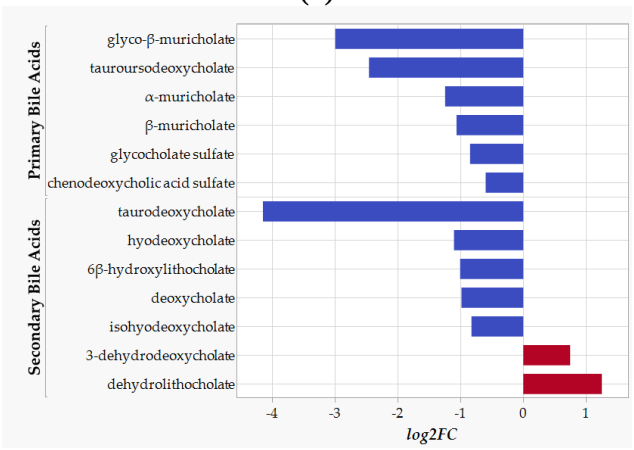

(**b**)

Figure IV.3. Bar plots of bile acid changes in bean versus control samples in (**a**) liver and (**b**) cecal samples. Only metabolites with $q < 0.1$ are depicted. Blue color indicates a decrease and red color indicates an increase in bean compared to control.

Fewer differences were observed in plasma bile acids (**Supplementary Table IV.S2** and **Figure IV.S5**). Presumably, this is due to the fact that not all samples had detectable signals for bile acids, which contributed to a lack of significant clustering and separation of the data seen in the PCoA (**Figure IV.2c**). Among 12 identified primary and 10 secondary bile acids, only taurochenodeoxycholate and 7-ketodeoxycholate approached a significant increase in the bean-fed animals, both approaching $p = 0.05$ cut-off but with insignificant

q-values. However, taurochenodeoxycholate was detected only in half of the control samples. Secondary taurodeoxycholate and ursocholate also showed a trend to increase, while taurohyodeoxycholic acid—to decrease, but with $0.1 > p\text{-value} > 0.05$.

These data demonstrate that bean consumption significantly alters the qualitative composition of bile acids in the cecal contents, liver, and plasma. The statistical emphasis appears to be skewed towards secondary bile acids as more differences in their levels were observed in mice that consumed bean.

3.3. Bean Affects Host Synthesis of Bile Acids

RNA-seq analysis of liver tissue samples from males and females of the same study that untargeted metabolomics were performed on was queried for effects on bile acid synthesis. DEGs in the RNA-seq data overlapped with a number of canonical pathways associated with the bile acids (**Figure IV.3**). Patterns of gene expression affected by consumption of bean in liver tissue indicated increased bile acid and bile salt metabolism (z-score = 3.962, p-value = 9.45×10^{-12}) and bile acid biosynthesis (z-score = 2, p-value = 3.56×10^{-4}). Liver X receptor and retinoid X receptor (LXR/RXR) activation also reached marked upregulation by bean with z-score = 3.55 and p-value = 8.57×10^{-16}, which is consistent with LXR function inducing bile acid synthesis [207] and with observed higher levels of its agonist, taurohyocholate, in the liver [250, 251]. Concomitantly, the pathway for hepatic cholestasis—a disorder associated with the accumulation of bile acids in the liver—was downregulated based on the gene expression data in the bean group (z-score = -2.466, p-value = 5.18×10^{-4}). Similarly, the MASLD signaling pathway was also inhibited based on the patterns of bean-induced hepatic gene expression (z-score = -2.16, p-value = 5.53×10^{-4}).

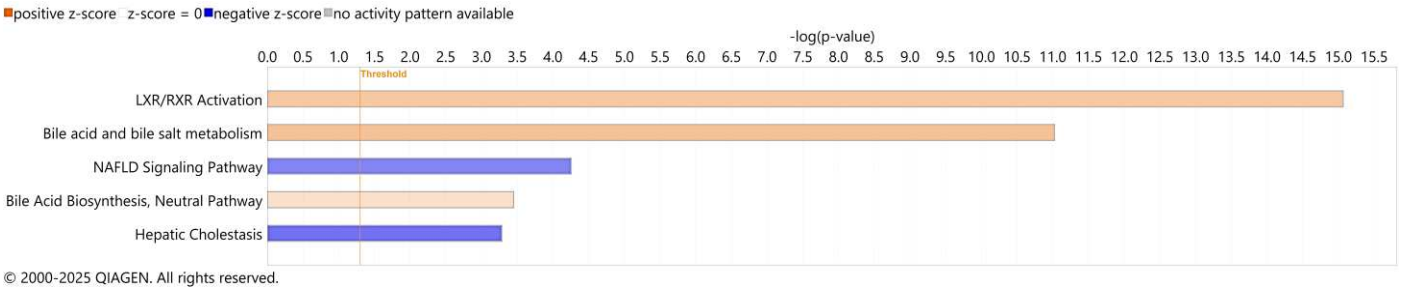

Figure IV.4. Canonical pathways analysis of bean-induced gene expression patterns associated with bile acid metabolism. Colors represent activation (shades of orange) or inhibition (shades of blue) of respective pathway. Features were deemed statistically significant with both activation $|z|$-score > 2 and p-value of overlap < 0.05.

Canonically, bile acid synthesis is regulated by FGF15-FXR-SHP signaling. Synthesis of FGF15 is induced by bile acids in the small intestine as a feedback loop to activate the FXR-SHP pathway in the liver and suppress the synthesis of bile acids. In RNA-seq analysis, we detected a slight increase in *Nr1h4 (Fxr)*, *Nr0b2 (Shp)*, and FGF15 receptor *Fgfr4* levels, albeit with a minor effect size (**Table IV.1**).

Table IV.1. RNA-seq results of hepatic *Fxr-Shp* signaling in bean vs. control.

DEG	ID	Expr Log Ratio	Expr *p*-Value	Expr *q*-Value
Fgfr4	ENSMUSG00000005320	0.27	0.00103	0.01
Shp (Nr0b2)	ENSMUSG00000037583	0.4	0.00017	0.0026
Fxr (Nr1h4)	ENSMUSG00000047638	0.3	0.000736	0.00848

When we analyzed the protein level of FGF15 in the liver, we observed a minor increase ($\log_2$FC = 0.567) in bean vs. control (**Figure IV.5**). Although the antibodies for FXR and SHP in the liver were of insufficient quality, qPCR analysis of hepatic *Nr1h4 (Fxr)* and *Nr0b2 (Shp)* did not achieve significant *p*-values to confirm their increase in the liver (**Table IV.2**).

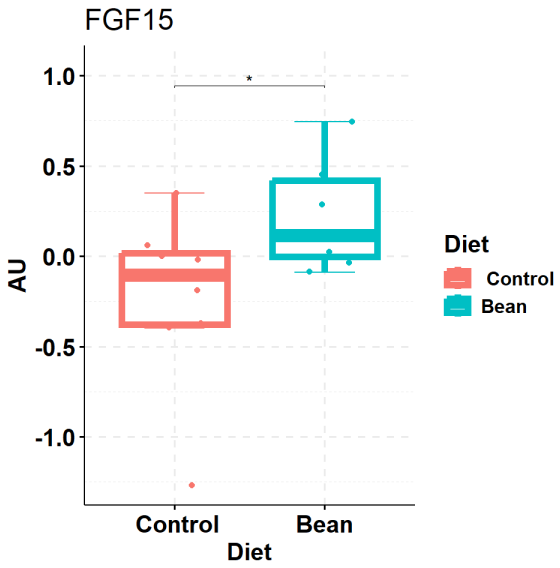

Figure IV.5. Box plot of protein levels of FGF15 from liver samples of animals fed control and bean diets. * indicates significant $p < 0.05$. AU—arbitrary units of signal peak area.

Table IV.2. qPCR results of hepatic *Fxr* and *Shp* in bean vs. control.

Bean vs. Control				
Gene	**Avg ΔCt Control**	**Avg ΔCt Bean**	**-ΔΔCt**	***p*-value**
Fxr (Nr1h4)	2.2485	2.1105	0.138	0.387
Shp (Nr0b2)	3.798	3.2855	0.5125	0.523

FGF15-FXR-SHP signaling regulates bile acid synthesis upstream, so we looked into genes directly involved in bile acid production. In mice, 75% of primary bile acids are synthesized in the classical pathway, the rate-limiting enzyme of which is CYP7A1. Analogically, CYP7B1 catalyzes the rate-limiting step in the acidic pathway of 25% of primary bile acids in mice. Both enzymes perform 7α-hydroxylation reaction, albeit on different targets: CYP7A1 acts directly on cholesterol, while CYP7B1—on oxysterols [252]. RNA-seq analysis of the liver tissue in the bean-fed mice revealed that expression of both *Cyp7a1* ($\log_2$FC = 1.06, *p*-value = 1.1×10^{-11}, *q*-value = 1.09×10^{-9}) and *Cyp7b1* ($\log_2$FC = 1.14, *p*-value = 2.23×10^{-15}, *q*-value = 5.39×10^{-13}) is markedly enhanced compared to the control. This increase was also confirmed on the protein level (**Figure IV.6**).

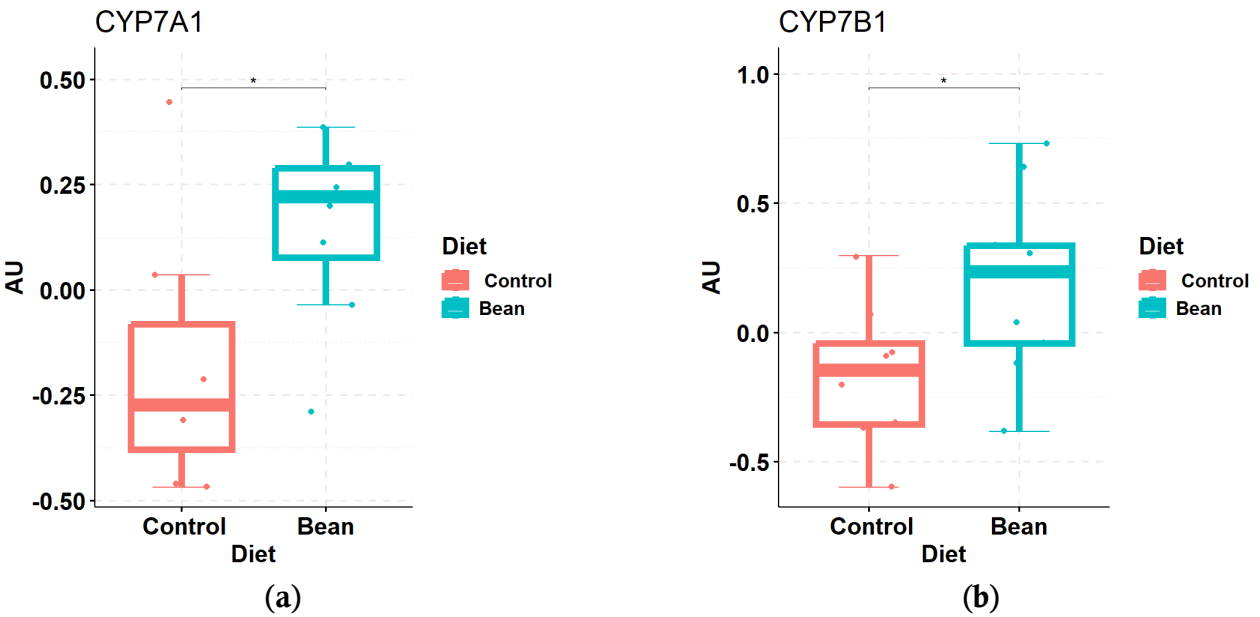

Figure IV.6. Box plots of protein levels of rate-limiting enzymes in bile acid biosynthesis: (**a**) CYP7A1 and (**b**) CYP7B1 in the liver samples of bean vs. control. * indicates significant $p < 0.05$. AU—arbitrary units of signal peak area.

Moderate upregulation was observed in downstream genes within bile acid biosynthetic pathways, such as *Cyp27a1, Amacr,* and *Acox2* (**Figure IV.7; Supplementary Table IV.S3**). To reduce the hydrophobicity of bile acids and retain them in the lumen of the small intestine, bile acids are conjugated to taurine in mice by hepatic *Baat*, whose expression was also slightly increased by bean. Expression of *Cyp3a11* (ortholog of human CYP3A4), which produces hyocholic acid from chenodeoxycholic acid [207] and can bypass *Cyp7b1* and *Cyp27a1* in the acidic pathway [253], was also markedly enhanced by bean. RNA-seq analysis of liver tissue has also revealed that *Slco1a1* and *Slco1b3* (coding organic anion transporters OATP1 and OATP1B3, respectively) and, to a smaller extent, *Abcb11* (BSEP) were expressed more in bean-fed animals, suggesting higher capacity to import free bile acids into the liver and to efflux bile salts out of the hepatocytes, respectively. Unlike humans, mice rely more on phase I hydroxylation for detoxification of bile acids, where *Cyp3a11* takes an important part [208] together with *Cyp2b10*, which was also upregulated in mice.

Nevertheless, mouse-specific *Cyp2a12/Cyp2a22,* which also enables rehydroxylation of secondary bile acids back to primary ones, was increased by bean in the liver [207, 254], indicating that the livers of the bean-fed animals might deal with an increase in secondary bile acids. However, sulfonation (phase II), albeit a minor detoxification pathway in mice [208], may be enhanced in bean-fed mice owing to higher expression of *Sult2a1* and *Sult2a8* (**Supplementary Table IV.S3**).

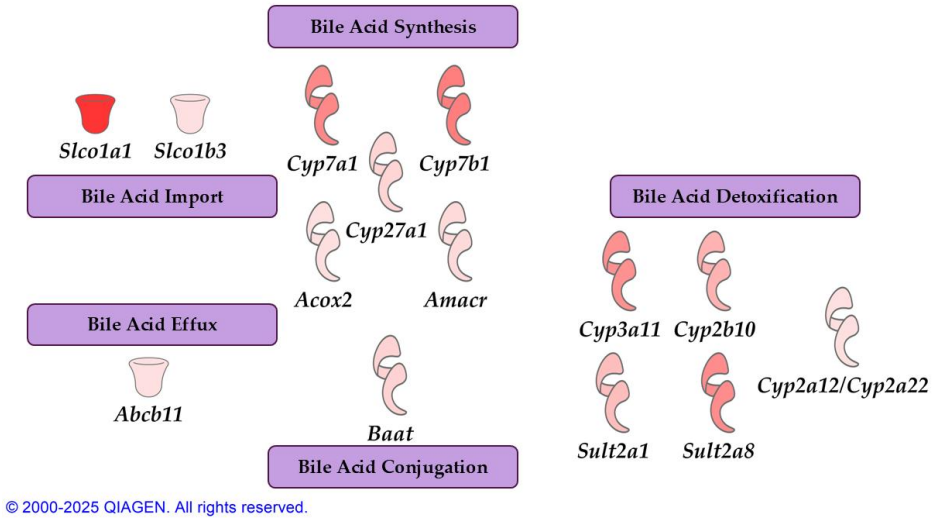

Figure IV.7. RNA-seq results on DEGs associated with bile acid metabolism in the liver tissue samples of bean-fed mice. Shades of red indicate $\log_2$FC. All depicted DEGs had $q < 0.05$.

3.4. Bean Consumption Enhances Microbial Contribution to the Bile Acid Metabolism

Most bile acids affected by bean consumption appear to be secondary and thus derive from microbial metabolism. Bacteria are capable of deconjugating hydrophilic bile salt into the hydrophobic form of bile acid, releasing the amino acid moiety. Using functional predictions from 16S rRNA gene data, we observed a slight increase in the primary and secondary bile acid biosynthesis pathway (ko00120, ko00121; $\log_2$FC = 0.15, p-value = 2.09×10^{-4}, q-value = 5.05×10^{-4}). Bile salt hydrolase (i.e., choloyglycine

hydrolase, K01442, EC:3.5.1.24) upon bean consumption was also increased (**Table IV.3**), indicating a higher potential of bean-induced microbiome to deconjugate bile salts. Within the *bai* operon responsible for bacterial transformation of primary bile acids into secondary, functional predictions revealed only a significant reduction in NADH:flavin-dependent oxidoreductase (**Table IV.3**), i.e., NAD^+-dependent 7β-hydroxy-3-oxo bile acid-CoA-ester 4-dehydrogenase (*baiH*). This enzyme catalyzes the intermediate step in the dehydroxylation of ursodeoxycholic acid (the 7β-epimer of chenodeoxycholic acid) metabolites and other 7β-hydroxy bile acids [255]. Such a marked reduction in predicted *baiH*-carrying bacteria infers that bean consumption promotes dehydroxylation of bile acids rather at the 7α position, instead. Bean consumption also predicted a small reduction in 7α-hydroxysteroid dehydrogenase (7α-HSDH, *hdhA*, K00076, EC:1.1.1.159), which is involved in 7-O.epimerization of deconjugated cholate and chenodeoxycholate into ursocholate and ursodeoxycholate, respectively. This is consistent with the observed reduction in taurine-conjugated ursodeoxycholate in the ceca of the bean-fed animals. PICRUSt2 also predicted increased bile acid:Na^+ symporter in the cecal microbiome of bean-fed animals (**Table IV.3**), consistent with our observations that bean-induced bacteria have a higher capacity to import and metabolize bile acids.

Table IV.3. PICRUSt2-predicted metagenome of cecal microbiota in bean vs. control.

Gene/Enzyme	log_2FC	*p*-values	*q*-values	ID
BSH, choloylglycine hydrolase	0.57	5.84×10^{-31}	2.39×10^{-30}	K01442
hdhA; 7-alpha-hydroxysteroid dehydrogenase [EC:1.1.1.159]	-0.22	7.62×10^{-13}	6.12×10^{-2}	K00076
baiH; NAD+-dependent 7beta-hydroxy-3-oxo bile acid-CoA-ester 4-dehydrogenase	-2.45	8.19×10^{-49}	1.73×10^{-47}	K15873
TC.BASS; bile acid:Na^+ symporter, BASS family	0.98	7.59×10^{-32}	3.29×10^{-31}	K03453
SLC10A7, P7; solute carrier family 10 (sodium/bile acid cotransporter), member 7	-0.21	0.574	0.608	K14347

Among the putative bacterial genera metabolizing bile acids [211, 256-258], we observed an overall reduction in more taxa than increased upon bean consumption (**Figure IV.8**), consistent with our previous report [259]. However, relative abundances of bean-enhanced bacteria were higher than those suppressed, particularly *Alistipes, Bacteroides*, and *Parasutterella*. On average, the cumulative abundance of bile acid-associated bacteria was 28.442% in the control and 37.183% in bean, indicating higher microbial capacity, albeit lower diversity, to metabolize bile acids. This is particularly important considering that bean-fed animals also exhibited larger ceca with more cecal content (**Supplementary Figure IV.S1**); thus, the net output of microbial contribution to bile acid metabolism in the colon of mice and their exposure to microbial metabolites of bile acids are even greater.

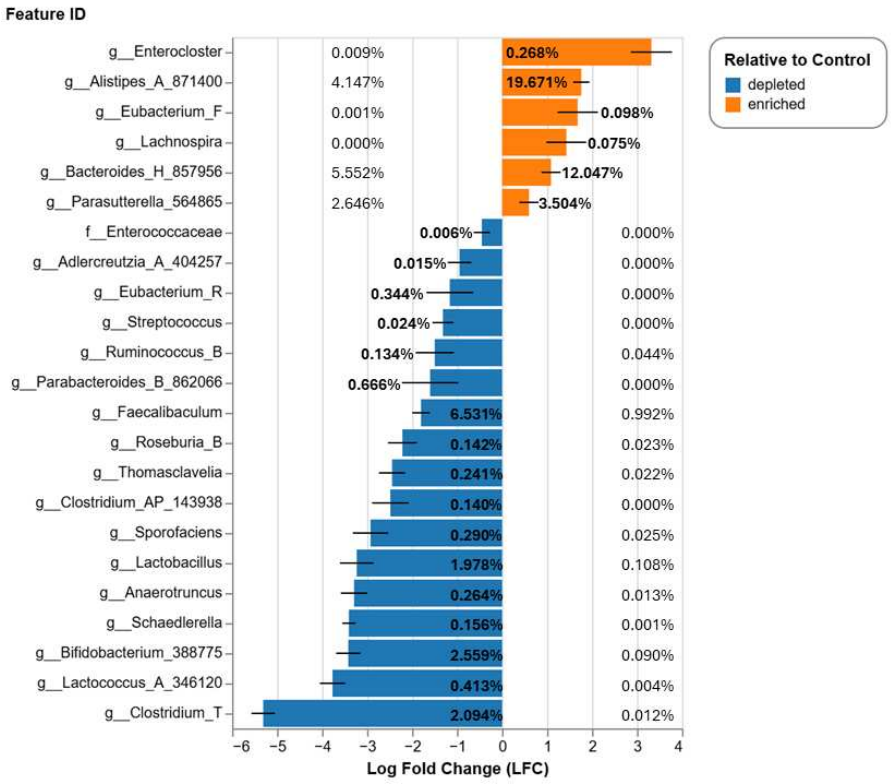

Figure IV.8. Results of differential abundance analysis of cecal microbiota in bean vs. control using ANCOM-BC. Only genera associated with bile acid metabolism and q-value < 0.05 are displayed. The numbers on each bar denote average relative abundance of bacterium in

control (on the left) and in bean (on the right) groups. Additional details on ANCOM-BC can be found in **Supplementary Table IV.S4**.

In a different study, we applied shotgun metagenomic analysis on the cecal contents of bean and control diet-fed mice. Using liberal quality controls, we identified 61 MAGs in the control and 73 MAGs in the bean group (**Supplementary Table IV.S5**). After mapping to the Genome Taxonomy Database (GTDB), we identified 19 unique taxa in control, 33 in bean, and 9 shared by both (**Figure IV.9**). Some of these taxa were not canonically recognized as bile acid-metabolizing bacteria, and the presence of bile salt hydrolase was the largest (36 hits out of 74), perhaps indicating horizontal transfer of the gene encoding this enzyme, which has been reported [260, 261]. Additionally, only bean MAGs possessed $NADP^+$-dependent 3α-hydroxycholanate dehydrogenase (EC:1.1.1.392, K22605).

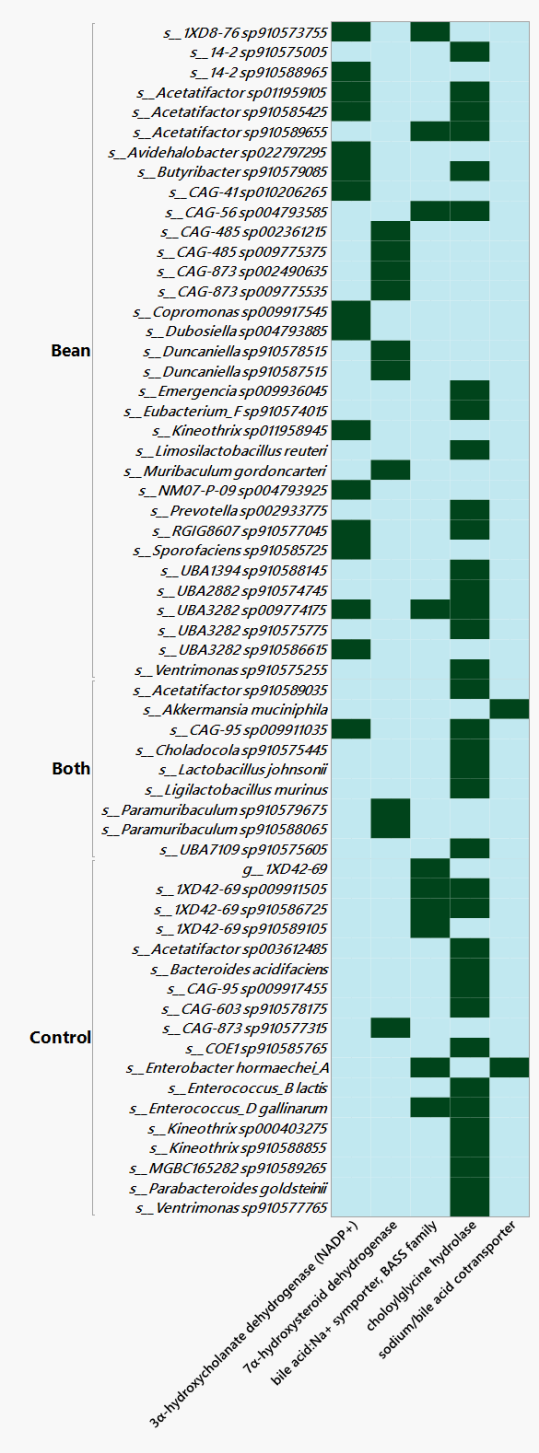

Figure IV.9. Summary of bile acid-associated genes found in the shotgun metagenomics analysis. Green color indicates the presence of the respective enzyme in identified MAGs. Choloylglycine hydrolase [EC:3.5.1.24; K01442]; 3α-hydroxycholanate dehydrogenase ($NADP^+$) [EC:1.1.1.392; K22605]; 7α-hydroxysteroid dehydrogenase [EC:1.1.1.159; K00076]; bile acid:Na^+ symporter, BASS family [K03453]; sodium/bile acid cotransporter [SLC10A7; K14347].

4. Discussion

The role of bile acids in modulating many aspects of metabolic dysfunction associated with the obesity pandemic is receiving considerable attention [205, 252]. Because the metabolic pathways regulated by bile acids, e.g., cholesterol metabolism and lipid homeostasis, overlap with the reported effects of consumption of therapeutic amounts of cooked bean [262, 263], the proof-of-concept experiments reported herein were conceived. We expected that the consumption of cooked bean would bind bile acids based on several reports that bean components sequester bile acids as detected using in vitro assays [264-266] and in vivo [267-269]. The data in **Figure IV.1** are consistent with the hypothesis that cooked bean sequesters bile acids, resulting in increased fecal bile acid elimination, which is considered a definitive biomarker for bile acid sequestration [213, 270]. Dietary fiber, protein, and even bean phytosterols are capable of binding bile acids [38, 214, 271]. This differs from earlier reports, indicating that only the soluble component of dietary fiber sequesters bile acids [272, 273] and is of particular importance in view of the fact that about 60% of bean fiber is insoluble [216]. Moreover, bean and other pulses have an amount of protein in essentially a 1:1 ratio (*w*/*w*) with dietary fiber [199]. Thus, the fact that bean protein also sequesters bile acids is significant [214]. Bean protein has a lower digestibility than familiar animal sources of the protein, suggesting that protein-sequestered bile acids arrive in the colon, where a mixture of fiber and protein undergoes microbial metabolism, rendering bile acids accessible for microbial metabolism as well. The biotransformational chemistry is supported by enriched microbial eco-groups, which we have previously reported [259], and is therefore of interest relative to host exposure to gut microbiota-derived bioactive compounds. In this regard, the effects of the bean are expected to be different than clinically prescribed bile acid

sequestering resins, either of the first (cholestyramine and colestipol) or second generation (colesevelam) that precipitate bile acids in the intestine, and those complexes are nonreactive and are excreted [213, 270].

While bean consumption increased bile acid excretion in the feces, it also increased the total bile acid content in the cecum, the first segment of the colon (**Figure IV.1**). Principal coordinates analysis (PCoA) of the bile acid data from global metabolomic analyses showed complete separation between the bean and the control group (**Figure IV.2; Supplementary Figures IV.S2–S4**). Further examination of these data indicated that conjugated primary bile acids were deconjugated in the cecum as well as converted to secondary bile acids. Thus, at least some of the bile acids reaching the colon are biologically active and participate in biotransformation reactions within the cecal microbiome.

Nonconjugated bile acid metabolites can be absorbed via passive diffusion in the colon and transported in the blood to the liver and other tissues, where they have been reported to exert hormone-like effects. Of particular interest in this regard are recently published data showing that caloric restriction of mice in the same mouse model resulted in increased conversion of primary bile acids to derivatives of lithocholic acid [274]. Reported changes in mTOR pathway signaling were partly mediated by the induction of AMP-activated protein kinase (AMPK) by lithocholate, a secondary bile acid. This observation has particular significance in that we have reported that bean feeding limits weight gain in obesogenic rodent models, an effect also observed in response to caloric restriction [219, 226]. The effects of bean consumption on weight regulation have also been reported in population studies [275, 276]. Moreover, we have previously reported the activation of AMPK by bean consumption in rat models of diet-induced obesity and breast cancer [204]. In addition, the AMPK-regulated

node of the mTOR signaling network, which is also induced by metformin, is associated with longevity extension [274, 277]. Bean consumption has also been associated with longevity extension in human population centers called blue zones [278].

Studies in preclinical models to identify differences in the relative abundance of microbial taxa of bean-fed versus control mice generally target fecal material [36, 279, 280]. Our work has moved the focus of analysis from the stool, which reflects the end stage of microbial impacts on the host, to the cecal content, recognizing that the cecum is the first segment of the colon at the end stage of host digestion. In a series of studies in rodents, a consistent relandscaping of the cecal microbiome has been observed in response to bean consumption, and variation across studies in the induced, unaffected, and suppressed bacterial genera and species have also been noted, a common observation in microbiome research [36]. However, herein, we reported 16S rRNA gene amplicon data (**Figure IV.8**) and shotgun metagenomics (**Figure IV.9**) that provide evidence of an enhanced ability to metabolize bile acids in bean-fed mice. Moreover, the metagenomic data provide insights for future follow-up experiments, i.e., the primers designed to permit quantitative assessment of bean-driven effects at the species and strain taxonomic level using methods like those proposed in [281].

Given these observations, we predicted that the liver's FXR and SHP transcript levels would not differ or be reduced in bean-fed versus control mice. qPCR data showed no significant difference (**Table IV.2**). Next, we found strong evidence for an increased rate of bile acid synthesis in bean-fed mice via both the canonical (produces both cholic and chenodeoxycholic acid) and the acidic pathway (produces chenodeoxycholic acid). We assessed protein levels of CYP7A1 and CYP7B1 hydroxylases, rate-limiting steps in bile acid

synthesis, the synthesis of which is inhibited by FGF15-FXR-SHIP signaling [282, 283]. This finding is consistent with our previous work, which showed that transcript levels of *Cyp7a1* were also induced by feeding a similar amount of cooked bean in a rat model [284]. The combined data indicate that this effect is observed in two rodent species and is consistent with the expectation that bile acid sequestration by bean would not be species-dependent. Chenodeoxycholic acid serves as a precursor for other primary bile acids, such as hyocholic and ursodeoxycholic. These differences were consistent with the global metabolomic analyses data, which showed complete separation between bile acid profiles of bean-fed versus control-fed mice (**Figure IV.2**). However, it is important to note that total bile acids were measured in the liver, and no differences were observed between the bean- and control-treated mice (**Figure IV.1c**). This finding indicates bean does not induce bile acid accumulation in the liver due to cholestasis, a condition where the flow of bile from the liver to the small intestine is impaired, which can also result in higher circulating levels of bile acids. This is consistent with observed RNA-seq patterns of increased transport of bile acids to (OATP1/3) and from (BSEP) hepatocytes (**Supplementary Table IV.S3**). These findings are also consistent with our previous report that no evidence of hepatotoxicity was observed in rats fed cooked bean in the diet [284]. The caveat is that the total bile acid assay relies on the 3α-hydroxysteroid dehydrogenase enzymatic reaction and thus would not detect epimers with 3β-OH and other 3α-dehydroxylated metabolites of bile acids. This underscores the importance of targeted bile acid analyses that detect a broad range of metabolites, given the diversity of bile acids recently reported to be generated during microbial metabolism [211, 285, 286]. Bean-induced microbial biotransformation of bile acids is not limited to just 7α-hydroxylation, as evidenced by the increase in dehydro-, keto-/oxo-forms of secondary bile acids. Moreover, bean

upregulates the mouse host capacity to rehydroxylate secondary bile acids. We also showed a relative decrease in cholate and deoxycholate with a shift towards their microbial metabolites, potentially carrying a health benefit, given that an increase in these two 12α-hydroxylated bile acids has been associated with metabolic morbidities [252, 287]. Finally, we show that bean consumption affects the metabolism of health-associated bile acid—hyocholic acid [251]—by increasing hepatic taurohyocholate yet reducing its microbial metabolites in the liver and cecum.

Therefore, bean must modulate bile acid metabolism beyond just sequestration and elimination of bile acids or altering microbial community and its net access to and capacity to metabolize bile acids. Previously, we have reported that feeding bean to mice and rats reduces serum levels of cholesterol and LDL [219], which was consistent with our later report that bean also impedes *de novo* synthesis of fatty acids and triglycerides and affects their packaging into lipid droplets and VLDL structures. Shown herein, the increase in bile acid synthetic pathways, their chelation, and elimination with fecal pellets suggest additional impact on cholesterol metabolism, redistributing its molecules towards bile acid metabolism and away from hepatic and potentially systemic lipotoxicity. Understandably, this would require future work on fasted animals to elucidate further bean effects on cholesterol synthesis, biotransformation, and circulating levels regulation. Moreover, additional multi-focal studies are required to outline which effects of bean consumption are direct (driven by dietary components of cooked bean and its host-mediated metabolites) versus indirect (mediated by the activity of bean-induced microbial eco-groups). The latter, one might say, would also include changes in host physiology owing to changes induced by direct effects of bean components and their metabolites. For example, here, we show direct effects of dietary bean

components on sequestering bile acids and increasing the colonic bacteria exposure to them, which, in turn, would affect cholesterol metabolism and absorption of other lipids in the lower small intestine. Therefore, it is important to understand that the multifactorial effect of bean consumption should not be underestimated yet must be accounted for in the future studies of its mechanisms.

Limitations. The work reported herein was retrospective, using biospecimens from preclinical studies designed for other purposes. While this is a strength in some respects, quantitative collection of feces for three to five days, which is recommended for assessing bile acid sequestration in rodent models, was not undertaken. In addition, it needs to be recognized that host exposure to various bile acid metabolites needs to be assessed. This will require a targeted analysis of a comprehensive panel of bile acid metabolites in which values are normalized to the dry matter weight of the biospecimen and further corrected for differences in mass of the luminal content or amount of feces excreted. For the cecum and presumably other colon segments, the luminal content mass generally exceeds that of the control by a factor of 1.5 or more in bean-fed rodents. Moreover, the same argument needs to be considered in quantifying the effects of bean on gut microbiota since relative abundance data limit insights concerning host exposure to specific microbiota and their products of metabolism [288]. Finally, to fully elucidate cardiometabolic health status, other derivatives of cholesterol, such as circulating lipoproteins (HDL, LDL, VLDL), need to be considered. Since our biospecimen collection was performed on animals not in a fasting state, any interpretation of cholesterol data was of limited value. However, future quantitative work on unraveling the effects of cooked bean consumption in an obesogenic environment on the bile acid composition and metabolism would benefit significantly from the data on fasted

cholesterol levels not only in the serum, but also in the liver and gastrointestinal tract, given that cholesterol is also synthesized in the lower ileum.

5. Conclusions

Collectively, the data reported here provide strong support for the prospective investigation of bile acid mediation of bean-driven health benefits. The consumption of cooked bean modulates all levels of bile acid metabolism: their synthesis rate, host modification, and gut microbial modification. Given the chelating properties of bean-derived chyme in the small intestine, bean consumption potentially also affects lipid metabolism and thus the host's absorption of cholesterol and other lipid species. Given that in most of our studies, mice are fed obesogenic diets (including the bean-containing ones), such multifactorial protection of animals from an obesogenic challenge points to the importance of this type of food as a source of plant-based protein, dietary fiber, and other bioactive food components.

CHAPTER V. Synthesis, Limitations, and Future Directions

Pulses, such as common beans, chickpeas, lentils, and dry peas, are famed for their health benefits, the extensive list of which only keeps growing. Nevertheless, such an advantage from their consumption stems from their nature as a *staple food* in the diet [289], not an occasional vegetable side dish. By the traditional definition, a staple food is one that is eaten regularly and in such quantities as to constitute a dominant part of the diet and supply a major proportion of energy and nutrient needs. However, in the U.S. and other countries worldwide, consumption of pulses has declined over the decades [290-293], as the popularity of dietary patterns associated with poor food quality and the coincidental development of chronic diseases has increased at unprecedented rates [294-298]. When presented with the choice of eating an ultra-processed food or a pulse-based food, the latter should be the obvious, healthier option. However, consumers overwhelmingly fail to make this choice in part due to deficits in food literacy [299-301]. That is, lacking sufficient knowledge, skills, and behaviors to select and navigate foods based on their expected health impact. Since introducing changes to food literacy and eating behaviors in the population has been steadily challenging [300, 302], alternative approaches must be considered.

Common bean (*Phaseolus vulgaris* L.), as the top pulse crop grown and consumed worldwide [303], was used herein as an exemplary pulse type to investigate. Overall, the goal of the studies presented in this dissertation was to establish a foundation for determining the required dose of cooked pulse and its molecular mechanisms to achieve metabolic health benefits in the prevention and control of chronic diseases by protecting an organism from the deleterious effects of an unhealthy, obesogenic diet. In Chapter II, the work reported demonstrated that cooked bean consumption can restructure the entire gut microbial

ecosystem, which, in turn, is one of the critical determinants of the organism's health and well-being. In Chapter III, the role of the liver—a central organ in the regulation of metabolic health in the body, was shown to be positively impacted through the improvement of lipid metabolism in the face of an obesogenic dietary challenge. Both Chapters II and III establish the importance of the dose of cooked beans consumed in observing positive improvements in body weight gain, adiposity, cecal microbial diversity, and lipid deposition in the liver. Moreover, they describe the presence of minor differences in the biological sex response to the effects of cooked bean consumption. Finally, Chapter IV reveals alterations in bile acid metabolism as a potential candidate mechanism for the observed health benefits of beans, affecting both the cecal bacterial community and liver function. The results of these investigations reveal the potential therapeutic value of bean effects for the human population, particularly in the context of the current harm caused by contemporary ultra-processed dietary patterns that dominate globally.

Whole-body responses to the consumption of cooked bean in mice

In the background of an obesogenic diet for C57BL6/J mice, one of the aims was to determine the dose of cooked bean in the diet that is capable of significantly reducing body weight gain compared to the bean-free control, despite the equivalent amounts of dietary fat between the groups. A medium dose of bean (35% of total dietary protein from cooked bean powder) was enough to observe reduced body weight gained by females compared to control diet (**Figure V.1a**). Body weights driven by the medium bean dose were also statistically different from low (17.5%) and high (70%) bean dose, indicating that females responded even further to bean consumption. In contrast, only a high dose of bean showed a significant reduction of body weight gained by male mice. Therein, the high bean diet (70% of total

dietary protein derived from cooked bean) was statistically different from all other diets in the study, except for low-fat control (**Figure V.1a**). This is opposed to female mice which gained even less body weight upon low-fat control compared with the high dose of bean, indicating that females' body weights overall were more sensitive to the diet composition than males'. As expected, males overall had higher body weights at the end of the study compared to female counterparts (**Figure V.1b**).

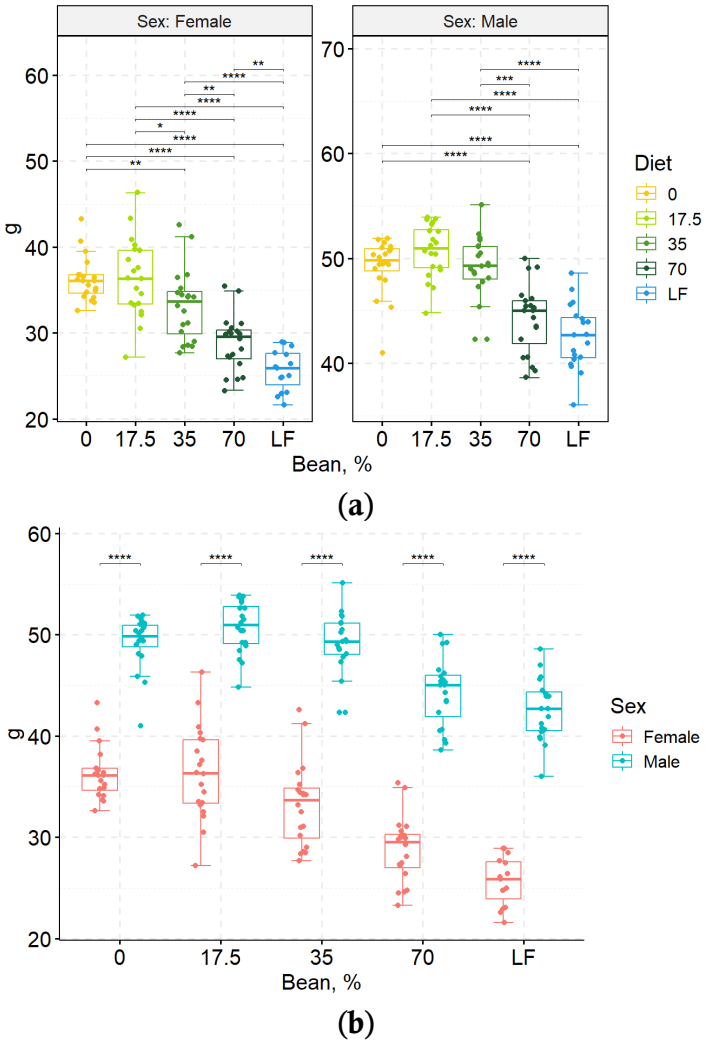

Figure V.1. Effect of dietary bean on body weight. Box plots display final body weights in g at the end of the study across the diet groups and sex cohorts. (**a**) Pairwise comparisons between the diet group using Wilcoxon test; (**b**) Pairwise comparison between sex cohorts were tested with the Mann-Whitney *U* test. The Benjamini–Hochberg method was used for

the multiple testing correction of *p*-values. * *p*-value < 0.05; ** *p*-value < 0.01; *** *p*-value < 0.001; **** *p*-value < 0.0001.

To further investigate anti-obesogenic function of cooked bean consumption, we also assessed the weights of subcutaneous and mesenteric adipose depots, indicative of metabolic health in mice (**Figure V.2**). Despite a visual dose-dependent trend across all groups, statistically lower weights of subcutaneous fat in both females and males were observed only at the 70% bean dose compared to bean-free control (**Figure V.2a**). This effect was potent enough to render differences with the low-fat control also insignificant. In contrast, females gained even less mesenteric fat weight on the low-fat control compared to the high bean dose, while males did not (**Figure V.2c**). Nevertheless, 70% of total dietary protein derived from bean was the dose at which both sex cohorts of mice gained less fat in the mesenteric depot compared to not only bean-free control, but also low and medium doses of bean. In both adipose depots, males consistently exhibited higher weights compared to females (**Figure V.2b** and **V.2d**). Patterns of weight gain reduction in the mesenteric adipose depot of female mice correspond to those observed in the body weights (**Figure V.1a**) and suggest that females are more sensitive to the dietary changes and consumption of bean than males. This is no surprise as the mesenteric fat depot has a greater function in the whole-body metabolic homeostasis maintenance compared to the subcutaneous fat [304], which emphasizes the potency of the preventative effects of bean consumption even more.

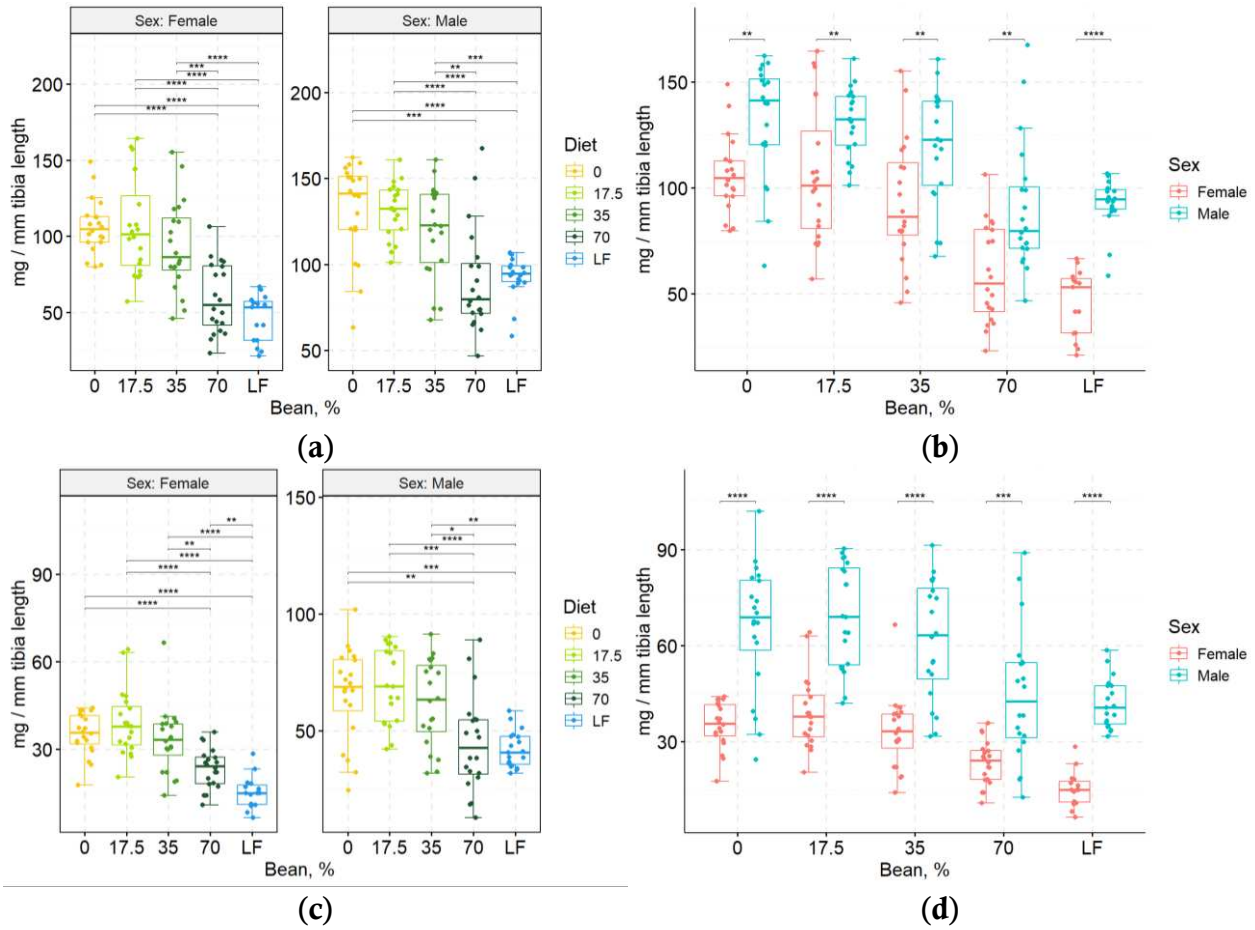

Figure V.2. Effect of dietary bean on adipose tissue weights. Box plots adipose depot weights in mg normalized to the mm of tibia lengths. (**a, b**) Differences between the diet groups and sex cohorts in the gained weights of the subcutaneous fat; (**c, d**) Differences between the diet groups and sex cohorts in the gained weights of the mesenteric fat. (**a, c**) Pairwise comparisons between the diet group using Wilcoxon test; (**b, d**) Pairwise comparison between sex cohorts were tested with the Mann-Whitney *U* test. The Benjamini–Hochberg method was used for the multiple testing correction of *p*-values. * *p*-value < 0.05; ** *p*-value < 0.01; *** *p*-value < 0.001; **** *p*-value < 0.0001.

Collectively, these data further complement the investigations reported in Chapters II–IV, demonstrating that cooked bean consumption exerts multifaceted protection against the metabolic dysregulation driven by high dietary fat: from molecular changes observed in the liver, cecal contents, and plasma to the morphometric changes in body weights, adipose depots, and lipid content in the liver. In the context of the latter, it is important to note that bean-induced suppression of hepatic lipid accumulation in males at medium (35%) bean dose

was marginally insignificant with p-value = 0.028 and q-value = 0.056 using Dunn test (**Figure III.1a**). When we reanalyzed the data with the less conservative Mann-Whitney U test, males also reached statistically significant reduction in liver lipid levels at 35% dose compared to bean-free control (p-value = 0.015 and q-value = 0.031), albeit retaining lack of differences with the 17.5% dose which was observed in females. Altogether, our studies suggest that despite microbial differences observed even at the lowest dose of bean, metabolically significant minimal dose of consumed bean in our studies remains 35% of total dietary protein derived from whole-food cooked bean.

Understanding the dose of bean necessary to achieve health benefits

As reported in Chapters II and III, inter-group differences in microbial populations (i.e., β-diversity) were significant even at the low bean dose (17.5% of total dietary protein or 10% w/w). Reduction of accumulated lipid as well as transcriptomic changes in the liver were detected at the medium dose but were more pronounced at the high dose, i.e., at 35% total protein, or 20% (w/w of the daily diet), and 70% total protein, or 40% (w/w), respectively. Using USDA Food Data Central resource for cannellini bean that was used in the studies herein (FDC ID: 2644287; accounting for dry weight), low, medium, and high bean doses correspond approximately to half, one, and two cans of beans, respectively (presuming a typical can of beans contains ~255 g, or 1 cup, of rinsed cooked bean seed). These are not exaggerated amounts typically used in studies utilizing laboratory animal models to maximize the observability of the investigated effects of the tested food or chemical agents. Instead, our study design ensures the translatability of the observed effects of cooked beans in an obesogenic dietary environment (32% kcal from dietary fat) to human populations in real-world dietary patterns. Approximately 80% of American adults fail to meet the recommended

pulse intake [1], typically consuming about 0.1 cup (25 g) per day [305]. Currently, DGA recommends eating one and a half cups of cooked pulses weekly (70 g/day) [306], whereas countries within the European Union, on average, range from one to three cups per week, albeit 100 g a day in Denmark [307]. Suggested doses of bean/pulse consumption from our studies, therefore, exceed both those normally consumed and the recommended amounts. Nevertheless, they do not exceed amounts consumed regularly, especially by those who prefer plant-based dietary patterns, as they represent only around 600 kcal from cooked bean a day (less than 30% of a typical 2,000 kcal diet).

In a systematic review of 20 human randomized controlled dietary interventions using cooked pulses, consumption of 150 g/day (minimum-maximum: 54–360 g/day) was associated with improvements in the blood lipid profile, blood pressure, inflammatory biomarkers, and body composition [34]. Similar outcomes were summarized in a scoping review of 30 articles reporting an average consumption of 0.5–1 cups of pulses [40]. A 4-week investigation of 1.5 cups of cooked beans per 2000 kcal daily resulted in significantly lower glycemic index, glycemic load, and fasting plasma leptin levels in men, regardless of their insulin resistance status [308]. Of note, this study used an amount of cooked beans equivalent to our high bean dose. Using data from the National Health and Nutrition Examination Survey (NHANES; 2001–2018), Papanikolaou et al. determined that dietary patterns with 1.7–2 servings (170–200 g) of cooked beans per day corresponded to significantly lower BMI, decreased body weight, and improved waist circumference relative to bean-free dietary patterns [276]. The authors concluded that bean-containing dietary patterns enhanced intake of choline, alpha-linolenic acid, folate, vitamin E, iron, magnesium, potassium, calcium, dietary fiber, and other shortfall micronutrients of public health concern, as well as

significantly improved diet quality (healthy eating index, HEI [309]) scores overall. In Beans to Enrich the Gut microbiome vs. Obesity's Negative Effects (BE GONE) study by Zhang et al. [310], 1 cup per day of cooked navy beans (reported to provide 16 g of dietary fiber; 14 g of protein, and 220 kcal overall) for 8 weeks in obese surveillance patients with a history of colorectal cancer was sufficient to enhance the diversity and composition of gut microbiota with parallel shifts in nutrient and microbiome-derived metabolites (e.g., increased pipecolic acid and decreased indole), immune and inflammatory biomarkers (e.g., increased fibroblast-growth factor-19 and decreased IL-10 receptor-α). Recently, Kaimila et al. determined that regular consumption of 80 g of pulses and other legumes was associated with a 3.7 point increase in a sustainable diet quality score (EAT-Lancet index) as well as higher intakes of fiber, vitamins (e.g., vitamin E, thiamine, folate, biotin) and minerals (e.g., sodium, potassium, phosphorus, magnesium, iron, zinc, and manganese), but lower intakes of saturated fats, total and free sugars, with higher plasma selenium and total carotenoid concentrations in UK populations [311]. The study also found that, just like their American counterparts, average UK adults consumed markedly less pulses on a daily basis at 15.0±21.0 g/day. In a 16-week, single-blind, parallel-design, randomized controlled study by Wu et al. [11], 127 Singaporean Chinese participants with prediabetes were given a calorie-restricted (500 kcal deficit) yet pulse-enriched (200 g mixed pulses/day) diet. Compared to the pulse-free control diet (also calorie-restricted, isocaloric, and meat-based), the intervention group exhibited significantly greater reductions in circulating LDL cholesterol, total cholesterol, and glycated hemoglobin (HbA1c), as well as an increase in dietary fiber-degrading species (e.g., *Eubacterium, Roseburia, Bifidobacterium*). These effects were reportedly mediated through metabolites such as bile acids (e.g., decreased hyocholic acid species) and amino acids (e.g.,

decreased fecal branched-chain and aromatic). Therefore, the dose-related findings of our work in mice correspond well to human equivalents of pulse-enriched diets in several investigations, ensuring the translational value of the studies presented herein. This highlights that consumption of medium and even high doses of beans by the human population is not only feasible but also practical, given the culinary versatility of cooked beans (and pulses overall). Should greater awareness of the health benefits from pulse consumption not be enough to incorporate them into people's dietary patterns in sufficient amounts, more information on how to motivate habitual consumption of pulses is available here [31].

Understanding the response to bean's protein and fiber

Microbial changes in the composition and diversity that we observed in our study are a significant indicator that cooked bean may convey its health benefits through the gut microbial ecosystem. According to β-diversity analysis, differences in the richness and abundance of detected bacteria in the cecum were observed at the lowest experimental dose of bean. As a source of dietary protein, albeit limited in its concentration of the essential sulfur-containing amino acids (methionine and cysteine) and tryptophan [303, 312], cooked bean suppressed *Allobaculum, Enterococcus*, *Parabacteroides*, *Streptococcus, Lactobacillus, Lactococcus, Eubacterium_R*, *Bifidobacterium, Faecalibaculum, Clostridium,* and *Turicibacter*—bacteria known for their proteolytic metabolism [129, 313, 314]. Presuming that casein, the control source of dietary protein, was not fully digested by the murine organism, these would be the genera of detected bacteria that were driven, at least in part, by undigested remnants of the dietary protein. At the same time, *Alistipes*, *Bacteroides*, *Eubacterium_F,* and *Sutterella* were enhanced in the bean-based diet compared to the bean-free control. On the surface, consumption of bean provides dietary protein of plant origin that is markedly less

digestible by the mammalian host enzymes and thus increases the probability of its undigested contents reaching the large intestine and becoming accessible to microbial metabolism. Scientific literature [313, 314] generally refers to a high-animal-protein diet as harmful, due to the putrefactive microbial products of proteolytic fermentation, such as amines, ammonia, hydrogen sulfide, phenols, and indoles. These compounds have been linked to a number of diseases, including inflammatory bowel disease and colorectal cancer. Important here was, at least partly, the accessibility of dietary protein, peptides, and amino acids to the colonic bacteria. However, consumption of plant-based protein, after extensive research, has been shown to induce positive changes in the host that are associated with the prevention and treatment of intestinal and whole-body metabolic diseases. Plant-based protein, by definition, is less digestible and thus is more likely to be metabolized by gut bacteria. This highlights the importance of the protein type to which the microbiota are exposed. In our studies, where consumption of beans had markedly beneficial host effects compared to the bean-free diet, total dietary protein contents were comparable in amount yet different in quality: the control diet was comprised of purified protein sources, predominantly casein, and experimental diets had an increasing fraction of total dietary protein comprised of bean protein. Given that none of the aforementioned bacteria are strict protein-degraders, although they were reported to be increased by diets enriched in casein [129, 313, 314], we can only speculate that their suppression by the bean-based diets may be associated with the reduction of dietary casein. Either way, the number of suppressed and enhanced bacteria by the cooked bean suggests that its effects are mediated instead by a different dietary component—dietary fiber.

Even though beans, as a staple food, are known as a rich source of dietary protein, it is essential to recognize that it is also a rich source of dietary fiber, which studies herein

emphasize. Fiber is the predominant substrate for the gut microbiome as mammalian hosts are unable to digest and extract energy from its consumption, and the ratio of protein to fiber is 1:1 in cooked bean. This is an important fact to consider, as the rise of metabolic diseases is directly proportional to the decline in dietary fiber consumption. In the U.S., less than 10% (9% of women and 5% of men [315]) of the population consumes the recommended 28 g of dietary fiber per 2,000 kcal daily [306]. While adequate consumption of dietary fiber has positive outcomes for obesity, diabetes, cardiovascular diseases, autoimmune diseases, neurological aspects, and cancer prevention, not all dietary fibers are created equal [316]. The importance of the latter statement may be superseded by the logical deduction that consumption of any kind of dietary fiber is already better than none, but the work presented herein also suggests that mice benefited from cooked bean's fiber more than from equivalent amounts of purified dietary fiber.

Dietary fiber consists of various complex carbohydrates, many of which are accessible to the microbiota in the gut (MACs). Short-chain fatty acids (SCFAs), such as acetate, propionate, and butyrate, are the most renowned metabolites of gut bacteria produced from the fermentation of MACs. Metabolic profiling of the cecal contents detected only butyrate, albeit undistinguished by Metabolon from its branched isoform isobutyrate, and statistical analysis showed a significant increase in its levels compared to the bean-free control in male mice ($\log_2$FC = 1.496, p-value = 2.76×10^{-6}, q-value = 3.45×10^{-5}). Butyrate is a major energy source for colonic enterocytes, aids in the maintenance of the gut barrier, promotes anti-inflammatory signaling, modulates histone acetylation, and is implicated in other health benefits [317]. Levels of butyrate were reported to be reduced during high-fat diet consumption in mice and associated with the development of fatty liver disease, which was

reversed by consumption of dietary fiber [318]. However, we did not explore the potential of cecum-derived butyrate mediating the effects we observed in the liver because metabolomics showed a lack of difference in butyrate/isobutyrate levels in liver tissue samples ($log_2FC = 0.176$, p-value = 0.812, q-value = 0.878).

In Chapter IV, we addressed the effects of bean-derived chyme and colonic bacteria on bile acid composition in the cecum. Evidence that the former exerts bile acid-sequestering properties was provided without further investigation on whether such effects were due to bean-derived protein remnants or dietary fiber. Both have been reported to possess such chelating properties, nonetheless [38, 214, 271]. However, the importance of further investigating bile acid metabolism in the context of pulse-derived protection from dietary obesogenicity, partly owing to the dietary fat, surpasses that of the differential function of bean-derived protein and fiber. Quantity-wise, we can speculate that dietary fiber appears to be more important, considering the digestibility of bean protein by the host is low yet present, and thus, the colonic microenvironment is impacted more by bean fiber. Our data on microbial ecosystem alteration by bean further support that statement.

Strengths and Limitations

While reporting results from prospective cohort studies or randomized clinical trials is desirable, the data from population studies on the health benefits associated with pulse consumption are promising but not definitive. Moreover, to our knowledge, no population-based studies have addressed the relationship between dose-dependent pulse consumption and metabolic dysfunction-associated liver diseases. Consequently, the use of preclinical studies employing a well-defined animal model for diet-induced obesity, and by extension, MASLD, to inform future human studies and address knowledge gaps is a strength.

An additional strength is the use of a tissue-pooling strategy to represent all animals from each dietary group, when tissue was available, from a large, long-duration common bean dose-response study that investigated both biological sexes. Nonetheless, there are limitations: 1) inability to determine if changes in bile acid metabolism preceded effects on the hepatic accumulation of lipid, 2) feasibility of having Metabolon evaluate all samples from the dose-response study without sample pooling, and 3) the use of global versus targeted profiling of metabolites and transcripts. However, given the magnitude of effects observed, a justification now exists for targeted analyses. Furthermore, without in-depth whole metagenomic profiling, we cannot fully connect the cecal microbiome changes to those observed in the liver and metabolomic data. Compositional profiling of cecal microbiota is limited to 16S rRNA gene presence, ignoring the impacts of viruses, fungi, and other microorganisms in the gut. Whole-genome sequencing traditionally enables the analysis of the intestinal microbiome from a functional repertoire of genes, particularly those involved in metabolic transformations. This would illuminate more mechanistic ties of metabolic transformations in the cecal samples, connecting the dots between affected microorganisms and the metabolites affecting, in turn, the host. Finally, the missing component is the biochemical composition of portal vein plasma, which serves as a proxy for the upstream molecules to which the liver is exposed following gastrointestinal processing of the bean-enriched diet. Such data would elucidate the composition and the net impact of host- and gut microbiota-derived metabolites on the liver, as well as provide crucial information on liver metabolism as a mediator between what the organism is exposed to (dietary components) and what the rest of the organism's system of organs is exposed to.

Significance

In the United States, one of the top risk factors associated with the majority of deaths is *diet* [319]. Poor dietary choices are associated with greater mortality than other diet-related cardiometabolic markers, such as elevated cholesterol or fasting plasma glucose, as well as systolic blood pressure, low bone mineral density, impaired kidney function, low physical activity, air pollution, occupational risks, alcohol and drug use, as well as tobacco use, to name a few. Even when represented as a percentage of disability-adjusted life-years, dietary risks are still in the top three following high body mass index and tobacco use. Thus, dietary choices are crucial determinants of a person's position on the health-disease coordinate system.

While understanding how poor dietary patterns contribute to a higher mortality risk in the U.S. population has garnered significant attention, the question of how diet fits into the context of longevity has also been explored. Analysis of overall dietary patterns of the world's longest-lived people suggests a noteworthy preference for plant-based foods over foods of animal origin or that are ultra-processed [320]. Americans who lived the longest were either vegans or pesco-vegetarians. In this longevity-promoting dietary pattern, macronutrient proportions are typically 65% carbohydrates, 20% fats, and 15% proteins, where animal-based foods constitute only 5% of total kilocalories. Of interest is that centenarians consume less than 2 oz of meat five times a month. Eating less dairy and eggs, as well as limited amounts of fish, was also associated with greater longevity. Naturally, ultra-processed foods and simple sugars are recommended to be replaced with nuts (as a snack), minimally processed foods (such as those cooked, ground, or fermented), and whole foods.

In a 16-year prospective cohort study involving more than 400,000 participants, researchers found that substituting animal-based protein with plant-based protein reduced the risk of overall mortality in both women and men [321]. Notably, substituting egg protein resulted in a greater risk reduction in males (24% versus 21% lower risk in women), while red-meat protein substitution resulted in a lower risk reduction in females (15% versus 12% lower risk in men). The study concluded that replacing as much as 3% of energy from animal protein with plant-based protein was sufficient to observe at least a 10% reduction in overall or cardiovascular disease mortality in both sexes, regardless of smoking status, diabetes, fruit consumption, supplemental vitamin use, or self-reported health status.

Should such interest in plant alternatives continue, the plant-based protein industry is expected to grow to over $27 billion by 2030 [312]. Globally, a substantial amount of plant protein is consumed from legumes of the botanical family Fabaceae. Within that family, the foods contributing to the protein are primarily either oilseed legumes (soy and peanut) or grain legumes, i.e., pulses. Oilseed legumes predominate in economically developed countries, while pulses—in the remainder of the world. Nevertheless, pulses are typical sources of protein across various types of plant-based diets, including vegan, ovo-vegetarian, lacto-vegetarian, lacto-ovo-vegetarian, pesco-vegetarian/pescatarian, and semi-vegetarian/flexitarian [322]. Thus, pulses are treated as a staple food crop, not a vegetable side dish. By definition, a staple food crop is eaten daily in large amounts as it supplies a significant proportion of energy and nutrients, and thus it dominates one's diet and is often affordable and accessible. Common bean, unsurprisingly, is the third most important legume crop grown worldwide, after soybeans and peanuts, making it the top pulse crop accordingly [303]. The abovementioned longevity-oriented food guidelines also recommend consuming

half a cup to one cup of beans per day [320]. Reportedly, centenarians eat at least four times more beans than the average American. In a decision support modeling study that predicts how dietary choices affect life expectancy, switching from a typical Western diet to an optimal diet would increase life expectancy by 10.7 years in women and 13.0 years in men in the U.S., with the most significant gains made by eating more legumes (2.2 years in women and 2.5 years in men).

Future Directions

Dietary patterns containing large amounts of ultra-processed foods, approximately 60% of dietary calories, are highly prevalent in developed and developing countries, along with their associated burden of chronic diseases [17]. However, this has not been the case throughout history. Consumption of a plant-based diet, low in saturated fat and high in disease-preventive phytochemicals, is more consistent with historically observed dietary patterns before the widespread availability and affordability of protein and fat from animal sources [323]. Therefore, as recently proposed by us [217, 324-326], a bean and other pulse-rich diet may represent a healthy and affordable alternative to prevalent yet metabolically dysfunctional Western dietary patterns. Cohort and case-control studies in the diet and colon cancer field suggest a minimum dose of 1 to 1.5 cups of cooked pulses per day is necessary for a reduced colorectal adenoma risk benefit. These levels of intake are representative of those studied herein [310, 327-330]. This dose of pulses is significantly higher than the recommended amount in the 2020–2025 U.S. Dietary Guidelines for Americans. However, both the U.S. NHANES and a similar national survey conducted in Canada document that Hispanic Americans and Asian Canadians within these populations consume these high levels of pulses [134, 331]. A practical approach to sustaining high levels of pulse

consumption is the increased availability of cooked whole food bean (and other pulse) flours to the public. Currently, these flours are commercially produced but are primarily available in bulk quantities (500 kg in 20 kg bags). Interestingly, these flours retain more than 90% of their original dietary protein and fiber and are prepared so that they readily absorb fluid (pre-gelled), which is an essential culinary consideration. A 100g portion of flour is equivalent to 1.5 cups of cooked bean. The same metrics apply to other pulses.

This work inspires further investigations into the biological effects of food components on the host from a pharmacological perspective. While classic pharmacology requires focus on singular compounds with known physicochemical properties, understanding the impact of the whole foods as a collection of biochemicals, their intermediate metabolism by the host and intestinal microorganisms (pharmacokinetics), and the resulting net impact on the host tissues (pharmacodynamics) is tremendously enriched when pharmacological principles are applied. Like drugs, food components undergo the same stages of host digestion and biotransformation. A deeper understanding of how bean components are digested by host enzymes versus microbial enzymes, what resulting metabolites are absorbed by the host versus excreted, and what further biotransformations occur in host tissues should be a goal for studying the health benefits of foods. Obviously, it is impossible to trace such a metabolic pathway of each biochemical within a whole food. However, even understanding the net impacts of a food's metabolome will be potentially groundbreaking in the deduction of molecular mechanisms. Bioavailability is a central concept in pharmacodynamics, particularly in the study of drug-receptor interactions at a molecular level. In terms of food pharmacology, the focus shifts from the net cellular response to a combined effect of food metabolites on an array of cellular receptors and resulting intracellular signaling. Just like

scientific understanding of the gut microbiota influence is shifting from presence and quantity of particular bacterial species and strains to the net impact of gut microbiome as a functional unit of intestinal environment and activity, combining those from the intra- and inter-symbiotic relations between the microorganisms and the host, respectively; so should the study of food components shift from the molecular impacts of one biochemical on a particular host cell type to the systematic effects of food on the collective alterations in tissue function, especially, in the context of chronic disease prevention and therapy. The etiology of these diseases suggests multifaceted changes in the body, which account for their effects on disease pathogenesis. While the influence of diet on these processes is already recognized, the multifaceted effects of foods on the host require the strategic application of principles of food pharmacology to elucidation of the underlying mechanisms accounting for the health benefits of pulse-based dietary patterns.

References

1. World Health Organization. *Obesity and overweight*. Fact sheets 2025 [cited 2025 July 25]; Available from: https://www.who.int/news-room/fact-sheets/detail/obesity-and-overweight.
2. WHO. *Noncommunicable diseases*. Fact sheets 2023 [cited 2024 March 12]; Available from: https://www.who.int/news-room/fact-sheets/detail/noncommunicable-diseases.
3. WHO, *World health statistics 2023: monitoring health for the SDGs, Sustainable Development Goals*. 2023, World Health Organization;: Geneva.
4. Rubino, F., et al., *Definition and diagnostic criteria of clinical obesity.* The Lancet Diabetes & Endocrinology, 2025. **13**(3): p. 221-262.
5. Sookoian, S., C.J. Pirola, and A.J. Sanyal, *MASLD as a non-communicable disease.* Nat Rev Gastroenterol Hepatol, 2025. **22**(3): p. 148-149.
6. Rinella, M.E., et al., *A multisociety Delphi consensus statement on new fatty liver disease nomenclature.* Journal of Hepatology, 2023. **79**(6): p. 1542-1556.
7. Chan, K.E., et al., *Global Prevalence and Clinical Characteristics of Metabolic-associated Fatty Liver Disease: A Meta-Analysis and Systematic Review of 10 739 607 Individuals.* The Journal of Clinical Endocrinology & Metabolism, 2022. **107**(9): p. 2691-2700.
8. Ramírez-Mejía, M.M., et al., *Breaking new ground: MASLD vs. MAFLD—which holds the key for risk stratification?* Hepatology International, 2024. **18**(1): p. 168-178.
9. Lazarus, J.V., et al., *Advancing the global public health agenda for NAFLD: a consensus statement.* Nature Reviews Gastroenterology & Hepatology, 2022. **19**(1): p. 60-78.
10. Lazarus, J.V., et al., *The global NAFLD policy review and preparedness index: Are countries ready to address this silent public health challenge?* Journal of Hepatology, 2022. **76**(4): p. 771-780.
11. Fedacko, J., et al., *Chapter 1 - Western diets and risk of non-communicable diseases*, in *Functional Foods and Nutraceuticals in Metabolic and Non-Communicable Diseases*, R.B. Singh, S. Watanabe, and A.A. Isaza, Editors. 2022, Academic Press. p. 3-21.
12. Akter, S., et al., *Dietary carbohydrates: Pathogenesis and potential therapeutic targets to obesity-associated metabolic syndrome.* BioFactors, 2022. **48**(5): p. 1036-1059.
13. Neuhouser, M.L., *The importance of healthy dietary patterns in chronic disease prevention.* Nutr Res, 2019. **70**: p. 3-6.
14. Bovolini, A., et al., *Metabolic syndrome pathophysiology and predisposing factors.* International Journal of Sports Medicine, 2021. **42**(03): p. 199-214.
15. WHO. *Healthy diet*. Fact sheets 2020 [cited 2024 March 12]; Available from: https://www.who.int/news-room/fact-sheets/detail/healthy-diet.
16. Valicente, V.M., et al., *Ultra-processed foods and obesity risk: a critical review of reported mechanisms.* Advances in nutrition, 2023.
17. Nees, S., T. Lutsiv, and H.J. Thompson, *Ultra-Processed Foods-Dietary Foe or Potential Ally?* Nutrients, 2024. **16**(7).
18. Menichetti, G., et al., *Machine learning prediction of the degree of food processing.* Nature Communications, 2023. **14**(1): p. 2312.
19. Ioannidis, J.P.A., *The Challenge of Reforming Nutritional Epidemiologic Research.* JAMA, 2018. **320**(10): p. 969-970.

20. Mozaffarian, D., I. Rosenberg, and R. Uauy, *History of modern nutrition science—implications for current research, dietary guidelines, and food policy.* BMJ, 2018. **361**: p. k2392.
21. Cámara, M., et al., *Food-Based Dietary Guidelines around the World: A Comparative Analysis to Update AESAN Scientific Committee Dietary Recommendations.* Nutrients, 2021. **13**(9): p. 3131.
22. U.S. Department of Agriculture, U.S.D.o.H.a.H.S., *Dietary Guidelines for Americans, 2020-2025.* . 2020, December: DietaryGuidelines.gov.
23. Ha, K., J.R. Sakaki, and O.K. Chun, *Nutrient Adequacy Is Associated with Reduced Mortality in US Adults.* J Nutr, 2021. **151**(10): p. 3214-3222.
24. Bailey, R.L., et al., *A Proposed Framework for Identifying Nutrients and Food Components of Public Health Relevance in the Dietary Guidelines for Americans.* The Journal of Nutrition, 2021. **151**(5): p. 1197-1204.
25. McBurney, M.I., et al., *Beyond Nutrient Deficiency-Opportunities to Improve Nutritional Status and Promote Health Modernizing DRIs and Supplementation Recommendations.* Nutrients, 2021. **13**(6).
26. Stefano, J.T., et al., *Non-pharmacological management options for MAFLD: a practical guide.* Ther Adv Endocrinol Metab, 2023. **14**: p. 20420188231160394.
27. Zhu, Y., et al., *Dietary fiber intake and non-alcoholic fatty liver disease: The mediating role of obesity.* Front Public Health, 2022. **10**: p. 1038435.
28. Makki, K., et al., *The Impact of Dietary Fiber on Gut Microbiota in Host Health and Disease.* Cell Host & Microbe, 2018. **23**(6): p. 705-715.
29. Tanes, C., et al., *Role of dietary fiber in the recovery of the human gut microbiome and its metabolome.* Cell Host & Microbe, 2021. **29**(3): p. 394-407.e5.
30. So, D., et al., *Dietary fiber intervention on gut microbiota composition in healthy adults: a systematic review and meta-analysis.* The American Journal of Clinical Nutrition, 2018. **107**(6): p. 965-983.
31. Didinger, C. and H. Thompson, *Motivating pulse-centric eating patterns to benefit human and environmental well-being.* Nutrients, 2020. **12**(11): p. 3500.
32. Didinger, C. and H.J. Thompson, *Defining nutritional and functional niches of legumes: A Call for clarity to distinguish a future role for pulses in the Dietary Guidelines for Americans.* Nutrients, 2021. **13**(4): p. 1100.
33. Didinger, C., et al., *Nutrition and Human Health Benefits of Dry Beans and Other Pulses*, in *Dry Beans and Pulses*. 2022. p. 481-504.
34. Ferreira, H., et al., *Benefits of pulse consumption on metabolism and health: A systematic review of randomized controlled trials.* Critical Reviews in Food Science and Nutrition, 2021. **61**(1): p. 85-96.
35. Hall, C., C. Hillen, and J. Garden Robinson, *Composition, Nutritional Value, and Health Benefits of Pulses.* Cereal Chemistry, 2017. **94**(1): p. 11-31.
36. John, H.S., É. Doucet, and K.A. Power, *Dietary pulses as a means to improve the gut microbiome, inflammation, and appetite control in obesity.* Obesity Reviews, 2023. **24**(9): p. e13598.
37. Kazemi, M., et al., *Pulses and Prevention and Management of Chronic Disease*, in *Health Benefits of Pulses*, W.J. Dahl, Editor. 2019, Springer International Publishing: Cham. p. 55-72.

38. Singh, B., et al., *Bioactive constituents in pulses and their health benefits.* Journal of Food Science and Technology, 2017. **54**(4): p. 858-870.
39. Viguiliouk, E., et al., *Can pulses play a role in improving cardiometabolic health? Evidence from systematic reviews and meta-analyses.* Annals of the New York Academy of Sciences, 2017. **1392**(1): p. 43-57.
40. Zhao, N., et al., *Pulse Consumption and Health Outcomes: A Scoping Review.* Nutrients, 2024. **16**(10): p. 1435.
41. Didinger, C. and H.J. Thompson, *The role of pulses in improving human health: A review.* Legume Science, 2022. **4**(4).
42. Thompson, H.J., *The Dietary Guidelines for Americans (2020–2025): Pulses, Dietary Fiber, and Chronic Disease Risk—A Call for Clarity and Action.* Nutrients, 2021. **13**(11): p. 4034.
43. Mitchell, D.C., et al., *Pulse Intake Improves Nutrient Density among US Adult Consumers.* Nutrients, 2021. **13**(8): p. 2668.
44. Lutsiv, T., et al., *Compositional Changes of the High-Fat Diet-Induced Gut Microbiota upon Consumption of Common Pulses.* Nutrients, 2021. **13**(11): p. 3992.
45. McGinley, J.N., et al., *Pulse Crop Effects on Gut Microbial Populations, Intestinal Function, and Adiposity in a Mouse Model of Diet-Induced Obesity.* Nutrients, 2020. **12**(3): p. 593.
46. Thompson, H.J., et al., *Beneficial Effects of Common Bean on Adiposity and Lipid Metabolism.* Nutrients, 2017. **9**(9): p. 998.
47. Neil, E.S., et al., *White Kidney Bean (Phaseolus Vulgaris L.) Consumption Reduces Fat Accumulation in a Polygenic Mouse Model of Obesity.* Nutrients, 2019. **11**(11): p. 2780.
48. Jiang, W., et al., *Identification of a molecular signature underlying inhibition of mammary carcinoma growth by dietary N-3 fatty acids.* Cancer Res, 2012. **72**(15): p. 3795-3806.
49. Mensack, M.M., J.N. McGinley, and H.J. Thompson, *Metabolomic analysis of the effects of edible dry beans (Phaseolus vulgaris L.) on tissue lipid metabolism and carcinogenesis in rats.* British Journal of Nutrition, 2012. **108**(S1): p. S155-S165.
50. World Health Organization. *Noncommunicable diseases*. 2021, April 13 [cited 2021 December 21]; Available from: https://www.who.int/news-room/fact-sheets/detail/noncommunicable-diseases.
51. Neuhouser, M.L., *The importance of healthy dietary patterns in chronic disease prevention.* Nutrition research (New York, N.Y.), 2019. **70**: p. 3-6.
52. Johnson, M., *Diet and nutrition: Implications to cardiometabolic health.* Journal of Cardiology and Cardiovascular Sciences, 2019. **3**(2).
53. Oren, A. and G.M. Garrity, *Valid publication of the names of forty-two phyla of prokaryotes.* International Journal of Systematic and Evolutionary Microbiology, 2021. **71**(10).
54. Lagkouvardos, I., et al., *Sequence and cultivation study of Muribaculaceae reveals novel species, host preference, and functional potential of this yet undescribed family.* Microbiome, 2019. **7**(1): p. 28.
55. Zhang, C., C.L. Franklin, and A.C. Ericsson, *Consideration of Gut Microbiome in Murine Models of Diseases.* Microorganisms, 2021. **9**(5): p. 1062.
56. Hugenholtz, F. and W.M. de Vos, *Mouse models for human intestinal microbiota research: a critical evaluation.* Cell Mol Life Sci, 2018. **75**(1): p. 149-160.
57. Chu, D.T., et al., *C57BL/6J mice as a polygenic developmental model of diet-induced obesity.* Physiol Rep, 2017. **5**(7).
58. Jang, H., *High-Fat Diets for Diet-Induced Obesity (DIO) Models.* 2017.

59. Lee, D.M., et al., *SGLT2 inhibition via dapagliflozin improves generalized vascular dysfunction and alters the gut microbiota in type 2 diabetic mice.* Cardiovascular Diabetology, 2018. **17**(1): p. 62.
60. Bolyen, E., et al., *Reproducible, interactive, scalable and extensible microbiome data science using QIIME 2.* Nature Biotechnology, 2019. **37**(8): p. 852-857.
61. Callahan, B.J., et al., *DADA2: High-resolution sample inference from Illumina amplicon data.* Nature Methods, 2016. **13**(7): p. 581-583.
62. Bokulich, N.A., et al., *Optimizing taxonomic classification of marker-gene amplicon sequences with QIIME 2's q2-feature-classifier plugin.* Microbiome, 2018. **6**(1): p. 90.
63. McDonald, D., et al., *An improved Greengenes taxonomy with explicit ranks for ecological and evolutionary analyses of bacteria and archaea.* The ISME Journal, 2012. **6**(3): p. 610-618.
64. Price, M.N., P.S. Dehal, and A.P. Arkin, *FastTree 2 – Approximately Maximum-Likelihood Trees for Large Alignments.* PLOS ONE, 2010. **5**(3): p. e9490.
65. Katoh, K. and D.M. Standley, *MAFFT Multiple Sequence Alignment Software Version 7: Improvements in Performance and Usability.* Molecular Biology and Evolution, 2013. **30**(4): p. 772-780.
66. Dhariwal, A., et al., *MicrobiomeAnalyst: a web-based tool for comprehensive statistical, visual and meta-analysis of microbiome data.* Nucleic Acids Research, 2017. **45**(W1): p. W180-W188.
67. Chong, J., et al., *Using MicrobiomeAnalyst for comprehensive statistical, functional, and meta-analysis of microbiome data.* Nature Protocols, 2020. **15**(3): p. 799-821.
68. Foster, Z.S.L., T.J. Sharpton, and N.J. Grünwald, *Metacoder: An R package for visualization and manipulation of community taxonomic diversity data.* PLOS Computational Biology, 2017. **13**(2): p. e1005404.
69. Segata, N., et al., *Metagenomic biomarker discovery and explanation.* Genome biology, 2011. **12**(6): p. R60-R60.
70. Douglas, G.M., et al., *PICRUSt2 for prediction of metagenome functions.* Nature Biotechnology, 2020. **38**(6): p. 685-688.
71. Barbera, P., et al., *EPA-ng: Massively Parallel Evolutionary Placement of Genetic Sequences.* Systematic Biology, 2018. **68**(2): p. 365-369.
72. Czech, L., P. Barbera, and A. Stamatakis, *Genesis and Gappa: processing, analyzing and visualizing phylogenetic (placement) data.* Bioinformatics, 2020. **36**(10): p. 3263-3265.
73. Louca, S. and M. Doebeli, *Efficient comparative phylogenetics on large trees.* Bioinformatics, 2017. **34**(6): p. 1053-1055.
74. Ye, Y. and T.G. Doak, *A Parsimony Approach to Biological Pathway Reconstruction/Inference for Genomes and Metagenomes.* PLOS Computational Biology, 2009. **5**(8): p. e1000465.
75. Caspi, R., et al., *The MetaCyc database of metabolic pathways and enzymes.* Nucleic acids research, 2018. **46**(D1): p. D633-D639.
76. Parks, D.H., et al., *STAMP: statistical analysis of taxonomic and functional profiles.* Bioinformatics (Oxford, England), 2014. **30**(21): p. 3123-3124.
77. Ganesan, K. and B. Xu, *Polyphenol-Rich Dry Common Beans (Phaseolus vulgaris L.) and Their Health Benefits.* International journal of molecular sciences, 2017. **18**(11): p. 2331.

78. de Almeida Costa, G.E., et al., *Chemical composition, dietary fibre and resistant starch contents of raw and cooked pea, common bean, chickpea and lentil legumes.* Food chemistry, 2006. **94**(3): p. 327-330.
79. Kleintop, A.E., et al., *Adaptation of the AOAC 2011.25 integrated total dietary fiber assay to determine the dietary fiber and oligosaccharide content of dry edible beans.* Journal of agricultural and food chemistry, 2013. **61**(40): p. 9719-9726.
80. Sender, R., S. Fuchs, and R. Milo, *Revised Estimates for the Number of Human and Bacteria Cells in the Body.* PLOS Biology, 2016. **14**(8): p. e1002533.
81. Org, E., et al., *Sex differences and hormonal effects on gut microbiota composition in mice.* Gut Microbes, 2016. **7**(4): p. 313-322.
82. Kim, Y.S., et al., *Sex Differences in Gut Microbiota.* wjmh, 2019. **38**(1): p. 48-60.
83. Koo, S.H., et al., *A pilot study to examine the association between human gut microbiota and the host's central obesity.* JGH Open, 2019. **3**(6): p. 480-487.
84. Del Chierico, F., et al., *Gut Microbiota Markers in Obese Adolescent and Adult Patients: Age-Dependent Differential Patterns.* Frontiers in microbiology, 2018. **9**: p. 1210-1210.
85. Crovesy, L., D. Masterson, and E.L. Rosado, *Profile of the gut microbiota of adults with obesity: a systematic review.* European Journal of Clinical Nutrition, 2020. **74**(9): p. 1251-1262.
86. Ye, J., et al., *Pu-erh tea ameliorates obesity and modulates gut microbiota in high fat diet fed mice.* Food Res Int, 2021. **144**: p. 110360.
87. Li, A., et al., *Modulation effect of chenpi extract on gut microbiota in high-fat diet-induced obese C57BL/6 mice.* Journal of Food Biochemistry, 2021. **45**(4): p. e13541.
88. Liu, Y., et al., *The ameliorative effect of Lactobacillus plantarum Y44 oral administration on inflammation and lipid metabolism in obese mice fed with a high fat diet.* Food & Function, 2020. **11**(6): p. 5024-5039.
89. Murga-Garrido, S.M., et al., *Gut microbiome variation modulates the effects of dietary fiber on host metabolism.* Microbiome, 2021. **9**(1): p. 117.
90. Wang, Y., et al., *Phylogenomics of expanding uncultured environmental Tenericutes provides insights into their pathogenicity and evolutionary relationship with Bacilli.* BMC Genomics, 2020. **21**(1): p. 408.
91. Nayfach, S., et al., *New insights from uncultivated genomes of the global human gut microbiome.* Nature, 2019. **568**(7753): p. 505-510.
92. Ding, Y., et al., *Honokiol Ameliorates High-Fat-Diet-Induced Obesity of Different Sexes of Mice by Modulating the Composition of the Gut Microbiota.* Frontiers in Immunology, 2019. **10**(2800).
93. Cao, W., et al., *The role of gut microbiota in the resistance to obesity in mice fed a high fat diet.* International Journal of Food Sciences and Nutrition, 2020. **71**(4): p. 453-463.
94. Monk, J.M., et al., *Navy Bean Supplementation in Established High-Fat Diet-Induced Obesity Attenuates the Severity of the Obese Inflammatory Phenotype.* Nutrients, 2021. **13**(3): p. 757.
95. Tan, Y., et al., *Cooked Black Turtle Beans Ameliorate Insulin Resistance and Restore Gut Microbiota in C57BL/6J Mice on High-Fat Diets.* Foods, 2021. **10**(8): p. 1691.
96. Gomes Mariana, J.C., et al., *Common Bean (Phaseolus vulgaris L.) Flour Can Improve the Gut Microbiota Composition and Function in Mice Fed a High-Fat Diet.* Current Developments in Nutrition, 2021. **5**(Supplement_2): p. 1159-1159.

97. Jang, L.-G., et al., *The combination of sport and sport-specific diet is associated with characteristics of gut microbiota: an observational study.* Journal of the International Society of Sports Nutrition, 2019. **16**(1): p. 21.
98. Wang, L., et al., *Methionine Restriction Regulates Cognitive Function in High-Fat Diet-Fed Mice: Roles of Diurnal Rhythms of SCFAs Producing- and Inflammation-Related Microbes.* Molecular Nutrition & Food Research, 2020. **64**(17): p. 2000190.
99. Hwang, N., et al., *Genes and Gut Bacteria Involved in Luminal Butyrate Reduction Caused by Diet and Loperamide.* Genes, 2017. **8**(12): p. 350.
100. Wei, G., et al., *Effect of banana pulp dietary fibers on metabolic syndrome and gut microbiota diversity in high-fat diet mice.* Journal of Food Biochemistry, 2020. **44**(9): p. e13362.
101. Mallozzi, M., V.K. Viswanathan, and G. Vedantam, *Spore-forming Bacilli and Clostridia in human disease.* Future Microbiology, 2010. **5**(7): p. 1109-1123.
102. Wexler, A.G. and A.L. Goodman, *An insider's perspective: Bacteroides as a window into the microbiome.* Nature Microbiology, 2017. **2**(5): p. 17026.
103. Yoshida, N., et al., *Bacteroides spp. promotes branched-chain amino acid catabolism in brown fat and inhibits obesity.* iScience, 2021. **24**(11): p. 103342.
104. Castaner, O., et al., *The Gut Microbiome Profile in Obesity: A Systematic Review.* International journal of endocrinology, 2018. **2018**: p. 4095789-4095789.
105. Tseng, C.-H. and C.-Y. Wu, *The gut microbiome in obesity.* Journal of the Formosan Medical Association, 2019. **118**: p. S3-S9.
106. Chijiiwa, R., et al., *Single-cell genomics of uncultured bacteria reveals dietary fiber responders in the mouse gut microbiota.* Microbiome, 2020. **8**(1): p. 5.
107. Holscher, H.D., *Dietary fiber and prebiotics and the gastrointestinal microbiota.* Gut microbes, 2017. **8**(2): p. 172-184.
108. Hemsworth, G.R., et al., *Structural dissection of a complex Bacteroides ovatus gene locus conferring xyloglucan metabolism in the human gut.* Open Biol, 2016. **6**(7).
109. Nakajima, A., et al., *A Soluble Fiber Diet Increases Bacteroides fragilis Group Abundance and Immunoglobulin A Production in the Gut.* Applied and Environmental Microbiology, 2020. **86**(13): p. e00405-20.
110. Sukkar, S.G. and M. Muscaritoli, *A Clinical Perspective of Low Carbohydrate Ketogenic Diets: A Narrative Review.* Frontiers in nutrition, 2021. **8**: p. 642628-642628.
111. Tomova, A., et al., *The Effects of Vegetarian and Vegan Diets on Gut Microbiota.* Frontiers in nutrition, 2019. **6**: p. 47-47.
112. Lonnie, M., et al., *Protein for Life: Review of Optimal Protein Intake, Sustainable Dietary Sources and the Effect on Appetite in Ageing Adults.* Nutrients, 2018. **10**(3): p. 360.
113. Derbyshire, E. and J. Delange, *Chapter 2 - The nutritional value of whole pulses and pulse fractions*, in *Pulse Foods (Second Edition)*, B.K. Tiwari, A. Gowen, and B. McKenna, Editors. 2021, Academic Press. p. 9-29.
114. Maqbool, N., et al., *Cooking methods affect eating quality, bio-functional components, antinutritional compounds and sensory attributes of selected vegetables.* Italian Journal of Food Science, 2021. **33**(SP1): p. 150-162.
115. Wainaina, I., et al., *Thermal treatment of common beans (Phaseolus vulgaris L.): Factors determining cooking time and its consequences for sensory and nutritional quality.* Comprehensive Reviews in Food Science and Food Safety, 2021. **20**(4): p. 3690-3718.

116. Jha, R., et al., *Dietary Fiber and Intestinal Health of Monogastric Animals.* Frontiers in Veterinary Science, 2019. **6**.
117. Diether, N.E. and B.P. Willing, *Microbial Fermentation of Dietary Protein: An Important Factor in Diet¯Microbe¯Host Interaction.* Microorganisms, 2019. **7**(1): p. 19.
118. Yao, C.K., J.G. Muir, and P.R. Gibson, *Review article: insights into colonic protein fermentation, its modulation and potential health implications.* Alimentary Pharmacology & Therapeutics, 2016. **43**(2): p. 181-196.
119. Division, N.a.F.S., *FAO/INFOODS Global database for pulses on dry matter basis. Version 1.0 - PulsesDM1.0*. 2017, FAO: Rome, Italy. p. #33 p.
120. Thompson, H.J. and M.A. Brick, *Perspective: Closing the Dietary Fiber Gap: An Ancient Solution for a 21st Century Problem.* Advances in nutrition (Bethesda, Md.), 2016. **7**(4): p. 623-626.
121. Koh, A., et al., *From Dietary Fiber to Host Physiology: Short-Chain Fatty Acids as Key Bacterial Metabolites.* Cell, 2016. **165**(6): p. 1332-1345.
122. Xiang, S., et al., *Xylitol enhances synthesis of propionate in the colon via cross-feeding of gut microbiota.* Microbiome, 2021. **9**(1): p. 62.
123. Zaibi, M.S., et al., *Roles of GPR41 and GPR43 in leptin secretory responses of murine adipocytes to short chain fatty acids.* FEBS letters, 2010. **584**(11): p. 2381-2386.
124. Kumar, J., K. Rani, and C. Datt, *Molecular link between dietary fibre, gut microbiota and health.* Molecular Biology Reports, 2020. **47**(8): p. 6229-6237.
125. Iskandar, C.F., et al., *Review of lactose and galactose metabolism in Lactic Acid Bacteria dedicated to expert genomic annotation.* Trends in Food Science & Technology, 2019. **88**: p. 121-132.
126. Pessione, E., *Lactic acid bacteria contribution to gut microbiota complexity: lights and shadows.* Frontiers in Cellular and Infection Microbiology, 2012. **2**.
127. Zhao, F., et al., *A Short-Term Feeding of Dietary Casein Increases Abundance of Lactococcus lactis and Upregulates Gene Expression Involving Obesity Prevention in Cecum of Young Rats Compared With Dietary Chicken Protein.* Frontiers in microbiology, 2019. **10**: p. 2411-2411.
128. Centanni, M., et al., *Bifidobacterium pseudolongum in the Ceca of Rats Fed Hi-Maize Starch Has Characteristics of a Keystone Species in Bifidobacterial Blooms.* Applied and Environmental Microbiology, 2018. **84**(15): p. e00547-18.
129. Oliphant, K. and E. Allen-Vercoe, *Macronutrient metabolism by the human gut microbiome: major fermentation by-products and their impact on host health.* Microbiome, 2019. **7**(1): p. 91.
130. Ma, N., et al., *Contributions of the Interaction Between Dietary Protein and Gut Microbiota to Intestinal Health.* Curr Protein Pept Sci, 2017. **18**(8): p. 795-808.
131. Zhao, J., et al., *Dietary Protein and Gut Microbiota Composition and Function.* Curr Protein Pept Sci, 2019. **20**(2): p. 145-154.
132. Giuberti, G., et al., *Nutrients' and Antinutrients' Seed Content in Common Bean (Phaseolus vulgaris L.) Lines Carrying Mutations Affecting Seed Composition.* 2019. **9**(6): p. 317.
133. Rodríguez-Daza, M.C., et al., *Polyphenol-Mediated Gut Microbiota Modulation: Toward Prebiotics and Further.* Front Nutr, 2021. **8**: p. 689456.
134. Mudryj, A.N., et al., *Pulse consumption in Canadian adults influences nutrient intakes.* Br J Nutr, 2012. **108 Suppl 1**: p. S27-36.

135. Eslam, M., et al., *MAFLD: A Consensus-Driven Proposed Nomenclature for Metabolic Associated Fatty Liver Disease.* Gastroenterology, 2020. **158**(7): p. 1999-2014.e1.
136. Xian, Y.X., J.P. Weng, and F. Xu, *MAFLD vs. NAFLD: shared features and potential changes in epidemiology, pathophysiology, diagnosis, and pharmacotherapy.* Chin Med J (Engl), 2020. **134**(1): p. 8-19.
137. Nassir, F., et al., *Pathogenesis and Prevention of Hepatic Steatosis.* Gastroenterol Hepatol (N Y), 2015. **11**(3): p. 167-75.
138. Cholankeril, G., et al., *Liver transplantation for nonalcoholic steatohepatitis in the US: temporal trends and outcomes.* Digestive diseases and sciences, 2017. **62**(10): p. 2915-2922.
139. Goldberg, D., et al., *Changes in the Prevalence of Hepatitis C Virus Infection, Nonalcoholic Steatohepatitis, and Alcoholic Liver Disease Among Patients With Cirrhosis or Liver Failure on the Waitlist for Liver Transplantation.* Gastroenterology, 2017. **152**(5): p. 1090-1099.e1.
140. Riazi, K., et al., *The prevalence and incidence of NAFLD worldwide: a systematic review and meta-analysis.* The Lancet Gastroenterology & Hepatology, 2022.
141. Alalwani, J., et al., *The impact of health status, diet and lifestyle on non-alcoholic fatty liver disease: Narrative review.* Clinical Obesity, 2022. **12**(4): p. e12525.
142. *Sex Differences in Nonalcoholic Fatty Liver Disease: Estrogen Influence on the Liver–Adipose Tissue Crosstalk.* Antioxidants & Redox Signaling, 2021. **35**(9): p. 753-774.
143. Löfgren, L., G.-B. Forsberg, and M. Ståhlman, *The BUME method: a new rapid and simple chloroform-free method for total lipid extraction of animal tissue.* Scientific Reports, 2016. **6**(1): p. 27688.
144. Krämer, A., et al., *Causal analysis approaches in Ingenuity Pathway Analysis.* Bioinformatics, 2013. **30**(4): p. 523-530.
145. Marjot, T., et al., *Nonalcoholic Fatty Liver Disease in Adults: Current Concepts in Etiology, Outcomes, and Management.* Endocrine Reviews, 2020. **41**(1): p. 66-117.
146. Yoon, H., et al., *Lipid metabolism in sickness and in health: Emerging regulators of lipotoxicity.* Molecular Cell, 2021. **81**(18): p. 3708-3730.
147. Geng, Y., et al., *How does hepatic lipid accumulation lead to lipotoxicity in non-alcoholic fatty liver disease?* Hepatology International, 2021. **15**(1): p. 21-35.
148. Nassir, F., *NAFLD: Mechanisms, Treatments, and Biomarkers.* Biomolecules, 2022. **12**(6): p. 824.
149. Alves-Bezerra, M. and D.E. Cohen, *Triglyceride Metabolism in the Liver.* Compr Physiol, 2017. **8**(1): p. 1-8.
150. Ipsen, D.H., J. Lykkesfeldt, and P. Tveden-Nyborg, *Molecular mechanisms of hepatic lipid accumulation in non-alcoholic fatty liver disease.* Cellular and Molecular Life Sciences, 2018. **75**(18): p. 3313-3327.
151. Xiao, Y., M. Kim, and M.A. Lazar, *Nuclear receptors and transcriptional regulation in non-alcoholic fatty liver disease.* Molecular Metabolism, 2021. **50**: p. 101119.
152. Liang, N., et al., *The Nuclear Receptor-Co-repressor Complex in Control of Liver Metabolism and Disease.* Front Endocrinol (Lausanne), 2019. **10**: p. 411.
153. Sahoo, S., et al., *Emergent Properties of the HNF4α-PPARγ Network May Drive Consequent Phenotypic Plasticity in NAFLD.* Journal of Clinical Medicine, 2020. **9**(3): p. 870.

154. Loft, A., et al., *Liver-fibrosis-activated transcriptional networks govern hepatocyte reprogramming and intra-hepatic communication.* Cell Metabolism, 2021. **33**(8): p. 1685-1700.e9.
155. Shin, D.W., *Lipophagy: Molecular Mechanisms and Implications in Metabolic Disorders.* Mol Cells, 2020. **43**(8): p. 686-693.
156. Grefhorst, A., et al., *The Role of Lipophagy in the Development and Treatment of Non-Alcoholic Fatty Liver Disease.* Front Endocrinol (Lausanne), 2020. **11**: p. 601627.
157. Filali-Mouncef, Y., et al., *The ménage à trois of autophagy, lipid droplets and liver disease.* Autophagy, 2022. **18**(1): p. 50-72.
158. Ma, M., W. Xie, and X. Li, *Identification of Autophagy-Related Genes in the Progression from Non-Alcoholic Fatty Liver to Non-Alcoholic Steatohepatitis.* Int J Gen Med, 2021. **14**: p. 3163-3176.
159. Jarc, E. and T. Petan, *Lipid Droplets and the Management of Cellular Stress.* Yale J Biol Med, 2019. **92**(3): p. 435-452.
160. Hodson, L. and P.J. Gunn, *The regulation of hepatic fatty acid synthesis and partitioning: the effect of nutritional state.* Nature Reviews Endocrinology, 2019. **15**(12): p. 689-700.
161. Donnelly, K.L., et al., *Sources of fatty acids stored in liver and secreted via lipoproteins in patients with nonalcoholic fatty liver disease.* J Clin Invest, 2005. **115**(5): p. 1343-51.
162. Wang, C., et al., *Rapamycin-mediated CD36 translational suppression contributes to alleviation of hepatic steatosis.* Biochem Biophys Res Commun, 2014. **447**(1): p. 57-63.
163. Lehner, R. and A.D. Quiroga, *Chapter 5 - Fatty Acid Handling in Mammalian Cells*, in *Biochemistry of Lipids, Lipoproteins and Membranes (Sixth Edition)*, N.D. Ridgway and R.S. McLeod, Editors. 2016, Elsevier: Boston. p. 149-184.
164. Anderson, C.M. and A. Stahl, *SLC27 fatty acid transport proteins.* Mol Aspects Med, 2013. **34**(2-3): p. 516-28.
165. Ipsen, D.H., J. Lykkesfeldt, and P. Tveden-Nyborg, *Molecular mechanisms of hepatic lipid accumulation in non-alcoholic fatty liver disease.* Cell Mol Life Sci, 2018. **75**(18): p. 3313-3327.
166. Badmus, O.O., et al., *Molecular mechanisms of metabolic associated fatty liver disease (MAFLD): functional analysis of lipid metabolism pathways.* Clin Sci (Lond), 2022. **136**(18): p. 1347-1366.
167. Mashek, D.G., *Hepatic Fatty Acid Trafficking: Multiple Forks in the Road.* Advances in Nutrition, 2013. **4**(6): p. 697-710.
168. Talley, J.T. and S.S. Mohiuddin, *Biochemistry, Fatty Acid Oxidation*, in *StatPearls*. 2022, StatPearls Publishing

169. Schreurs, M., F. Kuipers, and F.R. Van Der Leij, *Regulatory enzymes of mitochondrial β-oxidation as targets for treatment of the metabolic syndrome.* Obesity Reviews, 2010. **11**(5): p. 380-388.
170. Diebold, I., et al., *HADHA and HADHB gene associated phenotypes - Identification of rare variants in a patient cohort by Next Generation Sequencing.* Molecular and Cellular Probes, 2019. **44**: p. 14-20.
171. Watkins, P.A., L. Chen, and N. Braverman, *Peroxisomal Disorders in Children*, in *Liver Disease in Children*, F.J. Suchy, R.J. Sokol, and W.F. Balistreri, Editors. 2021, Cambridge University Press: Cambridge. p. 671-697.

172. Wanders, R.J.A., et al., *Peroxisomes, lipid metabolism and lipotoxicity.* Biochimica et Biophysica Acta (BBA) - Molecular and Cell Biology of Lipids, 2010. **1801**(3): p. 272-280.
173. Scorletti, E. and R.M. Carr, *A new perspective on NAFLD: Focusing on lipid droplets.* Journal of Hepatology, 2022. **76**(4): p. 934-945.
174. Moya, M., et al., *Foxa1 reduces lipid accumulation in human hepatocytes and is down-regulated in nonalcoholic fatty liver.* PLoS One, 2012. **7**(1): p. e30014.
175. Popkin, B.M. and S.W. Ng, *The nutrition transition to a stage of high obesity and noncommunicable disease prevalence dominated by ultra-processed foods is not inevitable.* Obesity Reviews, 2022. **23**(1): p. e13366.
176. Chia, A., et al., *Social entrepreneurship in obesity prevention: A scoping review.* Obesity Reviews, 2022. **23**(3): p. e13378.
177. Wells, J.C., et al., *The double burden of malnutrition: aetiological pathways and consequences for health.* Lancet, 2020. **395**(10217): p. 75-88.
178. Lazarus, J.V., et al., *A sustainable development goal framework to guide multisectoral action on NAFLD through a societal approach.* Alimentary Pharmacology & Therapeutics, 2022. **55**(2): p. 234-243.
179. Naeem, M., et al., *Associations of liver volume and other markers of hepatic steatosis with all-cause mortality in the general population.* Liver International, 2022. **42**(3): p. 575-584.
180. Rada, P., et al., *Understanding lipotoxicity in NAFLD pathogenesis: is CD36 a key driver?* Cell Death & Disease, 2020. **11**(9): p. 802.
181. Pei, K., et al., *An Overview of Lipid Metabolism and Nonalcoholic Fatty Liver Disease.* Biomed Res Int, 2020. **2020**: p. 4020249.
182. Schönfeld, P. and L. Wojtczak, *Short- and medium-chain fatty acids in energy metabolism: the cellular perspective.* J Lipid Res, 2016. **57**(6): p. 943-54.
183. Wilson, C.G., et al., *Hepatocyte-Specific Disruption of CD36 Attenuates Fatty Liver and Improves Insulin Sensitivity in HFD-Fed Mice.* Endocrinology, 2016. **157**(2): p. 570-85.
184. Enjoji, M., M. Kohjima, and M. Nakamuta, *Lipid metabolism and the liver*, in *The Liver in Systemic Diseases*. 2016, Springer. p. 105-122.
185. Chella Krishnan, K., et al., *Integration of Multi-omics Data from Mouse Diversity Panel Highlights Mitochondrial Dysfunction in Non-alcoholic Fatty Liver Disease.* Cell Systems, 2018. **6**(1): p. 103-115.e7.
186. Kurt, Z., et al., *Tissue-specific pathways and networks underlying sexual dimorphism in non-alcoholic fatty liver disease.* Biology of Sex Differences, 2018. **9**(1): p. 46.
187. Goossens, G.H., J.W.E. Jocken, and E.E. Blaak, *Sexual dimorphism in cardiometabolic health: the role of adipose tissue, muscle and liver.* Nature Reviews Endocrinology, 2021. **17**(1): p. 47-66.
188. Link, J.C. and K. Reue, *Genetic Basis for Sex Differences in Obesity and Lipid Metabolism.* Annu Rev Nutr, 2017. **37**: p. 225-245.
189. Daniel, P.V. and P. Mondal, *Causative and Sanative dynamicity of ChREBP in Hepato-Metabolic disorders.* European Journal of Cell Biology, 2020. **99**(8): p. 151128.
190. Miao, L., et al., *Current status and future trends of the global burden of MASLD.* Trends in Endocrinology & Metabolism, 2024. **35**(8): p. 697-707.
191. Song, S.J., et al., *Can we use old NAFLD data under the new MASLD definition?* Journal of Hepatology, 2024. **80**(2): p. e54-e56.

192. He, L., et al., *Changing from NAFLD to MASLD: The new definition can more accurately identify individuals at higher risk for diabetes.* Journal of Hepatology, 2024. **80**(2): p. e85-e87.
193. Chan, W.K., et al., *Metabolic Dysfunction-Associated Steatotic Liver Disease (MASLD): A State-of-the-Art Review.* J Obes Metab Syndr, 2023. **32**(3): p. 197-213.
194. of, U.S.D.o.A.a.U.S.D. and H.a.H. Services., *Dietary Guidelines for Americans, 2020-2025.* 2020.
195. García, S., et al., *Ultra-Processed Food Consumption and Metabolic-Dysfunction-Associated Steatotic Liver Disease (MASLD): A Longitudinal and Sustainable Analysis.* Nutrients, 2025. **17**(3).
196. Wang, D., et al., *Research advances in the diagnosis and treatment of MASLD/MASH.* Annals of Medicine, 2025. **57**(1): p. 2445780.
197. Cominelli, E., et al., *Antinutritional factors, nutritional improvement, and future food use of common beans: A perspective.* Front Plant Sci, 2022. **13**: p. 992169.
198. Ha, V., et al., *Effect of dietary pulse intake on established therapeutic lipid targets for cardiovascular risk reduction: a systematic review and meta-analysis of randomized controlled trials.* Cmaj, 2014. **186**(8): p. E252-62.
199. Brick, M.A., et al., *Dry Bean: A Protein-Rich Superfood With Carbohydrate Characteristics That Can Close the Dietary Fiber Gap.* Front Plant Sci, 2022. **13**: p. 914412.
200. Li, M. and S. Ma, *A review of healthy role of dietary fiber in modulating chronic diseases.* Food Research International, 2024. **191**: p. 114682.
201. Fu, J., et al., *Dietary Fiber Intake and Gut Microbiota in Human Health.* Microorganisms, 2022. **10**(12).
202. Lutsiv, T., et al., *Thwarting Metabolic Dysfunction-Associated Fatty Liver Disease (MAFLD) with Common Bean: Dose- and Sex-Dependent Protection against Hepatic Steatosis.* Nutrients, 2023. **15**(3).
203. Fitzgerald, V.K., et al., *Common Bean Suppresses Hepatic Ceramide Metabolism in a Mouse Model of Metabolic Dysfunction-Associated Steatotic Liver Disease.* Nutrients, 2024. **16**(18).
204. Thompson, M.D., et al., *Cell signaling pathways associated with a reduction in mammary cancer burden by dietary common bean (Phaseolus vulgaris L.).* Carcinogenesis, 2012. **33**(1): p. 226-232.
205. Wang, Y., et al., *Dysregulated bile acid homeostasis: unveiling its role in metabolic diseases.* Medical Review, 2024. **4**(4): p. 262-283.
206. Bilson, J., et al., *Bile Acids as Emerging Players at the Intersection of Steatotic Liver Disease and Cardiovascular Diseases.* Biomolecules, 2024. **14**(7).
207. Fleishman, J.S. and S. Kumar, *Bile acid metabolism and signaling in health and disease: molecular mechanisms and therapeutic targets.* Signal Transduction and Targeted Therapy, 2024. **9**(1): p. 97.
208. Li, J. and P.A. Dawson, *Animal models to study bile acid metabolism.* Biochimica et Biophysica Acta (BBA) - Molecular Basis of Disease, 2019. **1865**(5): p. 895-911.
209. Mohanty, I., et al., *The changing metabolic landscape of bile acids - keys to metabolism and immune regulation.* Nat Rev Gastroenterol Hepatol, 2024. **21**(7): p. 493-516.
210. Callender, C., I. Attaye, and M. Nieuwdorp, *The Interaction between the Gut Microbiome and Bile Acids in Cardiometabolic Diseases.* Metabolites, 2022. **12**(1): p. 65.

211. Guzior, D.V. and R.A. Quinn, *Review: microbial transformations of human bile acids.* Microbiome, 2021. **9**(1): p. 140.
212. Cai, J., et al., *Bile acid metabolism and signaling, the microbiota, and metabolic disease.* Pharmacology & Therapeutics, 2022. **237**: p. 108238.
213. Lent-Schochet, D. and I. Jialal, *Antilipemic agent bile acid sequestrants.* 2019.
214. Li, M.-Z., et al., *Biopolymer-based sequestrants for lowering cholesterol: structures, in vitro bile acid anion binding effects, and interaction mechanisms.* Journal of Functional Foods, 2024. **113**: p. 106002.
215. Collins, S.L., et al., *Bile acids and the gut microbiota: metabolic interactions and impacts on disease.* Nature Reviews Microbiology, 2023. **21**(4): p. 236-247.
216. Kleintop, A.E., et al., *Adaptation of the AOAC 2011.25 integrated total dietary fiber assay to determine the dietary fiber and oligosaccharide content of dry edible beans.* J Agric Food Chem, 2013. **61**(40): p. 9719-26.
217. Didinger, C. and H.J. Thompson, *Defining Nutritional and Functional Niches of Legumes: A Call for Clarity to Distinguish a Future Role for Pulses in the Dietary Guidelines for Americans.* Nutrients, 2021. **13**(4).
218. Jackson, R., et al., *Protein combined with certain dietary fibers increases butyrate production in gut microbiota fermentation.* Food Funct, 2024. **15**(6): p. 3186-3198.
219. Zhu, Z., W. Jiang, and H.J. Thompson, *Edible dry bean consumption (Phaseolus vulgaris L.) modulates cardiovascular risk factors and diet-induced obesity in rats and mice.* Br J Nutr, 2012. **108 Suppl 1**: p. S66-73.
220. Reeves, P.G., *Components of the AIN-93 Diets as Improvements in the AIN-76A Diet12.* The Journal of Nutrition, 1997. **127**(5): p. 838S-841S.
221. Reeves, P.G., F.H. Nielsen, and G.C. Fahey, *AIN-93 Purified Diets for Laboratory Rodents: Final Report of the American Institute of Nutrition Ad Hoc Writing Committee on the Reformulation of the AIN-76A Rodent Diet.* The Journal of Nutrition, 1993. **123**(11): p. 1939-1951.
222. Ford, L., et al., *Precision of a Clinical Metabolomics Profiling Platform for Use in the Identification of Inborn Errors of Metabolism.* J Appl Lab Med, 2020. **5**(2): p. 342-356.
223. Jiang, C., et al., *Intestine-selective farnesoid X receptor inhibition improves obesity-related metabolic dysfunction.* Nat Commun, 2015. **6**: p. 10166.
224. Neil, E.S., et al., *White Kidney Bean (Phaseolus Vulgaris L.) Consumption Reduces Fat Accumulation in a Polygenic Mouse Model of Obesity.* Nutrients, 2019. **11**(11).
225. Livak, K.J. and T.D. Schmittgen, *Analysis of relative gene expression data using real-time quantitative PCR and the 2(-Delta Delta C(T)) Method.* Methods, 2001. **25**(4): p. 402-8.
226. Thompson, H.J., et al., *Beneficial Effects of Common Bean on Adiposity and Lipid Metabolism.* Nutrients, 2017. **9**(9).
227. Walker, J.M., *The Bicinchoninic Acid (BCA) Assay for Protein Quantitation*, in *Basic Protein and Peptide Protocols*, J.M. Walker, Editor. 1994, Humana Press: Totowa, NJ. p. 5-8.
228. Thompson, H.J., et al., *Consumption of Common Bean Suppresses the Obesogenic Increase in Adipose Depot Mass: Impact of Dose and Biological Sex.* Nutrients, 2023. **15**(9): p. 2015.
229. McDonald, D., et al., *Greengenes2 unifies microbial data in a single reference tree.* Nature Biotechnology, 2024. **42**(5): p. 715-718.
230. Lin, H. and S.D. Peddada, *Analysis of compositions of microbiomes with bias correction.* Nat Commun, 2020. **11**(1): p. 3514.

231. Arkin, A.P., et al., *KBase: The United States Department of Energy Systems Biology Knowledgebase.* Nature Biotechnology, 2018. **36**(7): p. 566-569.
232. Chivian, D., et al., *Metagenome-assembled genome extraction and analysis from microbiomes using KBase.* Nature Protocols, 2023. **18**(1): p. 208-238.
233. Li, D., et al., *MEGAHIT: an ultra-fast single-node solution for large and complex metagenomics assembly via succinct de Bruijn graph.* Bioinformatics, 2015. **31**(10): p. 1674-6.
234. Wu, Y.-W., B.A. Simmons, and S.W. Singer, *MaxBin 2.0: an automated binning algorithm to recover genomes from multiple metagenomic datasets.* Bioinformatics, 2015. **32**(4): p. 605-607.
235. Wu, Y.-W., et al., *MaxBin: an automated binning method to recover individual genomes from metagenomes using an expectation-maximization algorithm.* Microbiome, 2014. **2**(1): p. 26.
236. Kang, D.D., et al., *MetaBAT, an efficient tool for accurately reconstructing single genomes from complex microbial communities.* PeerJ, 2015. **3**: p. e1165.
237. Alneberg, J., et al., *Binning metagenomic contigs by coverage and composition.* Nature Methods, 2014. **11**(11): p. 1144-1146.
238. Sieber, C.M., et al., *Recovery of genomes from metagenomes via a dereplication, aggregation and scoring strategy.* Nature microbiology, 2018. **3**(7): p. 836-843.
239. Camacho, C., et al., *BLAST+: architecture and applications.* BMC Bioinformatics, 2009. **10**(1): p. 421.
240. Parks, D.H., et al., *CheckM: assessing the quality of microbial genomes recovered from isolates, single cells, and metagenomes.* Genome research, 2015. **25**(7): p. 1043-1055.
241. Shaffer, M., et al., *DRAM for distilling microbial metabolism to automate the curation of microbiome function.* Nucleic Acids Research, 2020. **48**(16): p. 8883-8900.
242. Chaumeil, P.-A., et al., *GTDB-Tk: a toolkit to classify genomes with the Genome Taxonomy Database*. 2020, Oxford University Press.
243. Parks, D.H., et al., *GTDB: an ongoing census of bacterial and archaeal diversity through a phylogenetically consistent, rank normalized and complete genome-based taxonomy.* Nucleic Acids Research, 2021. **50**(D1): p. D785-D794.
244. Team, R.D.C., *R: A language and environment for statistical computing.* (No Title), 2010.
245. Kassambara, A., *rstatix: Pipe-friendly framework for basic statistical tests.* CRAN: Contributed Packages, 2019.
246. Kassambara, A., *ggpubr:'ggplot2'based publication ready plots.* R package version, 2018: p. 2.
247. Sievert, C., *Interactive web-based data visualization with R, plotly, and shiny*. 2020: Chapman and Hall/CRC.
248. Grobe, S., et al., *Highly selective bile acid hydroxylation by the multifunctional bacterial P450 monooxygenase CYP107D1 (OleP).* Biotechnol Lett, 2020. **42**(5): p. 819-824.
249. Deng, F., et al., *Engineering Regioselectivity of P450 BM3 Enables the Biosynthesis of Murideoxycholic Acid by 6β-Hydroxylation of Lithocholic Acid.* Biotechnology Journal, 2024. **19**(11): p. e202400518.
250. Song, C., R.A. Hiipakka, and S. Liao, *Selective activation of liver X receptor alpha by 6α-hydroxy bile acids and analogs.* Steroids, 2000. **65**(8): p. 423-427.
251. Zheng, D., et al., *Novel microbial modifications of bile acids and their functional implications.* Imeta, 2024. **3**(5): p. e243.

252. Cadena Sandoval, M. and R.A. Haeusler, *Bile acid metabolism in type 2 diabetes mellitus.* Nature Reviews Endocrinology, 2025. **21**(4): p. 203-213.
253. Pandak, W.M. and G. Kakiyama, *The acidic pathway of bile acid synthesis: Not just an alternative pathway(☆).* Liver Res, 2019. **3**(2): p. 88-98.
254. Gillard, J., et al., *A gut microbiota-independent mechanism shapes the bile acid pool in mice with MASH.* JHEP Reports, 2024. **6**(11): p. 101148.
255. Wise, J.L. and B.P. Cummings, *The 7-α-dehydroxylation pathway: An integral component of gut bacterial bile acid metabolism and potential therapeutic target.* Frontiers in Microbiology, 2023. **13**.
256. Larabi, A.B., H.L.P. Masson, and A.J. Bäumler, *Bile acids as modulators of gut microbiota composition and function.* Gut Microbes, 2023. **15**(1): p. 2172671.
257. Song, Z., et al., *Taxonomic profiling and populational patterns of bacterial bile salt hydrolase (BSH) genes based on worldwide human gut microbiome.* Microbiome, 2019. **7**(1): p. 9.
258. Yang, Y., et al., *Systematic identification of secondary bile acid production genes in global microbiome.* mSystems, 2024. **10**(1): p. e00817-24.
259. Lutsiv, T., et al., *Relandscaping the Gut Microbiota with a Whole Food: Dose-Response Effects to Common Bean.* Foods, 2022. **11**(8).
260. Agolino, G., et al., *Bile salt hydrolase: The complexity behind its mechanism in relation to lowering-cholesterol lactobacilli probiotics.* Journal of Functional Foods, 2024. **120**: p. 106357.
261. Kusada, H. and H. Tamaki, *Evidence for the Worldwide Distribution of a Bile Salt Hydrolase Gene in Enterococcus faecium Through Horizontal Gene Transfer.* International Journal of Molecular Sciences, 2025. **26**(2): p. 612.
262. Anderson, J.W. and A.W. Major, *Pulses and lipaemia, short- and long-term effect: potential in the prevention of cardiovascular disease.* Br J Nutr, 2002. **88 Suppl 3**: p. S263-71.
263. Rebello, C.J., F.L. Greenway, and J.W. Finley, *A review of the nutritional value of legumes and their effects on obesity and its related co-morbidities.* Obesity Reviews, 2014. **15**(5): p. 392-407.
264. Kahlon, T., G. Smith, and Q. Shao, *In vitro binding of bile acids by kidney bean (Phaseolus vulgaris), black gram (Vigna mungo), bengal gram (Cicer arietinum) and moth bean (Phaseolus aconitifolins).* Food chemistry, 2005. **90**(1-2): p. 241-246.
265. Lin, T., et al., *Retention of primary bile salts by dry beans (Phaseolus vulgaris L.) during in vitro digestion: Role of bean components and effect of food processing.* Food Research International, 2020. **137**: p. 109337.
266. Lin, T., et al., *Manipulation of the dry bean (Phaseolus vulgaris L.) matrix by hydrothermal and high-pressure treatments: Impact on in vitro bile salt-binding ability.* Food Chemistry, 2020. **310**: p. 125699.
267. Alves, P.L.S., et al., *Black, pinto and white beans lower hepatic lipids in hamsters fed high fat diets by excretion of bile acids.* Food Production, Processing and Nutrition, 2020. **2**(1): p. 25.
268. Ngoh, Y.-Y., S.B. Choi, and C.-Y. Gan, *The potential roles of Pinto bean (Phaseolus vulgaris cv. Pinto) bioactive peptides in regulating physiological functions: Protease activating, lipase inhibiting and bile acid binding activities.* Journal of Functional Foods, 2017. **33**: p. 67-75.

269. Nakatani, A., et al., *Dietary mung bean protein reduces high-fat diet-induced weight gain by modulating host bile acid metabolism in a gut microbiota-dependent manner.* Biochemical and Biophysical Research Communications, 2018. **501**(4): p. 955-961.
270. Feng, H.J.X., et al., *Recent Advances in the Management of Dyslipidemia: A Systematic Review.* Cureus, 2025. **17**(3).
271. Singh, J., et al., *Review on Bile Acids: Effects of the Gut Microbiome, Interactions with Dietary Fiber, and Alterations in the Bioaccessibility of Bioactive Compounds.* J Agric Food Chem, 2019. **67**(33): p. 9124-9138.
272. Story, J.A., E.J. Furumoto, and K.K. Buhman, *Dietary fiber and bile acid metabolism—an update.* Dietary fiber in health and disease, 1997: p. 259-266.
273. Vahouny, G.V., et al., *Dietary Fibers VI: Binding of Fatty Acids and Monolein from Mixed Micelles Containing Bile Salts and Lecithin1.* Proceedings of the Society for Experimental Biology and Medicine, 1981. **166**(1): p. 12-16.
274. Qu, Q., et al., *Lithocholic acid phenocopies anti-ageing effects of calorie restriction.* Nature, 2024.
275. Tucker, L.A., *Bean Consumption Accounts for Differences in Body Fat and Waist Circumference: A Cross-Sectional Study of 246 Women.* J Nutr Metab, 2020. **2020**: p. 9140907.
276. Papanikolaou, Y., J. Slavin, and V.L. Fulgoni, *Adult dietary patterns with increased bean consumption are associated with greater overall shortfall nutrient intakes, lower added sugar, improved weight-related outcomes and better diet quality.* Nutrition Journal, 2024. **23**(1): p. 36.
277. Penugurti, V., et al. *AMPK: the Energy Sensor at the Crossroads of Aging and Cancer*. in *Seminars in Cancer Biology*. 2024. Elsevier.
278. Buettner, D. and S. Skemp, *Blue Zones: Lessons From the World's Longest Lived.* Am J Lifestyle Med, 2016. **10**(5): p. 318-321.
279. Feng, Q., et al., *Protective Effects of White Kidney Bean (Phaseolus vulgaris L.) against Diet-Induced Hepatic Steatosis in Mice Are Linked to Modification of Gut Microbiota and Its Metabolites.* Nutrients, 2023. **15**(13): p. 3033.
280. Kadyan, S., et al., *Prebiotic mechanisms of resistant starches from dietary beans and pulses on gut microbiome and metabolic health in a humanized murine model of aging.* Frontiers in Nutrition, 2023. **10**.
281. Li, F., et al., *Highly accurate and sensitive absolute quantification of bacterial strains in human fecal samples.* Microbiome, 2024. **12**(1): p. 168.
282. Chiang, J.Y. and J.M. Ferrell, *Bile acid receptors FXR and TGR5 signaling in fatty liver diseases and therapy.* American Journal of Physiology-Gastrointestinal and Liver Physiology, 2020. **318**(3): p. G554-G573.
283. Xue, R., et al., *Bile Acid Receptors and the Gut-Liver Axis in Nonalcoholic Fatty Liver Disease.* Cells, 2021. **10**(11).
284. Daniell, E.L., et al., *Dietary dry bean effects on hepatic expression of stress and toxicity-related genes in rats.* British Journal of Nutrition, 2012. **108**(S1): p. S37-S45.
285. Mohanty, I., et al., *The underappreciated diversity of bile acid modifications.* Cell, 2024. **187**(7): p. 1801-1818.e20.
286. Winston, J.A. and C.M. Theriot, *Diversification of host bile acids by members of the gut microbiota.* Gut Microbes, 2020. **11**(2): p. 158-171.

287. Xie, G., et al., *Conjugated secondary 12α-hydroxylated bile acids promote liver fibrogenesis.* EBioMedicine, 2021. **66**: p. 103290.
288. Barlow, J.T., S.R. Bogatyrev, and R.F. Ismagilov, *A quantitative sequencing framework for absolute abundance measurements of mucosal and lumenal microbial communities.* Nat Commun, 2020. **11**(1): p. 2590.
289. USDA. *Feeding the future with Pulse Crops*. 2016 [cited 2025 July]; Available from: https://agresearchmag.ars.usda.gov/2016/feb/pulsecrops/.
290. Mudryj, A.N., *Pulse Consumption: A Global Perspective*, in *Health Benefits of Pulses*, W.J. Dahl, Editor. 2019, Springer International Publishing: Cham. p. 19-33.
291. Joshi, P.K. and P.P. Rao, *Global pulses scenario: status and outlook.* Annals of the New York Academy of Sciences, 2017. **1392**(1): p. 6-17.
292. Ferraro, D.M., et al., *Historical food consumption declines and the role of alternative foods.* Environmental Research Letters, 2022. **17**(1): p. 014020.
293. Lane, L., R. Wells, and C. Reynolds, *Beans, peas and pulses for improved public and planetary health: Changing UK consumption patterns.* Proceedings of the Nutrition Society, 2024. **83**(OCE2): p. E203.
294. Bhardwaj, R.L., et al., *An Alarming Decline in the Nutritional Quality of Foods: The Biggest Challenge for Future Generations' Health.* Foods, 2024. **13**(6).
295. Levy, R.B., et al., *Ultra-processed food consumption and type 2 diabetes incidence: A prospective cohort study.* Clinical Nutrition, 2021. **40**(5): p. 3608-3614.
296. Wood, B., et al., *Using a systems thinking approach to map the global rise of ultra-processed foods in population diets.* Obesity Reviews, 2025. **26**(4): p. e13877.
297. Watson, K.B., et al., *Trends in Multiple Chronic Conditions Among US Adults, By Life Stage, Behavioral Risk Factor Surveillance System, 2013–2023.* Preventing Chronic Disease, 2025. **22**: p. E15.
298. Hacker, K., *The Burden of Chronic Disease.* Mayo Clin Proc Innov Qual Outcomes, 2024. **8**(1): p. 112-119.
299. Daneshmand, R., *Challenges in Promoting Plant Protein Food Consumption*, in *Plant Protein Foods*, A. Manickavasagan, L.-T. Lim, and A. Ali, Editors. 2022, Springer International Publishing: Cham. p. 503-510.
300. Silva, P., et al., *Nutrition and Food Literacy: Framing the Challenges to Health Communication.* Nutrients, 2023. **15**(22).
301. Taylor, M.K., et al., *Nutrition literacy predicts adherence to healthy/unhealthy diet patterns in adults with a nutrition-related chronic condition.* Public Health Nutr, 2019. **22**(12): p. 2157-2169.
302. Murakami, K., et al., *Food literacy and eating motivation in relation to diet quality and general and abdominal obesity: A cross-sectional study.* Appetite, 2025. **209**: p. 107968.
303. Lisciani, S., et al., *Legumes and common beans in sustainable diets: nutritional quality, environmental benefits, spread and use in food preparations.* Frontiers in Nutrition, 2024. **Volume 11 - 2024**.
304. Thompson, H.J., et al., *Consumption of Common Bean Suppresses the Obesogenic Increase in Adipose Depot Mass: Impact of Dose and Biological Sex.* Nutrients, 2023. **15**(9).
305. Bowman, S., et al., *Food Patterns Equivalents Intakes from Food: Mean Amounts Consumer per Individual, What We Eat in America, NHANES 2011-12; Tables 1-4.* Agricultural

Research Service. https://www. ars. usda. gov/research/publications/publication, 2014.
306. *U.S. Department of Agriculture and U.S. Department of Health and Human Services. Dietary Guidelines for Americans, 2020-2025. 9th Edition. December 2020. Available at DietaryGuidelines.gov. [(accessed on 7 May 2024)].*
307. Commission, E. *Food-Based Dietary Guidelines recommendations for legumes*. Knowledge for Policy, 2025.
308. Zhang, Z., et al., *A high-legume low-glycemic index diet reduces fasting plasma leptin in middle-aged insulin-resistant and -sensitive men.* European Journal of Clinical Nutrition, 2011. **65**(3): p. 415-418.
309. Service, U.S.D.o.A.F.a.N. *Healthy eating index (HEI)*. 2025 [cited 2025 July 17]; Available from: https://www.fns.usda.gov/cnpp/healthy-eating-index-hei.
310. Zhang, X., et al., *Modulating a prebiotic food source influences inflammation and immune-regulating gut microbes and metabolites: insights from the BE GONE trial.* eBioMedicine, 2023. **98**.
311. Kaimila, Y., et al., *Pulse and legume consumption is associated with a more optimal nutrient intake and a higher EAT-Lancet index in a representative UK population.* Eur J Nutr, 2025. **64**(3): p. 139.
312. Singh, A.K., et al., *Plant-based protein crops and their improvement: Current status and future perspectives.* Crop Science, 2025. **65**(1): p. e21389.
313. Wu, S., et al., *Effect of Dietary Protein and Processing on Gut Microbiota—A Systematic Review.* Nutrients, 2022. **14**(3): p. 453.
314. Bartlett, A. and M. Kleiner, *Dietary protein and the intestinal microbiota: An understudied relationship.* iScience, 2022. **25**(11).
315. Nutrition, A.S.f. *Most Americans are not getting enough fiber in our diets*. 2021 [cited 2025; Available from: https://nutrition.org/most-americans-are-not-getting-enough-fiber-in-our-diets/.
316. Ioniţă-Mîndrican, C.B., et al., *Therapeutic Benefits and Dietary Restrictions of Fiber Intake: A State of the Art Review.* Nutrients, 2022. **14**(13).
317. Hodgkinson, K., et al., *Butyrate's role in human health and the current progress towards its clinical application to treat gastrointestinal disease.* Clinical Nutrition, 2023. **42**(2): p. 61-75.
318. Pant, K., et al., *The Role of Gut Microbiome-Derived Short-Chain Fatty Acid Butyrate in Hepatobiliary Diseases.* The American Journal of Pathology, 2023. **193**(10): p. 1455-1467.
319. Collaborators, T.U.B.o.D., *The State of US Health, 1990-2016: Burden of Diseases, Injuries, and Risk Factors Among US States.* JAMA, 2018. **319**(14): p. 1444-1472.
320. BlueZones.com. *Food Guidelines - Blue Zones*. [cited 2025; Available from: https://www.bluezones.com/recipes/food-guidelines/.
321. Huang, J., et al., *Association Between Plant and Animal Protein Intake and Overall and Cause-Specific Mortality.* JAMA Internal Medicine, 2020. **180**(9): p. 1173-1184.
322. Rolands, M.R., et al., *Protein Adequacy, Plant Protein Proportion, and Main Plant Protein Sources Consumed Across Vegan, Vegetarian, Pescovegetarian, and Semivegetarian Diets: A Systematic Review.* The Journal of Nutrition, 2025. **155**(1): p. 153-167.

323. Abe-Inge, V., et al., *Plant-based dietary shift: Current trends, barriers, and carriers.* Trends in Food Science & Technology, 2024. **143**.
324. Didinger, C., M. Bunning, and H. Thompson, *A Translational Approach to Increase Pulse Intake and Promote Public Health through Developing an Extension Bean Toolkit.* Nutrients, 2023. **15**(19).
325. Didinger, C., M. Bunning, and H.J. Thompson, *Bean Cuisine: The Potential of Citizen Science to Help Motivate Changes in Pulse Knowledge and Consumption.* Foods, 2023. **12**(14).
326. Didinger, C. and H. Thompson, *Motivating Pulse-Centric Eating Patterns to Benefit Human and Environmental Well-Being.* Nutrients, 2020. **12**(11).
327. Lanza, E., et al., *High dry bean intake and reduced risk of advanced colorectal adenoma recurrence among participants in the polyp prevention trial.* J Nutr, 2006. **136**(7): p. 1896-903.
328. Wang, Y., et al., *Legume consumption and colorectal adenoma risk: a meta-analysis of observational studies.* PLoS One, 2013. **8**(6): p. e67335.
329. Agurs-Collins, T., et al., *Legume intake and reduced colorectal adenoma risk in African-Americans.* J Natl Black Nurses Assoc, 2006. **17**(2): p. 6-12.
330. Patel, L., et al., *Legume intake and cancer risk in a network of case-control studies.* Eur J Clin Nutr, 2024.
331. Mitchell, D.C., et al., *Consumption of dry beans, peas, and lentils could improve diet quality in the US population.* J Am Diet Assoc, 2009. **109**(5): p. 909-13.